



12TH INTERNATIONAL ORGANIZATION OF CHINESE
PHYSICISTS AND ASTRONOMERS ACCELERATOR SCHOOL



OCPA-2025

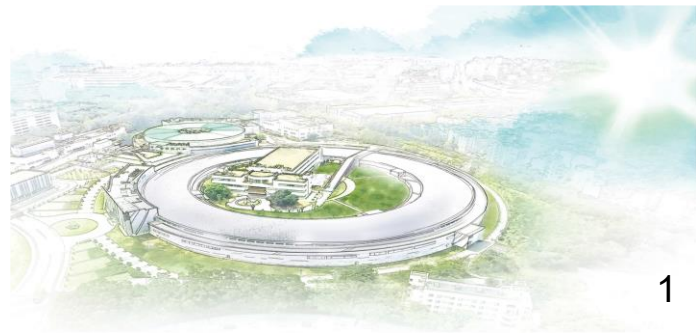
KHAOYAI, NAKHON RATCHASIMA, THAILAND | 29 JULY – 7 AUGUST 2025

RF Technology (T6)

W. Y. Chiang

National Synchrotron Radiation Research Center (NSRRC)

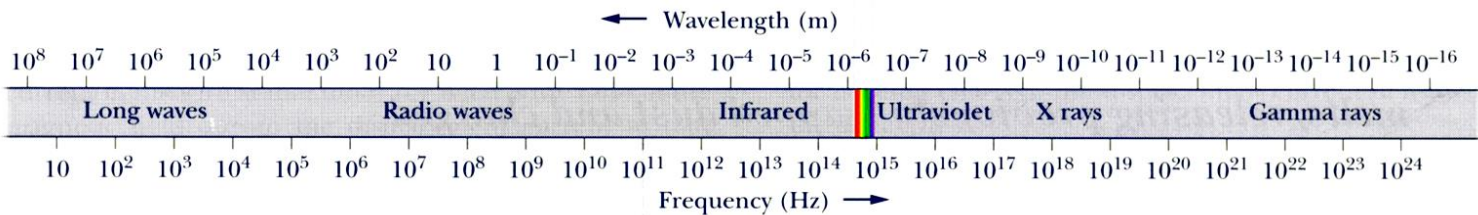
OCPA 2025, August 4, 2024



國家同步輻射研究中心
National Synchrotron Radiation Research Center

Outline

- Field Theory of Guided Waves - 1. Modes in a Waveguide
- Field Theory of Guided Waves – 2. Modes in Cavities
- Cavity Power Loss and Q
- Parameters of an Open-End Cavity
- Critical Coupling, Undercoupling, and Overcoupling
- Cavity application – SLED
- Microwave Tubes
- Line-type Modulator of Klystron



Frequency Bands for Household Electronics

AM broadcast band: 535-1605 kHz

Shortwave radio: 3-30 MHz

FM broadcast band: 88-108 MHz

VHF TV (channel 2-4): 54-72 MHz

VHF TV (channel 5-6): 76-88 MHz

UHF TV (channel 7-13): 174-216 MHz

UHF TV (channel 14-83): 470-890 MHz

Microwave Bands

L-band: 1 - 2 GHz

S-band: 2 - 4 GHz

C-band: 4 - 8 GHz

X-band: 8 - 12 GHz

Ku-band: 12 - 18 GHz

K-band: 18 - 26.5 GHz

Ka-band: 26.5 - 40 GHz

U-band: 40 - 60 GHz

V-band: 60 - 80 GHz

W-band (IEEE): 80 - 100 GHz

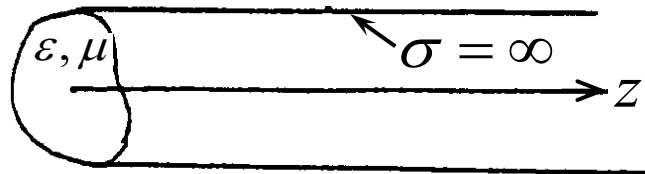
Field Theory of Guided Waves - 1. Modes in a Waveguide

Consider a hollow conductor of *infinite* length and *uniform* cross section of arbitrary shape (see figure). This is a structure which can be used to transport high-power EM waves, and hence is called a waveguide. Assume a *uniform, linear, and isotropic* filling medium

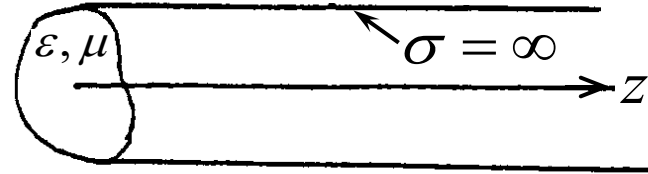
and let $\begin{cases} \mathbf{E}(\mathbf{x}, t) = \mathbf{E}(\mathbf{x})e^{-i\omega t} \\ \mathbf{B}(\mathbf{x}, t) = \mathbf{B}(\mathbf{x})e^{-i\omega t} \end{cases}$ and $\begin{cases} \mathbf{B}(\mathbf{x}) = \mu\mathbf{H}(\mathbf{x}) \\ \mathbf{D}(\mathbf{x}) = \varepsilon\mathbf{E}(\mathbf{x}) \end{cases}$, where ε and μ

are in general complex numbers. Usually, the filling medium is air ($\varepsilon \approx \varepsilon_0$, $\mu = \mu_0$). For now, we assume infinite wall conductivity. As before, $\mathbf{E}(\mathbf{x})$ and $\mathbf{B}(\mathbf{x})$ are complex phasers, and $\mathbf{E}(\mathbf{x}, t)$ or $\mathbf{B}(\mathbf{x}, t)$ is the real part of the RHS. Under these assumptions, Maxwell eqs. are

$$\begin{cases} \nabla \times \mathbf{E}(\mathbf{x}) = i\omega\mathbf{B}(\mathbf{x}) & (8) \\ \nabla \times \mathbf{B}(\mathbf{x}) = -i\mu\varepsilon\omega\mathbf{E}(\mathbf{x}) & (9) \\ \nabla \cdot \mathbf{E}(\mathbf{x}) = 0 & (10) \\ \nabla \cdot \mathbf{B}(\mathbf{x}) = 0 & (11) \end{cases}$$



$$\text{Rewrite } \begin{cases} \nabla \times \mathbf{E} = i\omega \mathbf{B} \\ \nabla \times \mathbf{B} = -i\mu\epsilon\omega \mathbf{E} \\ \nabla \cdot \mathbf{E} = 0 \\ \nabla \cdot \mathbf{B} = 0 \end{cases} \quad \begin{array}{l} (8) \\ (9) \\ (10) \\ (11) \end{array}$$



$$\begin{aligned} \nabla \times (8) &\Rightarrow \nabla \times \nabla \times \mathbf{E} = i\omega \nabla \times \mathbf{B} \\ &\Rightarrow \nabla(\nabla \cdot \mathbf{E}) - \nabla^2 \mathbf{E} = \mu\epsilon\omega^2 \mathbf{E} \\ &\Rightarrow \nabla^2 \mathbf{E} + \mu\epsilon\omega^2 \mathbf{E} = 0 \end{aligned} \quad (12a)$$

Similarly,

$$\nabla \times (9) \Rightarrow \nabla^2 \mathbf{B} + \mu\epsilon\omega^2 \mathbf{B} = 0 \quad (12b)$$

(12a,b) have the same form as the wave equations in infinite space. However, (12a,b) are now subject to boundary conditions on the walls. Most wave problems involving a boundary do not have exact solutions. The waveguide structure offers a rare case where exact solutions are possible (in particular, for rectangular and circular cross-sections). The structural uniformity in z suggests a solution with $e^{\pm ik_z z}$ dependence.

$$\text{Let } \begin{cases} \mathbf{E}(\mathbf{x}) = \mathbf{E}(\mathbf{x}_t) e^{\pm i k_z z} \\ \mathbf{B}(\mathbf{x}) = \mathbf{B}(\mathbf{x}_t) e^{\pm i k_z z} \end{cases} \quad (13)$$

then, $\begin{cases} \mathbf{E}(\mathbf{x}, t) = \mathbf{E}(\mathbf{x}_t) e^{\pm i k_z z - i \omega t} \\ \mathbf{B}(\mathbf{x}, t) = \mathbf{B}(\mathbf{x}_t) e^{\pm i k_z z - i \omega t} \end{cases}$

\mathbf{x}_t : coordinates transverse to z ,
 e.g. (x, y) or (r, θ)
 k_z here $\leftrightarrow k$ in Jackson

where, in general, ω and k_z are complex constants. To be specific, *we assume that the real parts of ω and k_z are both positive*. Then, $e^{i k_z z - i \omega t}$ and $e^{-i k_z z - i \omega t}$ have forward and backward *phase* velocities, respectively. As will be seen in (30), $e^{i k_z z - i \omega t}$ and $e^{-i k_z z - i \omega t}$ also have forward and backward *group* velocities, respectively. Hence, we call $e^{i k_z z - i \omega t}$ a forward wave and $e^{-i k_z z - i \omega t}$ a backward wave, both of which are traveling waves. With the assumed z dependences, we get

$$\begin{cases} \frac{\partial^2}{\partial z^2} \rightarrow -k_z^2 \\ \nabla^2 = \nabla_t^2 + \frac{\partial^2}{\partial z^2} = \nabla_t^2 - k_z^2 \end{cases}$$

$$\nabla_t^2 = \begin{cases} \frac{\partial^2}{\partial x^2} + \frac{\partial^2}{\partial y^2}, & \text{Cartesian} \\ \frac{1}{r} \frac{\partial}{\partial r} \left(r \frac{\partial}{\partial r} \right) + \frac{1}{r^2} \frac{\partial^2}{\partial \theta^2}, & \text{cylindrical} \end{cases}$$

Thus,

$$\begin{cases} \nabla^2 \mathbf{E}(\mathbf{x}) + \mu\epsilon\omega^2 \mathbf{E}(\mathbf{x}) = 0 \\ \nabla^2 \mathbf{B}(\mathbf{x}) + \mu\epsilon\omega^2 \mathbf{B}(\mathbf{x}) = 0 \end{cases} \Rightarrow \left(\nabla_t^2 + \mu\epsilon\omega^2 - k_z^2 \right) \begin{Bmatrix} \mathbf{E}(\mathbf{x}_t) \\ \mathbf{B}(\mathbf{x}_t) \end{Bmatrix} = 0 \quad (8.19)$$

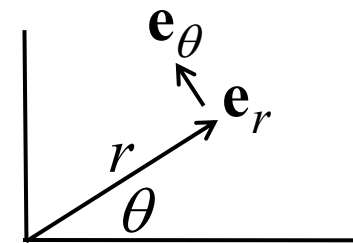
$$\Rightarrow \left(\nabla_t^2 + \mu\epsilon\omega^2 - k_z^2 \right) \begin{Bmatrix} E_z(\mathbf{x}_t) \\ B_z(\mathbf{x}_t) \end{Bmatrix} = 0 \quad (14)$$

It is in general not possible to obtain from (8.19) a simple equation like (14) for the other components of $\mathbf{E}(\mathbf{x}_t)$ and $\mathbf{B}(\mathbf{x}_t)$ [such as $E_\theta(\mathbf{x}_t)$, see Exercise below]. So our strategy here is to solve (14) for $E_z(\mathbf{x}_t)$ and $B_z(\mathbf{x}_t)$, and then express the other components of the fields [$\mathbf{E}_t(\mathbf{x}_t)$ and $\mathbf{B}_t(\mathbf{x}_t)$] in terms of $E_z(\mathbf{x}_t)$ and $B_z(\mathbf{x}_t)$.

Exercise:

Writing $\mathbf{E}(\mathbf{x}_t) = E_r \mathbf{e}_r + E_\theta \mathbf{e}_\theta + E_z \mathbf{e}_z$ and using the cylindrical coordinate system, derive the equations for E_r and E_θ from (8.19).

(hint: $\frac{\partial}{\partial \theta} \mathbf{e}_r = \mathbf{e}_\theta$, $\frac{\partial}{\partial \theta} \mathbf{e}_\theta = -\mathbf{e}_r$)



$$\text{Let } \begin{cases} \mathbf{E}(\mathbf{x}_t) = \mathbf{E}_t(\mathbf{x}_t) + E_z(\mathbf{x}_t)\mathbf{e}_z \\ \mathbf{B}(\mathbf{x}_t) = \mathbf{B}_t(\mathbf{x}_t) + B_z(\mathbf{x}_t)\mathbf{e}_z \\ \nabla = \nabla_t + \mathbf{e}_z \frac{\partial}{\partial z} = \nabla_t \pm ik_z \mathbf{e}_z \end{cases}$$

$$\nabla_t = \begin{cases} \mathbf{e}_x \frac{\partial}{\partial x} + \mathbf{e}_y \frac{\partial}{\partial y}, & \text{Cartesian} \\ \mathbf{e}_r \frac{\partial}{\partial r} + \mathbf{e}_\theta \frac{1}{r} \frac{\partial}{\partial \theta}, & \text{cylindrical} \end{cases}$$

$$\nabla \times \mathbf{E} = i\omega \mathbf{B} \Rightarrow (\nabla_t \pm ik_z \mathbf{e}_z) \times (\mathbf{E}_t + E_z \mathbf{e}_z) = i\omega (\mathbf{B}_t + B_z \mathbf{e}_z) \quad (15)$$

$$\nabla \times \mathbf{B} = -i\omega \mu \epsilon \mathbf{E} \Rightarrow (\nabla_t \pm ik_z \mathbf{e}_z) \times (\mathbf{B}_t + B_z \mathbf{e}_z) = -i\omega \mu \epsilon (\mathbf{E}_t + E_z \mathbf{e}_z) \quad (16)$$

Using the relations: $\left\{ \begin{array}{l} (\nabla_t \times \mathbf{E}_t) \parallel \mathbf{e}_z \\ (\nabla_t \times E_z \mathbf{e}_z) \perp \mathbf{e}_z \end{array} \right\}$ on (15), (16), and write down

the transverse components of (15) and (16):

$$\left\{ \begin{array}{l} \nabla_t \times E_z \mathbf{e}_z \pm ik_z \mathbf{e}_z \times \mathbf{E}_t = i\omega \mathbf{B}_t \\ \nabla_t \times B_z \mathbf{e}_z \pm ik_z \mathbf{e}_z \times \mathbf{B}_t = -i\mu \epsilon \omega \mathbf{E}_t \end{array} \right. \quad (17)$$

$$\left\{ \begin{array}{l} \nabla_t \times E_z \mathbf{e}_z \pm ik_z \mathbf{e}_z \times \mathbf{E}_t = i\omega \mathbf{B}_t \\ \nabla_t \times B_z \mathbf{e}_z \pm ik_z \mathbf{e}_z \times \mathbf{B}_t = -i\mu \epsilon \omega \mathbf{E}_t \end{array} \right. \quad (18)$$

Note: In (15)-(18), the $\left\{ \begin{array}{l} \text{upper} \\ \text{lower} \end{array} \right\}$ sign $\Rightarrow \left\{ \begin{array}{l} \text{forward} \\ \text{backward} \end{array} \right\}$ wave and the

the real parts of ω and k_z are both assumed to be positive.

$$\text{Rewrite } \begin{cases} \nabla_t \times E_z \mathbf{e}_z \pm ik_z \mathbf{e}_z \times \mathbf{E}_t = i\omega \mathbf{B}_t & (17) \\ \nabla_t \times B_z \mathbf{e}_z \pm ik_z \mathbf{e}_z \times \mathbf{B}_t = -i\mu\epsilon\omega \mathbf{E}_t & (18) \end{cases}$$

Assume E_z, B_z have already been solved from (14), then (17), (18) are algebraic (rather than differential) equations. We now manipulate (17), (18) to eliminate \mathbf{B}_t and thus express \mathbf{E}_t in terms of E_z and B_z .

$$\begin{aligned} \mathbf{e}_z \times (17) \Rightarrow \mathbf{e}_z \times (\underbrace{\nabla_t \times E_z \mathbf{e}_z}_{\nabla_t E_z \times \mathbf{e}_z + E_z \underbrace{\nabla_t \times \mathbf{e}_z}_0}) \pm ik_z \mathbf{e}_z \times \overbrace{(\mathbf{e}_z \times \mathbf{E}_t)}^{-\mathbf{E}_t} &= i\omega \mathbf{e}_z \times \mathbf{B}_t \\ \nabla_t E_z \times \mathbf{e}_z + E_z \underbrace{\nabla_t \times \mathbf{e}_z}_0 & \end{aligned}$$

$$\nabla \times \psi \mathbf{a} = \nabla \psi \times \mathbf{a} + \psi \nabla \times \mathbf{a}$$

If ψ, \mathbf{a} are both independent of z , then

$$\nabla_t \times \psi \mathbf{a} = \nabla_t \psi \times \mathbf{a} + \psi \nabla_t \times \mathbf{a}$$

$$\Rightarrow i\omega \mathbf{e}_z \times \mathbf{B}_t = \nabla_t E_z \mp ik_z \mathbf{E}_t \quad (19)$$

Sub. $i\omega\mathbf{e}_z \times \mathbf{B}_t = \nabla_t E_z \mp ik_z \mathbf{E}_t$ [(19)] into

$$\nabla_t \times B_z \mathbf{e}_z \pm ik_z \mathbf{e}_z \times \mathbf{B}_t = -i\mu\epsilon\omega\mathbf{E}_t \quad (18)$$

$$\Rightarrow \underbrace{\nabla_t \times B_z \mathbf{e}_z}_{\nabla_t B_z \times \mathbf{e}_z} \pm ik_z \frac{1}{i\omega} (\nabla_t E_z \mp ik_z \mathbf{E}_t) = -i\mu\epsilon\omega\mathbf{E}_t \quad (20)$$

Multiply (20) by $i\omega$: $i\omega\nabla_t B_z \times \mathbf{e}_z \pm ik_z \nabla_t E_z + k_z^2 \mathbf{E}_t = \mu\epsilon\omega^2 \mathbf{E}_t$

$$\Rightarrow (\mu\epsilon\omega^2 - k_z^2) \mathbf{E}_t = i(\omega\nabla_t B_z \times \mathbf{e}_z \pm k_z \nabla_t E_z)$$

$$\Rightarrow \mathbf{E}_t(\mathbf{x}_t) = \frac{i}{\mu\epsilon\omega^2 - k_z^2} [\pm k_z \nabla_t E_z(\mathbf{x}_t) - \omega\mathbf{e}_z \times \nabla_t B_z(\mathbf{x}_t)] \quad (8.26a)$$

Similarly,

$$\mathbf{B}_t(\mathbf{x}_t) = \frac{i}{\mu\epsilon\omega^2 - k_z^2} [\pm k_z \nabla_t B_z(\mathbf{x}_t) + \mu\epsilon\omega\mathbf{e}_z \times \nabla_t E_z(\mathbf{x}_t)] \quad (8.26b)$$

Thus, once $E_z(\mathbf{x}_t)$ and $B_z(\mathbf{x}_t)$ have been solved from (14), the solutions for $\mathbf{E}_t(\mathbf{x}_t)$ and $\mathbf{B}_t(\mathbf{x}_t)$ are given by (8.26a) and (8.26b).

Discussion:

- (i) \mathbf{E}_t , \mathbf{B}_t , E_z , B_z in (8.26a) and (8.26b) are functions of \mathbf{x}_t only.
- (ii) ε and μ can be complex. $\text{Im}(\varepsilon)$ or $\text{Im}(\mu)$ implies dissipation.
- (iii) By letting $B_z = 0$, we may obtain a set of solutions for E_z , \mathbf{E}_t , and \mathbf{B}_t from (14), (8.26a), and (8.26b), respectively. It can be shown that if the boundary condition on E_z is satisfied, then boundary conditions on \mathbf{E}_t and \mathbf{B}_t are also satisfied. Hence, this gives a set of valid solutions called the TM (transverse magnetic) modes. Similarly, by letting $E_z = 0$, we may obtain a set of valid solutions called the TE (transverse electric) modes.
- (iv) E_z is the generating function for the TM mode and B_z is the generating function for the TE mode. The generating function is denoted by Ψ in Jackson.

TM Mode of a Waveguide ($B_z = 0$): (see pp. 359-360)

$$\left\{ \begin{array}{l} (\nabla_t^2 + \gamma^2) E_z = 0 \text{ with boundary condition } E_z|_s = 0 \\ \mathbf{E}_t = \pm \frac{ik_z}{\gamma^2} \nabla_t E_z \\ \mathbf{H}_t = \pm \frac{\varepsilon\omega}{k_z} \mathbf{e}_z \times \mathbf{E}_t = \pm \frac{1}{Z_e} \mathbf{e}_z \times \mathbf{E}_t \\ \gamma^2 = \mu\varepsilon\omega^2 - k_z^2 \end{array} \right. \quad \begin{array}{l} (21) \\ (21a) \\ (21b) \\ (21c) \end{array}$$

Assume perfectly conducting wall.

$Z_e \equiv k_z / \varepsilon\omega$, wave impedance of TM modes

TE Mode of a Waveguide ($E_z = 0$): (see pp. 359-360)

$$\left\{ \begin{array}{l} (\nabla_t^2 + \gamma^2) H_z = 0 \text{ with boundary condition } \frac{\partial}{\partial n} H_z|_s = 0 \\ \mathbf{H}_t = \pm \frac{ik_z}{\gamma^2} \nabla_t H_z \\ \mathbf{E}_t = \mp \frac{\mu\omega}{k_z} \mathbf{e}_z \times \mathbf{H}_t = \mp Z_h \mathbf{e}_z \times \mathbf{H}_t \\ \gamma^2 = \mu\varepsilon\omega^2 - k_z^2 \end{array} \right. \quad \begin{array}{l} (22) \\ (22a) \\ (22b) \\ (22c) \end{array}$$

$Z_h \equiv \mu\omega / k_z$, wave impedance of TE modes

b.c. $\mathbf{n} \cdot \mathbf{H}|_s = 0$
 $\mathbf{n} \perp \mathbf{e}_z \Rightarrow \mathbf{n} \cdot \mathbf{H}_t|_s = 0$
 (22a) $\Rightarrow \mathbf{n} \cdot \nabla_t H_z|_s = 0$
 $\Rightarrow \frac{\partial}{\partial n} H_z|_s = 0$

Discussion:

- (i) Either (21) or (22) constitutes an eigenvalue problem (see Electrodynamics (I) lecture notes, Ch. 3, Appendix A). The eigenvalue γ^2 will be an infinite set of discrete values fixed by the boundary condition, each representing an eigenmode of the waveguide (An example will be provided below.)
- (ii) (21b) and (22b) show that \mathbf{E} is perpendicular to \mathbf{B} (also true in a cavity).
- (iii) (21b) and (22b) show that \mathbf{E}_t and \mathbf{B}_t are *in phase* if μ , ε , ω , k_z are all real (not true in a cavity).
- (iv) (21c) [or (22c)] is the dispersion relation, which relates ω and k_z for a given mode.
- (v) The wave impedance (Z_e or Z_h) gives the ratio of E_t to H_t in the waveguide.

TEM Mode of Coaxial and Parallel-Wire Transmission Lines

$(E_z = B_z = 0)$: (see Jackson p. 341)

$$\text{Rewrite } \begin{cases} \mathbf{E}_t = \frac{i}{\mu\epsilon\omega^2 - k_z^2} [\pm k_z \nabla_t E_z - \omega \mathbf{e}_z \times \nabla_t B_z] & (8.26a) \\ \mathbf{B}_t = \frac{i}{\mu\epsilon\omega^2 - k_z^2} [\pm k_z \nabla_t B_z + \mu\epsilon\omega \mathbf{e}_z \times \nabla_t E_z] & (8.26b) \end{cases}$$

These 2 equations fail for a different class of modes, called the TEM (transverse electromagnetic) mode, for which $E_z = B_z = 0$.

However, they give the condition for the existence of this mode:

$$\boxed{\omega^2 = \frac{k_z^2}{\mu\epsilon}} \left[\begin{array}{l} \text{Equations in rectangular boxes are} \\ \text{basic equations for the TEM mode.} \end{array} \right] \quad (8.27)$$

(8.27) is also the dispersion relation in infinite space. This makes the TEM mode very useful because it can propagate at any frequency.

To calculate \mathbf{E}_t and \mathbf{B}_t , we need to go back to Maxwell equations.

Let $\begin{cases} E_z = 0 \\ B_z = 0 \end{cases}$ and $\begin{cases} \mathbf{E}(\mathbf{x}) \\ \mathbf{B}(\mathbf{x}) \end{cases} = \begin{cases} \mathbf{E}_{\text{TEM}}(\mathbf{x}_t) \\ \mathbf{B}_{\text{TEM}}(\mathbf{x}_t) \end{cases} e^{\pm ik_z z}$.

$$\begin{aligned} \mathbf{E}_{\text{TEM}}(\mathbf{x}_t) &\perp \mathbf{e}_z \\ \mathbf{B}_{\text{TEM}}(\mathbf{x}_t) &\perp \mathbf{e}_z \end{aligned}$$

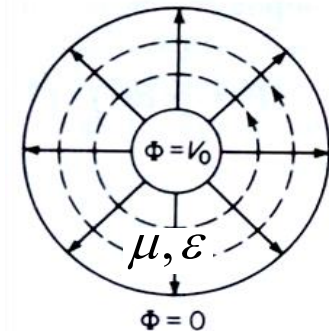
With $B_z = 0$, the z -component of $\nabla \times \mathbf{E}(\mathbf{x}) = i\omega \mathbf{B}(\mathbf{x})$ gives

$$\nabla_t \times \mathbf{E}_{\text{TEM}}(\mathbf{x}_t) = 0 \Rightarrow \boxed{\mathbf{E}_{\text{TEM}}(\mathbf{x}_t) = -\nabla_t \Phi_{\text{TEM}}(\mathbf{x}_t)},$$

[Note: $\nabla_t \times \mathbf{A}_t(\mathbf{x}_t) = 0 \Leftrightarrow \mathbf{A}_t(\mathbf{x}_t) = -\nabla_t \Phi(\mathbf{x}_t)$]

With $E_z = 0$, $\nabla \cdot \mathbf{E}(\mathbf{x}) = 0$ gives

$$\nabla_t \cdot \mathbf{E}_{\text{TEM}}(\mathbf{x}_t) = 0 \Rightarrow \boxed{\nabla_t^2 \Phi_{\text{TEM}}(\mathbf{x}_t) = 0}.$$



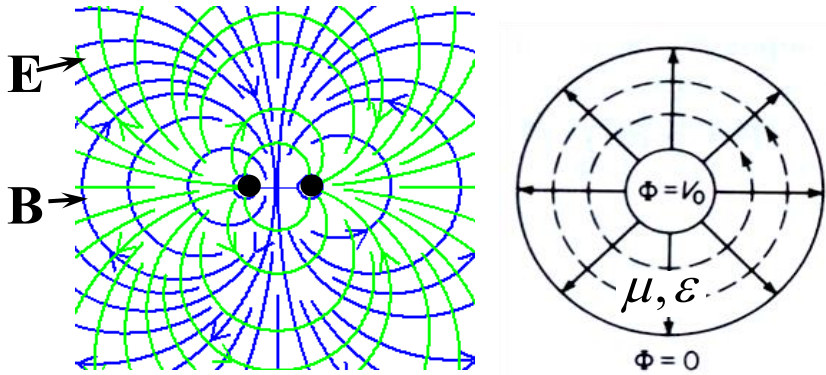
coaxial cable

The transverse component of $\nabla \times \mathbf{E}(\mathbf{x}) = i\omega \mathbf{B}(\mathbf{x})$ gives

$$\boxed{\mathbf{B}_{\text{TEM}}(\mathbf{x}_t) = \pm \frac{k_z}{\omega} \mathbf{e}_z \times \mathbf{E}_{\text{TEM}}(\mathbf{x}_t)}.$$

Because $\mathbf{E}_{\text{tan}} = 0$ ("tan": tangential) on the surface of a perfect conductor, we have Φ_{TEM} (on the boundary) = *const.* This gives $\Phi_{\text{TEM}} = \text{const.}$ or $\mathbf{E}_{\text{TEM}} = 0$ everywhere, if there is only one conductor. So, **TEM modes exist only in 2-conductor configurations**, such as coaxial and parallel-wire transmission lines.

In summary, the TEM modes are governed by

$$\left\{ \begin{array}{l} \nabla_t^2 \Phi_{\text{TEM}}(\mathbf{x}_t) = 0 \\ \mathbf{E}_{\text{TEM}} = -\nabla_t \Phi_{\text{TEM}}(\mathbf{x}_t) \\ \mathbf{B}_{\text{TEM}} = \pm \frac{k_z}{\omega} \mathbf{e}_z \times \mathbf{E}_{\text{TEM}} \end{array} \right. \quad \begin{array}{l} \mathbf{E} \rightarrow \\ \mathbf{B} \rightarrow \end{array} \quad \begin{array}{l} (23) \\ (23a) \\ (23b) \end{array}$$


$$\left(\text{or } \mathbf{H}_{\text{TEM}} = \pm \frac{k_z}{\omega \mu} \mathbf{e}_z \times \mathbf{E}_{\text{TEM}} = \pm \sqrt{\frac{\epsilon}{\mu}} \mathbf{e}_z \times \mathbf{E}_{\text{TEM}} = \pm Y \mathbf{e}_z \times \mathbf{E}_{\text{TEM}} \right)$$

$$\left\{ \begin{array}{l} \omega^2 = \frac{k_z^2}{\mu \epsilon} \end{array} \right. \quad (23c)$$

where $Y (= \sqrt{\frac{\epsilon}{\mu}})$ is the (intrinsic) admittance of the filling medium, which is defined in Ch. 2 of lecture notes following Eq. (26).

Since \mathbf{E}_{TEM} and \mathbf{B}_{TEM} are both $\perp \mathbf{e}_z$, the Poynting vector, $\langle \mathbf{S} \rangle_t = \frac{1}{2} \text{Re}[\mathbf{E}_{\text{TEM}}^* \times \mathbf{H}_{\text{TEM}}]$, is in the \mathbf{e}_z direction.

Question: If an electron moves from $\Phi_{\text{TEM}} = 0$ to $\Phi_{\text{TEM}} = V_0$, does its energy change by eV_0 ?

Discussion:

(i) For the TEM modes, we solve a 2-D equation $\nabla_t^2 \Phi_{\text{TEM}}(\mathbf{x}_t) = 0$ for $\Phi_{\text{TEM}}(\mathbf{x}_t)$. But this is not a 2-D problem because Φ_{TEM} is not the full solution. The full solution is $\begin{pmatrix} \mathbf{E}_t(\mathbf{x}, t) \\ \mathbf{B}_t(\mathbf{x}, t) \end{pmatrix} = \begin{pmatrix} \mathbf{E}_{\text{TEM}}(\mathbf{x}_t) \\ \mathbf{B}_{\text{TEM}}(\mathbf{x}_t) \end{pmatrix} e^{\pm i k_z z - i \omega t}$

with $\mathbf{E}_{\text{TEM}}(\mathbf{x}_t) = -\nabla_t \Phi_{\text{TEM}}(\mathbf{x}_t)$ and $\mathbf{B}_{\text{TEM}}(\mathbf{x}_t) = \pm \frac{k_z}{\omega} \mathbf{e}_z \times \mathbf{E}_{\text{TEM}}(\mathbf{x}_t)$.

For an actual 2-D electrostatic problem [$\Phi(\mathbf{x}) = \Phi(\mathbf{x}_t)$], we have $\nabla_t^2 \Phi(\mathbf{x}_t) = 0$, which gives the full solution $\mathbf{E}_t(\mathbf{x}_t) = -\nabla_t \Phi(\mathbf{x}_t)$.

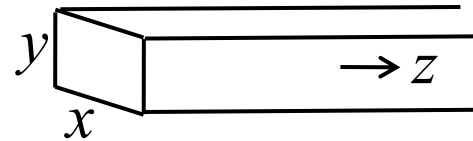
(ii) Note the difference between the scalar potential discussed here and those defined in electrostatics and electrodynamics.

$$\begin{cases} \mathbf{E}_{\text{TEM}}(\mathbf{x}_t) = -\nabla_t \Phi_{\text{TEM}}(\mathbf{x}_t), \text{ regard } \Phi_{\text{TEM}} \text{ as a mathematical tool.} \\ \mathbf{E}(\mathbf{x}) = -\nabla \Phi(\mathbf{x}) \text{ [electrostatics], regard } \Phi \text{ as a physical quantity.} \\ \mathbf{E}(\mathbf{x}, t) = -\nabla \Phi(\mathbf{x}, t) - \frac{\partial \mathbf{A}(\mathbf{x}, t)}{\partial t}, \text{ regard } \Phi \text{ and } \mathbf{A} \text{ as mathematical tools.} \end{cases}$$

Example 1: TE mode of a rectangular waveguide

Rewrite the basic equations for the TE mode:

$$\left\{ \begin{array}{l} (\nabla_t^2 + \gamma^2) H_z(\mathbf{x}_t) = 0 \text{ with boundary condition } \frac{\partial}{\partial n} H_z \Big|_s = 0 \quad (22) \\ \mathbf{H}_t(\mathbf{x}_t) = \pm \frac{ik_z}{\gamma^2} \nabla_t H_z(\mathbf{x}_t) \quad (22a) \\ \mathbf{E}_t(\mathbf{x}_t) = \mp \frac{\mu\omega}{k_z} \mathbf{e}_z \times \mathbf{H}_t(\mathbf{x}_t) = \mp Z_h \mathbf{e}_z \times \mathbf{H}_t(\mathbf{x}_t) \quad (22b) \\ \gamma^2 = \mu\epsilon\omega^2 - k_z^2 \quad (22c) \end{array} \right.$$



Rectangular geometry \Rightarrow Cartesian system $\Rightarrow \nabla_t^2 = \frac{\partial^2}{\partial x^2} + \frac{\partial^2}{\partial y^2}$

Hence, the wave equation in (22) becomes:

$$\left[\frac{\partial^2}{\partial x^2} + \frac{\partial^2}{\partial y^2} + \mu\epsilon\omega^2 - k_z^2 \right] H_z(x, y) = 0 \quad (24)$$

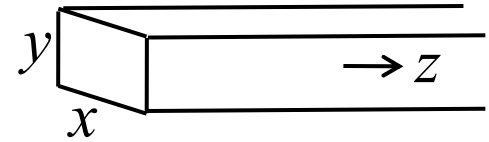
Rewrite (24):
$$\left[\frac{\partial^2}{\partial x^2} + \frac{\partial^2}{\partial y^2} + \mu\epsilon\omega^2 - k_z^2 \right] H_z(x, y) = 0 \quad (24)$$

Assuming $e^{ik_x x + ik_y y}$ dependence for $H_z(x, y)$, we obtain

$$\left[\mu\epsilon\omega^2 - k_x^2 - k_y^2 - k_z^2 \right] H_z(x, y) = 0$$

In order for $H_z(x, y) \neq 0$, we must have

$$\mu\epsilon\omega^2 - k_x^2 - k_y^2 - k_z^2 = 0,$$



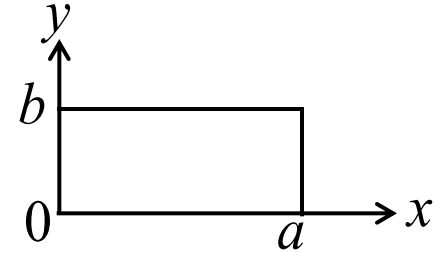
which is satisfied for $\pm k_x$, $\pm k_y$, $\pm k_z$. Since $(e^{ik_x x}, e^{-ik_x x})$, $(e^{ik_y y}, e^{-ik_y y})$, and $(e^{ik_z z}, e^{-ik_z z})$ are all linearly independent pairs, the full solution for H_z is

$$H_z(\mathbf{x}, t) = e^{-i\omega t} \left[A_1 e^{ik_x x} + A_2 e^{-ik_x x} \right] \left[B_1 e^{ik_y y} + B_2 e^{-ik_y y} \right] \cdot \left[C_+ e^{ik_z z} + C_- e^{-ik_z z} \right] \quad (25)$$

Applying boundary conditions [see (22)] to $H_z(\mathbf{x}, t)$ in (25):

$$H_z = e^{-i\omega t} \left[A_1 e^{ik_x x} + A_2 e^{-ik_x x} \right] \left[B_1 e^{ik_y y} + B_2 e^{-ik_y y} \right] \left[C_+ e^{ik_z z} + C_- e^{-ik_z z} \right]$$

$$\begin{cases} \frac{\partial}{\partial x} B_z(x=0) = 0 \Rightarrow ik_x A_1 - ik_x A_2 = 0 \Rightarrow A_1 = A_2 \\ \frac{\partial}{\partial y} B_z(y=0) = 0 \Rightarrow ik_y B_1 - ik_y B_2 = 0 \Rightarrow B_1 = B_2 \end{cases}$$



$$\Rightarrow H_z(\mathbf{x}, t) = \cos k_x x \cos k_y y \left[C_+ e^{-i\omega t + ik_z z} + C_- e^{-i\omega t - ik_z z} \right]$$

$$\begin{cases} \frac{\partial}{\partial x} B_z(x=a) = 0 \Rightarrow \sin k_x a = 0 \Rightarrow k_x = m\pi/a, \quad m = 0, 1, 2, \dots \\ \frac{\partial}{\partial y} B_z(y=b) = 0 \Rightarrow \sin k_y b = 0 \Rightarrow k_y = n\pi/b, \quad n = 0, 1, 2, \dots \end{cases}$$

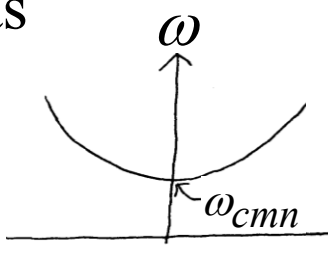
$$\Rightarrow H_z(\mathbf{x}, t) = \cos \frac{m\pi x}{a} \cos \frac{n\pi y}{b} \left[\underbrace{C_+ e^{ik_z z - i\omega t}}_{\text{forward wave}} + \underbrace{C_- e^{-ik_z z - i\omega t}}_{\text{backward wave}} \right] \quad (26)$$

Sub. $k_x = \frac{m\pi}{a}$, $k_y = \frac{n\pi}{b}$ into $\mu\epsilon\omega^2 - k_x^2 - k_y^2 - k_z^2 = 0$, we obtain

$$\mu\epsilon\omega^2 - k_z^2 - \pi^2 \left(\frac{m^2}{a^2} + \frac{n^2}{b^2} \right) = 0, \quad m, n = 0, 1, 2, \dots \quad (27)$$

Rewrite $\mu\varepsilon\omega^2 - k_z^2 - \pi^2\left(\frac{m^2}{a^2} + \frac{n^2}{b^2}\right) = 0$ [(27)] as

$$\mu\varepsilon\omega^2 - k_z^2 - \mu\varepsilon\omega_{cmn}^2 = 0 \quad [\text{for complex } \mu \text{ and } \varepsilon], \quad (28a)$$

where $\omega_{cmn} = \frac{\pi}{\sqrt{\mu\varepsilon}}\left(\frac{m^2}{a^2} + \frac{n^2}{b^2}\right)^{1/2}, \quad m, n = 0, 1, 2, \dots$  (28b)

(28) is the exact expression of the TE_{mn} mode dispersion relation for a rectangular waveguide with infinite wall conductivity and a uniform dielectric filling medium of (in general complex) ε and μ .

Each pair of (m, n) gives a normal mode (TE_{mn} mode) of the waveguide. The mode indices m and n cannot both be 0, because that will make the denominator in (22a) vanish.

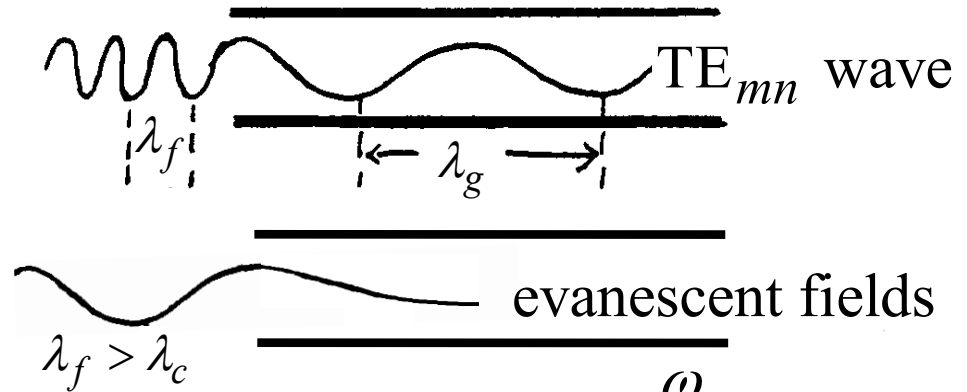
Special case: Unfilled waveguide (i.e. $\varepsilon = \varepsilon_0$ and $\mu = \mu_0$)

We have $\mu\varepsilon = \mu_0\varepsilon_0 = \frac{1}{c^2}$, and (28a,b) can be written

$$\omega^2 - k_z^2 c^2 - \omega_{cmn}^2 = 0 \quad [\text{for unfilled waveguide}], \quad (29a)$$

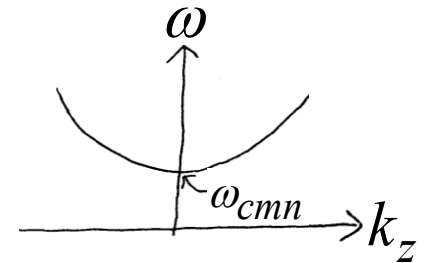
where $\omega_{cmn} = \pi c \left(\frac{m^2}{a^2} + \frac{n^2}{b^2}\right)^{1/2}, \quad m, n = 0, 1, 2, \dots$ (29b)

Rewrite
$$\begin{cases} \omega^2 - k_z^2 c^2 - \omega_{cmn}^2 = 0 \\ \omega_{cmn} = \pi c \left(\frac{m^2}{a^2} + \frac{n^2}{b^2} \right)^{\frac{1}{2}} \end{cases}$$



Definitions and terminology:

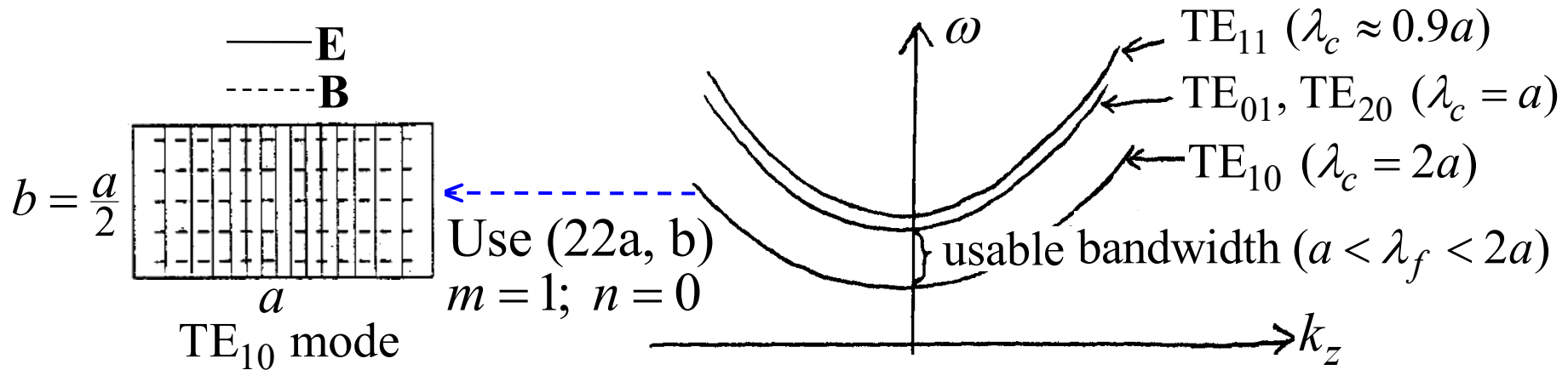
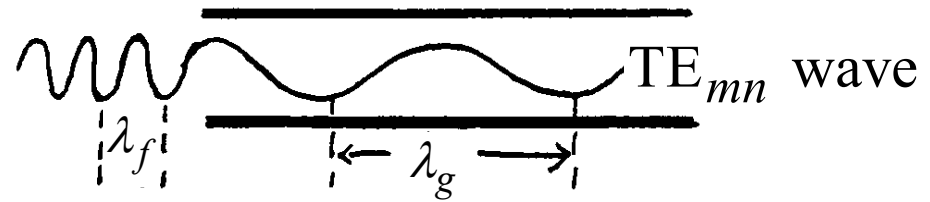
$$\begin{cases} \omega > \omega_{cmn} \Rightarrow k_z = \text{real} \Rightarrow \text{propagating waves} \\ \omega < \omega_{cmn} \Rightarrow k_z = \text{imaginary} \Rightarrow \text{evanescent fields.} \end{cases}$$



$$\begin{cases} \lambda_f = \text{free space wavelength} \equiv \frac{2\pi c}{\omega} \left[\begin{array}{l} \text{wavelength of an EM} \\ \text{wave in free space} \end{array} \right] \\ \lambda_g = \text{guide wavelength} \equiv \frac{2\pi}{k_z} \left[\begin{array}{l} \text{wavelength of the TE}_{mn} \\ \text{wave in the waveguide} \end{array} \right] \end{cases}$$

$$\begin{cases} \omega_{cmn} = \text{cutoff frequency} \left[\begin{array}{l} \text{lowest } \omega \text{ allowed to enter the waveguide} \\ \text{as a TE}_{mn} \text{ wave, i.e. when } k_z = 0 \text{ } (\lambda_g = \infty) \end{array} \right] \\ \lambda_c = \text{cutoff wavelength} \equiv \frac{2\pi c}{\omega_{cmn}} \left[\begin{array}{l} \text{longest } \lambda_f \text{ allowed to enter the} \\ \text{waveguide as a TE}_{mn} \text{ wave} \end{array} \right] \end{cases}$$

Rewrite
$$\begin{cases} \omega^2 - k_z^2 c^2 - \omega_{cmn}^2 = 0 \\ \omega_{cmn} = \pi c \left(\frac{m^2}{a^2} + \frac{n^2}{b^2} \right)^{\frac{1}{2}} \\ \lambda_f = \frac{2\pi c}{\omega} \quad [\text{wavelength of an EM wave in free space}] \\ \lambda_g = \frac{2\pi}{k_z} \quad [\text{wavelength of the TE}_{mn} \text{ wave in the waveguide}] \\ \lambda_c = \frac{2\pi c}{\omega_{cmn}} \quad \left[\begin{array}{l} \text{longest } \lambda_f \text{ allowed to enter the waveguide} \\ \text{as a TE}_{mn} \text{ wave} \end{array} \right] \end{cases}$$



Question 1: Why a typical waveguide has $a = 2b$? (discussed below)

Question 2: Can we use a waveguide to transport waves at 60 Hz?

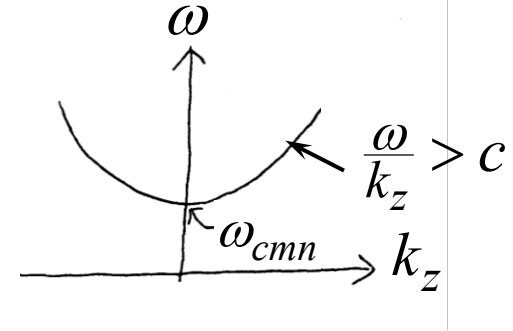
Other quantities of interest:

(1) Rewrite (29a): $\omega^2 - k_z^2 c^2 - \omega_{cmn}^2 = 0$ [for unfilled waveguide]

$$\Rightarrow v_{ph} = \frac{\omega}{k_z} > c \quad [\text{phase velocity}]$$

$$\frac{d}{dk_z} (29a) \Rightarrow 2\omega \frac{d\omega}{dk_z} - 2k_z c^2 = 0$$

$$\Rightarrow v_g = \frac{d\omega}{dk_z} = \frac{k_z c^2}{\omega} \quad [\text{group velocity}]$$



$$\Rightarrow \text{(i) } v_g < c; \quad \text{(ii) } v_{ph} v_g = c^2; \quad \text{(iii) } \begin{cases} v_{ph} \rightarrow \infty \text{ as } \omega \rightarrow \omega_{cmn} \\ v_g \rightarrow 0 \text{ as } \omega \rightarrow \omega_{cmn} \end{cases}$$

(2) The remaining field components (E_x , E_y , H_x , and H_y) can be obtained from $H_z(x, y)$ through

$$\mathbf{H}_t(x, y) = \pm \frac{ik_z}{\gamma^2} \nabla_t H_z(x, y) \quad \left[\gamma^2 = \mu_0 \epsilon_0 \omega^2 - k_z^2 = \frac{\omega_{cmn}^2}{c^2} \right] \quad (22a)$$

$$\mathbf{E}_t(x, y) = \mp \frac{\mu \omega}{k_z} \mathbf{e}_z \times \mathbf{H}_t(x, y) \quad \left[\text{see (22c) and (29).} \right] \quad (22b)$$

Note: The upper (lower) sign \Rightarrow forward (backward) wave. We have assumed $\text{Re}[k_z] > 0$. Since there is no loss, k_z is a real positive number.

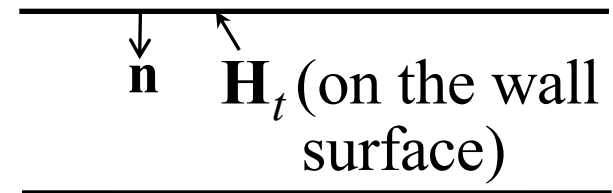
(3) Wall current

There are currents in the conductor flowing within a skin depth. When we apply boundary conditions to calculate the fields, effects of the wall currents are automatically accounted for

The wall current is given by

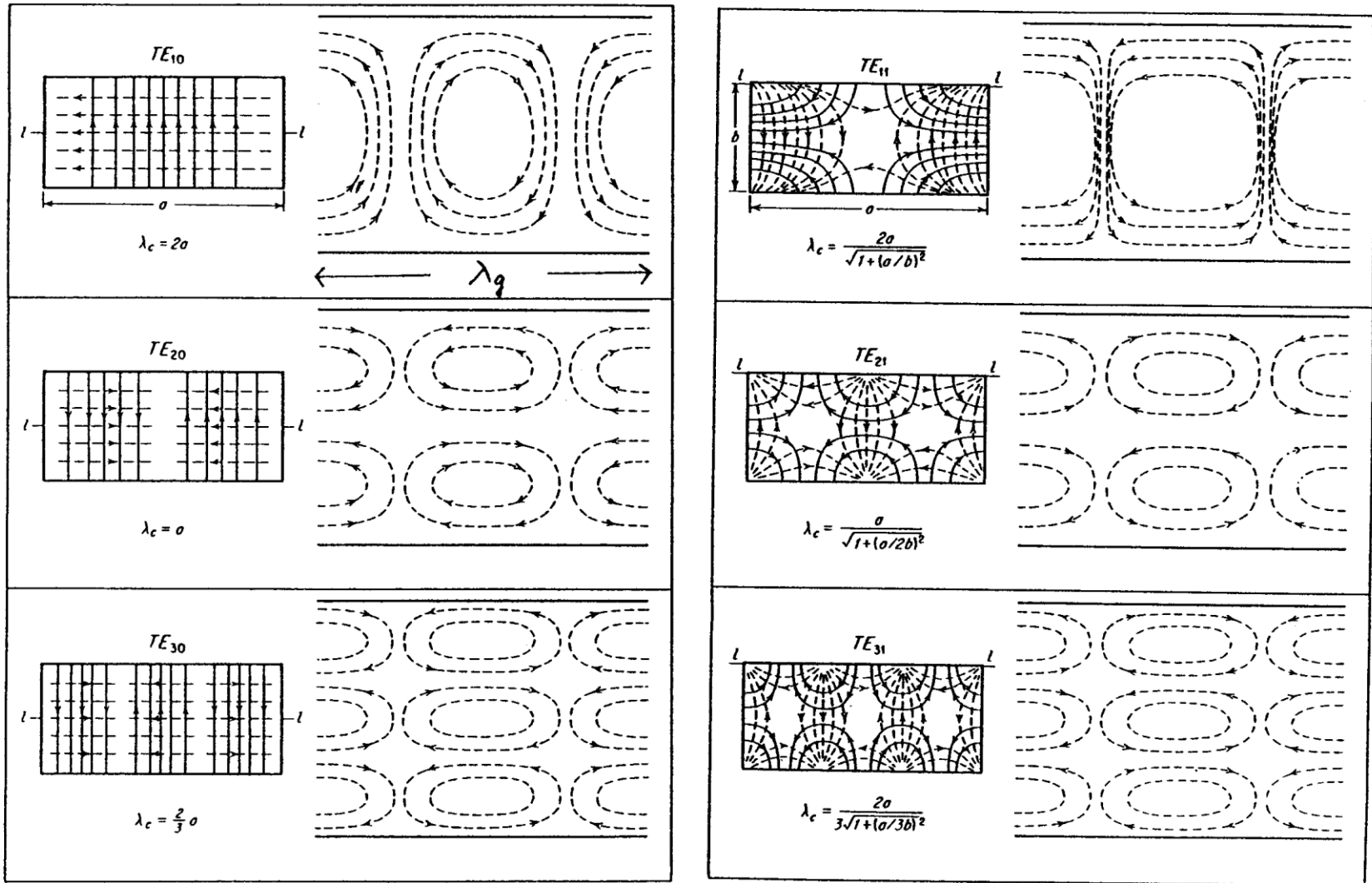
$$\mathbf{J}_s = \mathbf{n} \times \mathbf{H}_t \text{ (on the wall surface)}$$

[See lecture notes, Ch. 2, Eq. (29)
or Jackson Eq. (8.14)]



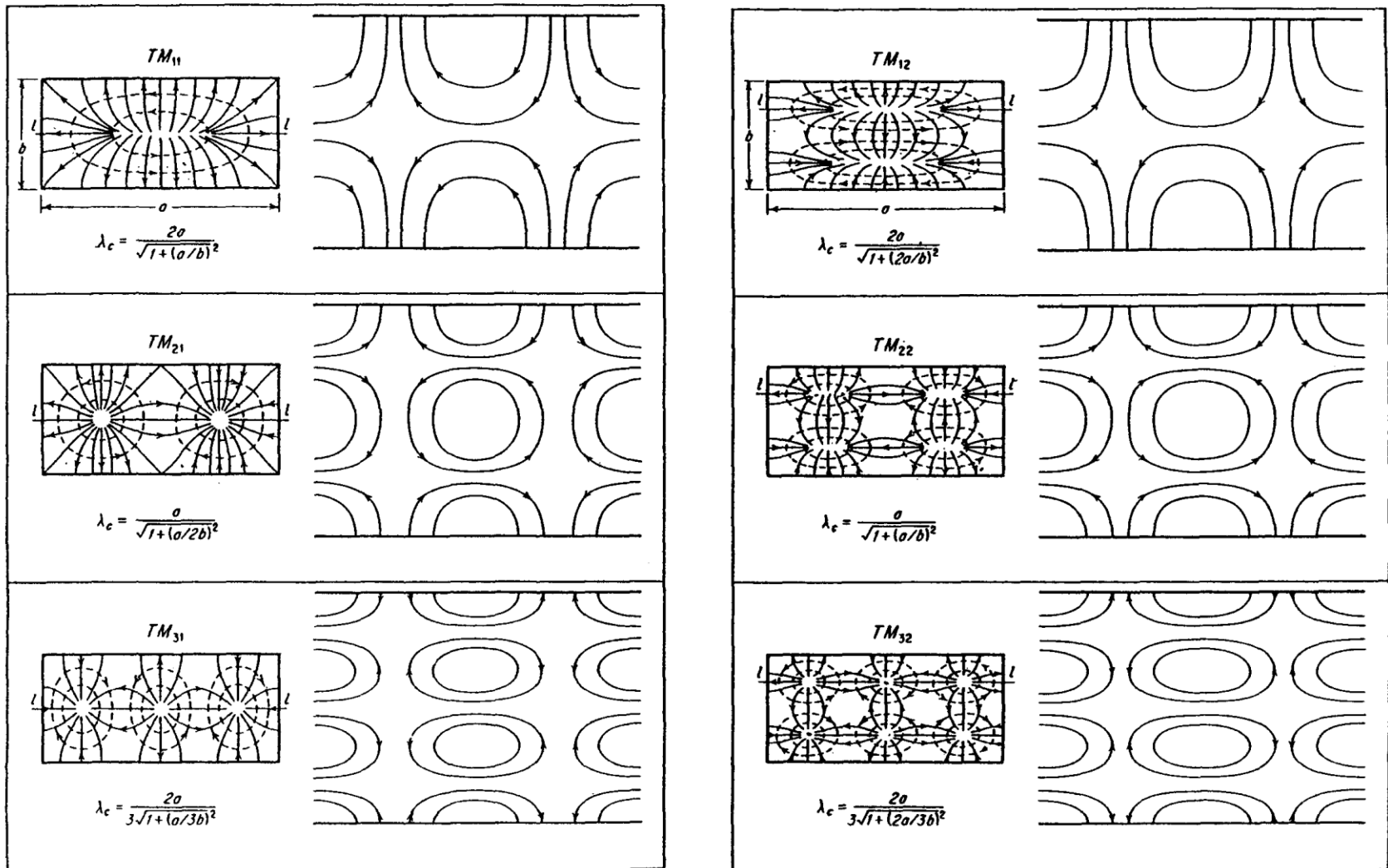
For infinite conductivity, the skin depth is zero. Hence, the wall current is a surface current.

TE mode field patterns of rectangular waveguide



from E. L. Ginzton, "Microwave measurements". λ_c : cutoff frequency
 solid curve: **E**-field lines; dashed curves: **B**-field lines

TM mode field patterns of rectangular waveguide

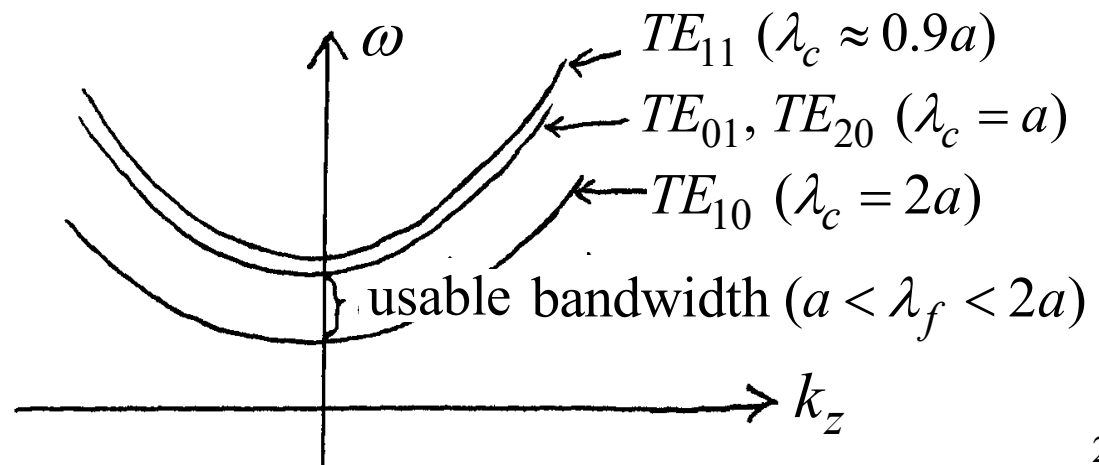
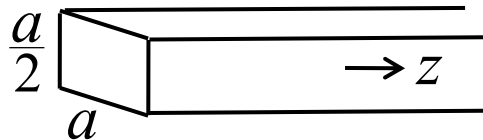


from E. L. Ginzton, "Microwave measurements". λ_c : cutoff frequency
 solid curve: **E**-field lines; dashed curves: **B**-field lines

Discussion: waveguide and microwaves

If $b \leq \frac{1}{2}a$, there is a maximum usable bandwidth ($a < \lambda_f < 2a$) over which only the TE_{10} mode can propagate (no mode conversion). A typical waveguide has $b = \frac{1}{2}a$ for maximum power capability & usable bandwidth. Microwaves are normally transported by the TE_{10} mode in the usable bandwidth. Waveguides come in different sizes. Usable bandwidths of practical waveguide dimensions ($0.1 \text{ cm} < a < 100 \text{ cm}$) cover the entire microwave band (300 MHz to 300 GHz).

The waveguide is capable of handling much higher power than the coaxial transmission lines. In a high-power radar system, for example, it is used to transport microwaves from the generator to the antenna.



Some Standard Size Waveguides

Guide	Size (inch)	Rec. (GHz)	f_c (GHz)	Band	(GHz)
WR650	6.500×3.250	1.12 - 1.70	0.91	<i>L</i>	(1.0 - 2.0)
WR284	2.840×1.340	2.60 - 3.95	2.08	<i>S</i>	(2.0 - 4.0)
WR187	1.872×0.872	3.95 - 5.85	3.15	<i>C</i>	(4.0 - 8.0)
WR90	0.900×0.400	8.20 - 12.40	6.56	<i>X</i>	(8.0 - 12.0)
WR62	0.622×0.311	12.40 - 18.00	9.49	<i>Ku</i>	(12.0 - 18.0)
WR42	0.420×0.170	18.00 - 26.50	14.05	<i>K</i>	(18.0 - 27.0)
WR28	0.280×0.140	26.50 - 40.00	21.08	<i>Ka</i>	(27.0 - 40.0)

Whittum, D.H. (1999). Introduction to Microwave Linacs. In: Ferbel, T. (eds) Techniques and Concepts of High Energy Physics X. NATO Science Series, vol 534. Springer.



TM Waves in a Circular Waveguides

Consider TM waves of a circular waveguide in vacuum with inner diameter :

$$[\nabla_t^2 + \gamma^2]E_z = 0$$

$$\nabla_t^2 = \frac{1}{\rho} \frac{\partial}{\partial \rho} \left(\rho \frac{\partial}{\partial \rho} \right) + \frac{1}{\rho^2} \frac{\partial^2}{\partial \phi^2}$$

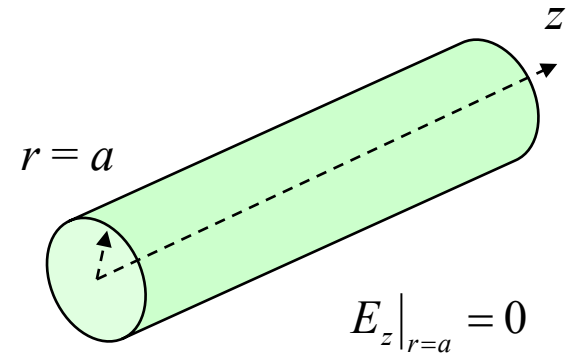
Solutions for E_z are:

$$E_z(\rho, \phi) = \hat{E}_z J_m(\gamma_{mn} \rho) e^{\pm im\phi} e^{-j(k_z z - \omega t)}$$

and the corresponding eigenvalues are:

$$\gamma_{mn} = \sqrt{\mu \epsilon \omega_{mn}^2} = \frac{x_{nm}}{a}$$

ω_{mn} are the cutoff frequency of the TM_{mn} waveguide modes,
 x_{nm} are the roots of the Bessel function



no. of roots	$J_0(x)$	$J_1(x)$	$J_2(x)$
1	2.4048	3.8317	5.1356
2	5.5201	7.0156	8.4172
3	8.6537	10.1735	11.6198

Field Theory of Guided Waves – 2. Modes in Cavities

We consider the example of a rectangular cavity (i.e. a rectangular waveguide with two ends closed by conductors), for which we have two additional boundary conditions at the ends: $z = 0$ and d .

$$\text{Rewrite (27): } H_z = \cos \frac{m\pi x}{a} \cos \frac{n\pi y}{b} \left[C_+ e^{ik_z z - i\omega t} + C_- e^{-ik_z z - i\omega t} \right]$$

$$\text{b.c. (i): } H_z(z = 0) = 0 \Rightarrow C_+ = -C_-$$

$$\Rightarrow H_z = H_{z0} e^{-i\omega t} \cos \frac{m\pi x}{a} \cos \frac{n\pi y}{b} \sin k_z z$$

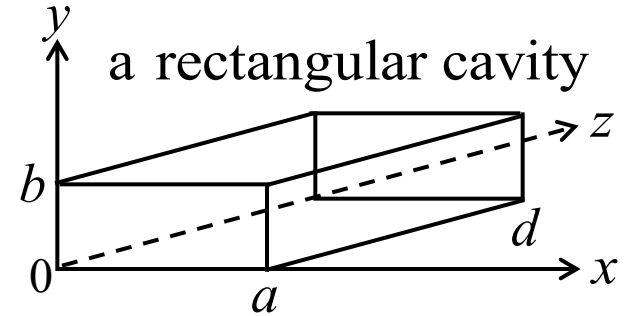
$$\text{b.c. (ii): } H_z(z = d) = 0$$

$$\Rightarrow \sin k_z d = 0 \Rightarrow k_z = \frac{l\pi}{d}, \quad l = 1, 2, \dots \quad (32)$$

$$\Rightarrow H_z = H_{z0} e^{-i\omega t} \cos \frac{m\pi x}{a} \cos \frac{n\pi y}{b} \sin \frac{l\pi z}{d}, \quad \left[\begin{array}{l} m, n = 0, 1, 2, \dots \\ l = 1, 2, \dots \end{array} \right] \quad (33)$$

$$\text{Sub. (32) into } \omega^2 - k_z^2 c^2 - \omega_{cmn}^2 = 0, \text{ where } \omega_{cmn} = \pi c \left(\frac{m^2}{a^2} + \frac{n^2}{b^2} \right)^{\frac{1}{2}}$$

$$\Rightarrow \omega = \omega_{mnl} = \pi c \left(\frac{m^2}{a^2} + \frac{n^2}{b^2} + \frac{l^2}{d^2} \right)^{1/2} \left[\begin{array}{l} \omega_{mnl} : \text{resonant frequency} \\ \text{of the TE}_{mnl} \text{ mode} \end{array} \right] \quad (34)$$



TM Modes in a Cylindrical Cavity

$$E_z = \hat{E}_z J_m(k_{mn}r) \cos m\theta \cos k_l z e^{j\omega t}$$

$$E_r = -\frac{jk_l}{k_{mn}} \hat{E}_z J'_m(k_{mn}r) \cos m\theta \sin k_l z e^{j\omega t}$$

$$E_\theta = -\frac{k_l m}{k_{mn}^2 r} \hat{E}_z J_m(k_{mn}r) \sin m\theta \sin k_l z e^{j\omega t}$$

$$B_r = \frac{\omega m}{k_{mn}^2 c r} \hat{E}_z J_m(k_{mn}r) \sin m\theta \cos k_l z e^{j\omega t}$$

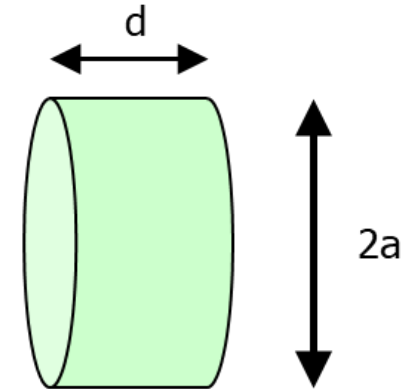
$$B_\theta = \frac{j\omega}{k_{mn} c} \hat{E}_z J'_m(k_{mn}r) \cos m\theta \cos k_l z e^{j\omega t}$$

$$B_z = 0$$

where $k_l = l\pi / d$ $l = 0, 1, 2, \dots$ and $k_{mn} = \frac{\omega_{mn}}{c} = \frac{x_{mn}}{a}$ ↪ the n^{th} zero of $J_m(x)$

$$f_{mnl} = \frac{c}{2\pi} \sqrt{\left(\frac{l\pi}{d}\right)^2 + \left(\frac{x_{mn}}{a}\right)^2}$$

for TM₀₁-modes $x_{01}=2.405$



End wall b.c. : $E_r = E_\theta = 0$, at $z = 0, d$

Side wall b.c. : $E_z = 0$, at $r = a$

TE Modes in a Cylindrical Cavity

$$B_z = \hat{B}_z J_m(k_{mn}r) \cos m\theta \sin k_l z e^{j\omega t}$$

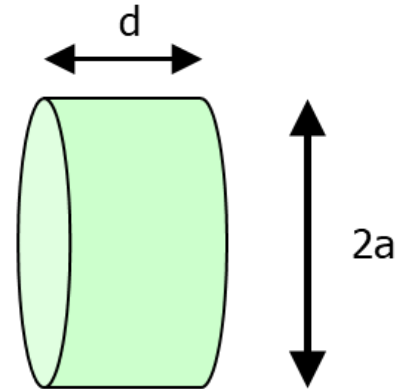
$$B_r = \frac{k_l}{k_{mn}} \hat{B}_z J'_m(k_{mn}r) \cos m\theta \cos k_l z e^{j\omega t}$$

$$B_\theta = -\frac{k_l m}{k_{mn}^2 r} \hat{B}_z J_m(k_{mn}r) \sin m\theta \cos k_l z e^{j\omega t}$$

$$E_r = \frac{j\omega m}{k_{mn}^2 c r} \hat{B}_z J_m(k_{mn}r) \sin m\theta \sin k_l z e^{j\omega t}$$

$$E_\theta = \frac{j\omega}{k_{mn} c} \hat{B}_z J'_m(k_{mn}r) \cos m\theta \sin k_l z e^{j\omega t}$$

$$E_z = 0$$



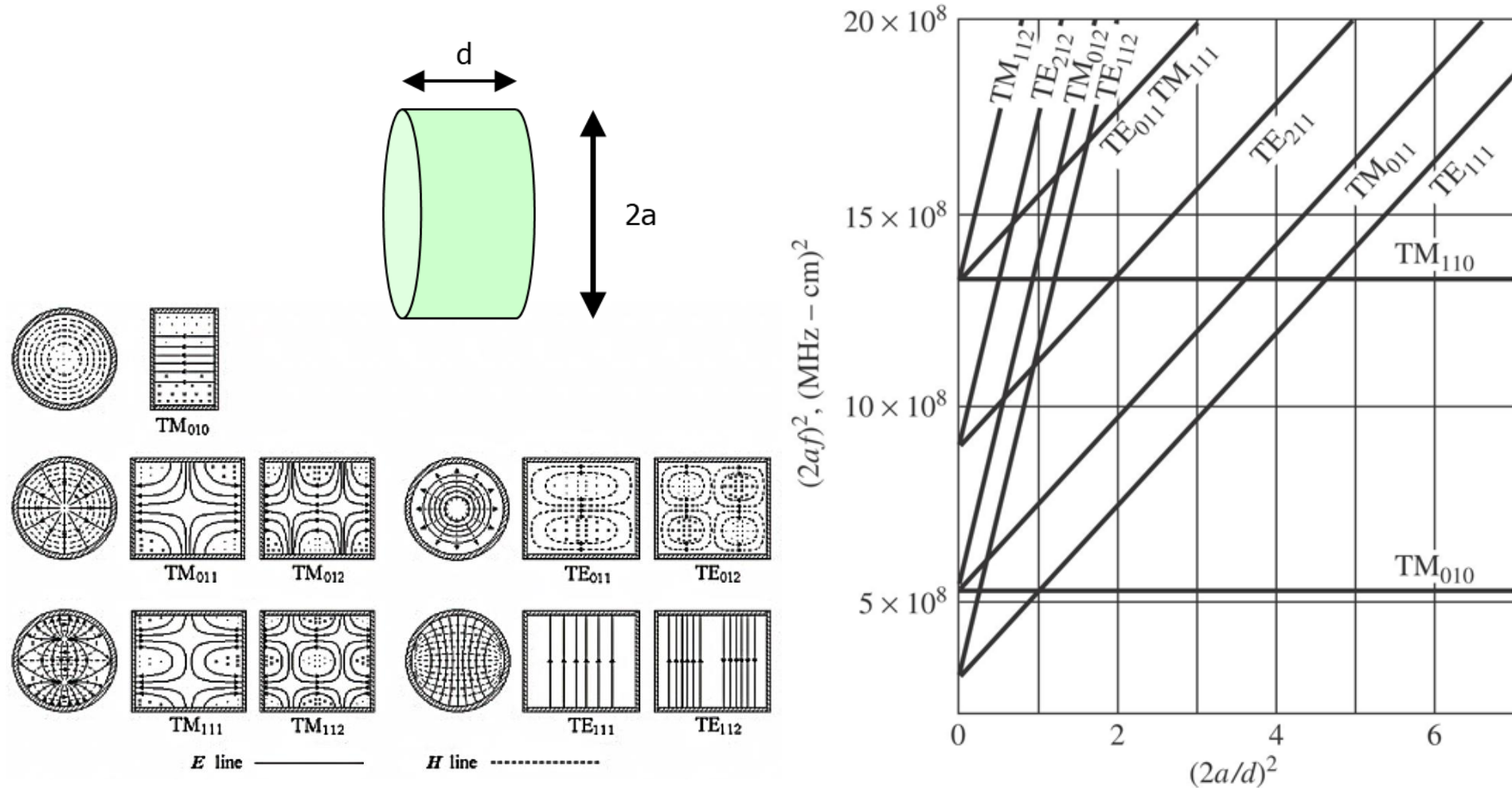
End wall b.c. : $B_z = 0$, at $z = 0, d$

Side wall b.c. : $\partial B_z / \partial B_r = 0$, at $r = a$

where $k_l = l\pi / d$ $l = 0, 1, 2, \dots$ and $k_{mn} = x'_{mn} / a$ ↘ the n^{th} zero of $J'_m(x)$

$$f_{mnl} = \frac{c}{2\pi} \sqrt{\left(\frac{l\pi}{d}\right)^2 + \left(\frac{x_{mn}}{a}\right)^2}$$

Higher Order Modes for a Cylindrical Cavity



Cavity Power Loss and Q

Definition of Q : Waves *propagates* in a waveguide. Hence, its attenuation is represented by a complex k_z . Since fields are *stored* in a cavity, any loss results in damping in time. The damping is then represented by a complex ω . We consider only the wall loss for now.

Assume fields at any point in the cavity have the time dependence:

$$E(t) = \begin{cases} E_0 e^{-i\omega_0 t}, & \sigma = \infty \\ E_0 e^{-i(\omega_0 + \Delta\omega - i\frac{\omega_0}{2Q})t} = E_0 e^{-i(\omega_0 + \Delta\omega)t - \frac{\omega_0}{2Q}t}, & \sigma \neq \infty \end{cases} \quad (8.88)$$

where ω_0 is the resonant frequency [e.g. (34)] without the wall loss.

(8.88) assumes that the wall loss modifies ω_0 by a small real part $\Delta\omega$ and a small imaginary part $\frac{\omega_0}{2Q}$, where $\Delta\omega$ and Q are to be determined.

Physical reason for $\Delta\omega$: Effective cavity size increases by $\sim \delta$ (skin depth). A larger cavity has a lower frequency. Hence, $\Delta\omega < 0$.

Physical reason for Q : Ohmic dissipation on the wall

$$U = \text{stored energy in the cavity} \left[\propto |E|^2 \propto e^{-i\omega t} \cdot e^{i\omega^* t} = e^{2\omega_i t} = e^{-\frac{\omega_0 t}{Q}} \right]$$

$$= U_0 e^{-\frac{\omega_0 t}{Q}}$$

$$\Rightarrow \frac{dU}{dt} = -\frac{\omega_0}{Q} U \quad [\text{power loss}]$$

$$\mathbf{E}(t) = E_0 e^{-i(\omega_0 + \Delta\omega)t - \frac{\omega_0}{2Q}t}$$

$$\Rightarrow \omega_i = -\frac{\omega_0}{2Q}$$
(8.87)

$$\Rightarrow Q = \omega_0 \frac{\text{stored energy}}{\text{power loss}} \quad [\text{time-space definition of } Q] \quad (8.86)$$

(8.88) represents a damped oscillation which does not have a single frequency. To examine the frequency of $E(t)$, we write

$$E(t) = \frac{1}{\sqrt{2\pi}} \int_{-\infty}^{\infty} E(\omega) e^{-i\omega t} d\omega,$$

where

Use (8.88), assume $E(t) = 0$ for $t < 0$

$$E(\omega) = \frac{1}{\sqrt{2\pi}} \int_{-\infty}^{\infty} E(t) e^{i\omega t} dt = \frac{1}{\sqrt{2\pi}} E_0 \int_0^{\infty} e^{-\frac{\omega_0}{2Q}t + i(\omega - \omega_0 - \Delta\omega)t} dt$$

$$= \frac{1}{\sqrt{2\pi}} \frac{E_0}{-i(\omega - \omega_0 - \Delta\omega) + \frac{\omega_0}{2Q}}$$

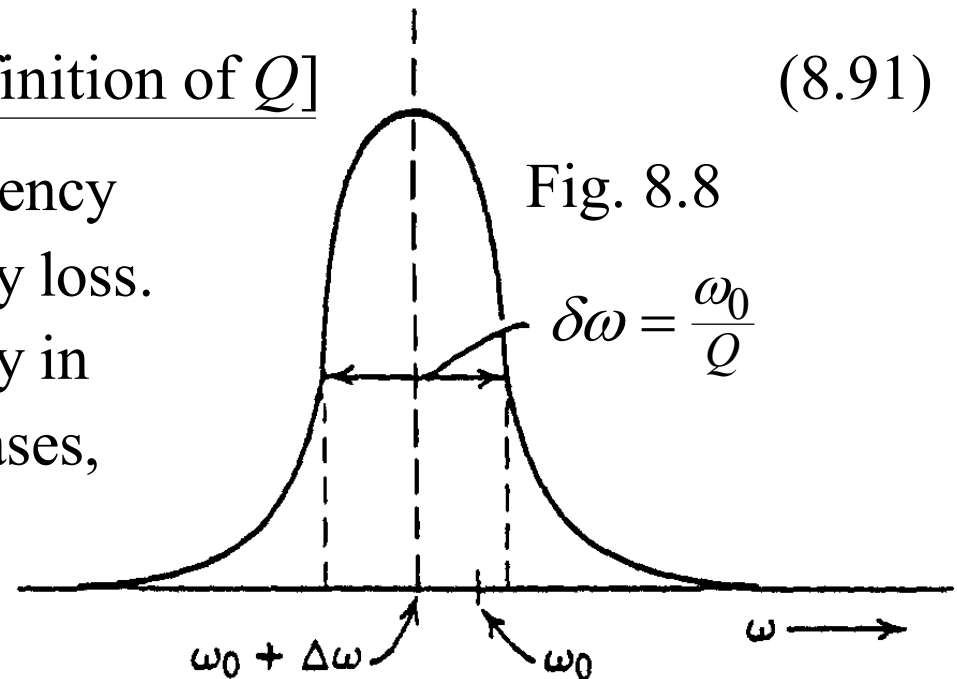
The frequency spectrum is best seen from the field energy distribution in ω -space

$$|E(\omega)|^2 \propto \frac{1}{(\omega - \omega_0 - \Delta\omega)^2 + (\frac{\omega_0}{2Q})^2} = \begin{cases} \text{max, } \omega = \omega_0 + \Delta\omega \\ \frac{1}{2} \text{ max, } \omega = \omega_0 + \Delta\omega \pm \frac{\omega_0}{2Q} \end{cases} \quad (8.90)$$

$$\Rightarrow \delta\omega = \left[\begin{array}{l} \text{full width at} \\ \text{half-maximum points} \end{array} \right] = \frac{\omega_0}{Q}$$

$$\Rightarrow Q = \frac{\omega_0}{\delta\omega} \quad [\text{frequency-space definition of } Q] \quad (8.91)$$

Note: ω_0 is the resonant frequency of the cavity in the absence of any loss. $\omega_0 + \Delta\omega$ is the resonant frequency in the presence of losses. In most cases, the difference is insignificant.



Physical Interpretation of Q :

(i) Use the time-space definition: $Q = \omega_0 \frac{\text{stored energy}}{\text{power loss}}$

$$\omega_0 = 2\pi f_0 = \frac{2\pi}{\tau_0} \leftarrow \text{wave period}$$

$$\frac{\text{stored energy}}{\text{power loss}} \approx \tau_d \leftarrow \text{decay time of stored energy}$$

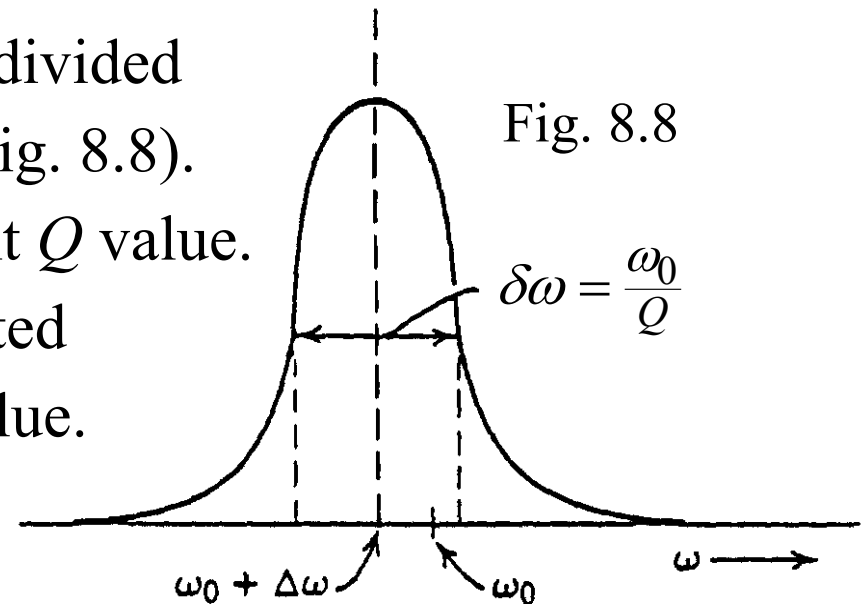
$$\Rightarrow Q = \omega_0 \frac{\text{stored energy}}{\text{power loss}} \approx 2\pi \frac{\tau_d}{\tau_0} \quad (48)$$

(48) shows that Q , which results from the power loss, is approximately 2π times the number of oscillations during the decay time. A larger Q value implies that the field energy can be stored in the cavity for a longer time. Hence, Q is commonly referred to as the quality factor. However, in some cases such as high-power microwave generation, a low Q value may often be desired. This is arranged not by increasing the Ohmic loss, but by a structure which couples the wave out of the cavity.

(ii) Use the frequency-space definition: $Q = \frac{\omega_0}{\delta\omega}$ (see Fig. 8.8)

For a lossy cavity, a resonant mode can be excited not just at one frequency (as is the case with a lossless cavity) but at a range of frequencies ($\delta\omega$). The resonant frequency ($\omega_0 + \Delta\omega$, see Fig. 8.8) of a lossy cavity is the frequency at which the cavity can be excited with the largest inside-field amplitude, given the same source power. The resonant width $\delta\omega$ of a mode is equal to the resonant frequency divided by the Q value of that mode (see Fig. 8.8). Note that each mode has a different Q value.

Figure 8.8 can be easily generated in experiment to measure the Q value.



$$Q = \omega_0 \frac{\text{stored energy}}{\text{power loss}}$$

Using the results of Sec. 8.1, we can calculate Q (but not $\Delta\omega$) due to the ohmic loss. We first calculate the zero order \mathbf{E} and \mathbf{H} of a specific cavity assuming $\sigma = \infty$, then use the zero order \mathbf{E} and \mathbf{H} to calculate U and power loss,

$$\text{stored energy} = \int_V (w_e + w_m) d^3x = \begin{cases} 2 \int_V w_e d^3x = \frac{\epsilon}{2} \int_V |\mathbf{E}|^2 d^3x \\ 2 \int_V w_m d^3x = \frac{\mu}{2} \int_V |\mathbf{H}|^2 d^3x \end{cases}$$

$$\text{power loss} \stackrel{(8.15)}{=} \frac{1}{2\sigma\delta} \oint_S |\mathbf{J}_s|^2 da$$

$$\stackrel{(8.14)}{=} \frac{1}{2\sigma\delta} \oint_S |\mathbf{n} \times \mathbf{H}|^2 da$$

$$\stackrel{(6.133)}{=}$$

Formulae for Q (due to ohmic loss) for rectangular and cylindrical cavities can be found in Collin, p. 503 and p. 506.

Q due to Other Types of Losses :

If there are several types of power losses in a cavity (e.g. due to a lossy filling medium or leakage through a coupling structure), Q can be expressed as

$$Q = \omega_0 \frac{\text{stored energy}}{\sum_n (\text{power loss})_n} \quad (49)$$

$$\Rightarrow \frac{1}{Q} = \sum_n \frac{1}{Q_n} \quad (50)$$

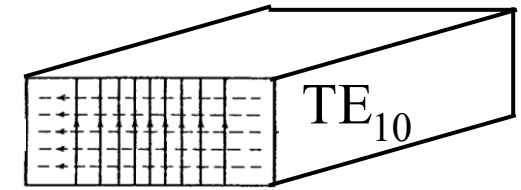
n-th type of power loss

where Q_n (Q due to the n -th type of power loss) is given by

$$Q_n = \omega_0 \frac{\text{stored energy}}{(\text{power loss})_n}$$

Parameters of an Open-End Cavity

In Ch. 3, we analyzed a simple, fully closed (ideal) cavity. The modes are standing waves, each characterized by a resonant frequency (ω_0) and a quality factor (Q , due to power losses).



An ideal cavity

In reality, a cavity is always connected to the outside in some way. Furthermore, it often has a complex shape to optimize its function.

Fig. 1 shows a commonly used cavity. It has a narrow channel for charged particles (but not waves) to pass through, and is shaped for the electric field to concentrate around a narrow gap, where the field either absorbs the electron energy (as in the klystron) or delivers energy to electrons or ions (as in an acceleration cavity). In this chapter, we put our focus on this type of cavity. However, the theory is general to all cavities.

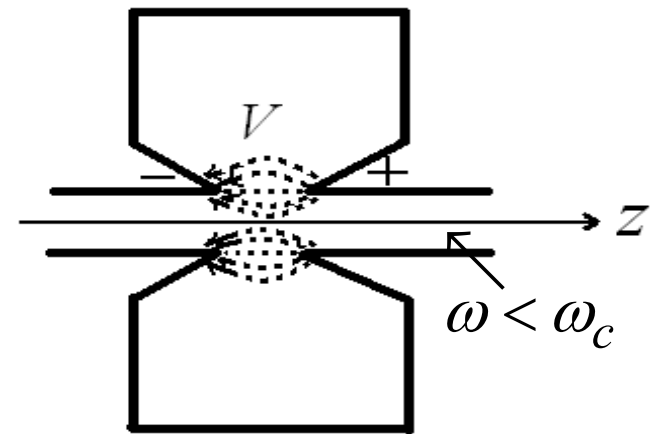


Fig. 1. An open-end cavity.

Gap Voltage and Shunt Impedance:

Assume a mode is present in the cavity in Fig. 1, the voltage difference across the gap is a parameter of interest.

Define the gap voltage V as

$$V \equiv -\int_a^b E_z(z) dz \quad [\text{Gap voltage}],$$

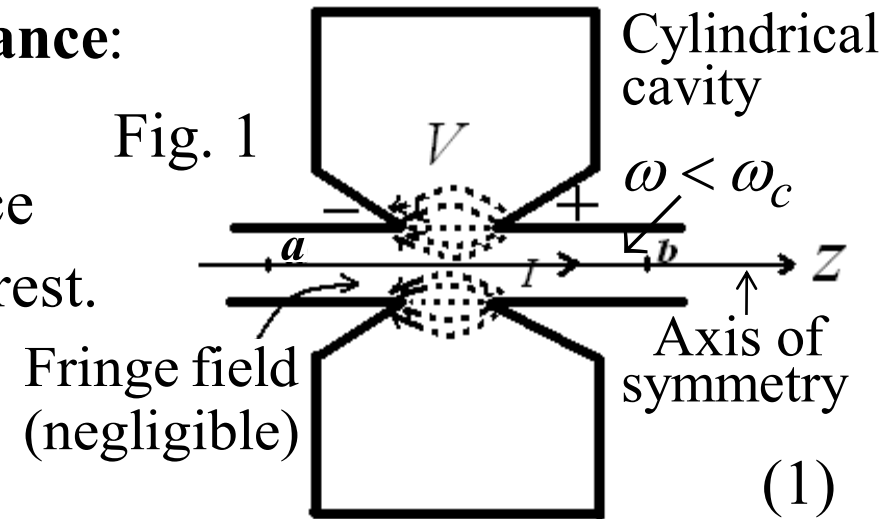
where the integration is along the z -axis.

Question: Can there be a voltage difference on the same conductor?

In (1), V and E_z are phasors (ω -space complex quantities), i.e. in t -space, we have $V(t) = \text{Re}[Ve^{j\omega t}]$ and $E_z(z, t) = \text{Re}[E_z(z)e^{j\omega t}]$.

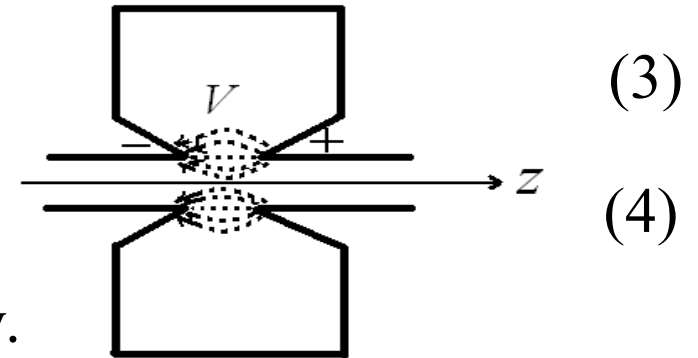
When V is defined as in (1), the reference polarity [direction of positive $V(t)$] is shown in Fig. 1. Let P_{loss} be the total power loss in the cavity (e.g. Ohmic loss). In terms of V and P_{loss} , we define a

shunt impedance as $R \equiv \frac{|V|^2}{2P_{\text{loss}}} \quad [\text{Shunt impedance}] \quad (2) \quad 43$



V and R are two new parameters not applicable to a fully closed cavity. On the other hand, the quality factor Q are defined in two consistent ways as for a closed cavity (Lecture Notes, Ch. 3, Sec. 4):

$$\begin{cases} Q = \frac{\omega_0 W_f}{P_{loss}} & [t\text{-space definition}] \\ Q = \frac{\omega_0}{\delta\omega} & [\omega\text{-space definition}] \end{cases} \quad (3)$$



where W_f is the field energy in the cavity.

Parameters V , R , and Q each gives a key property of the cavity:

1. The gap voltage V ($= -\int_a^b E_z(z)dz$) gives the maximum energy a charged particle can gain or lose in passing through the cavity.

2. Assume an RF power (P) is injected into a cavity to set up a gap voltage V . In the steady state, P is lost in the cavity. So, we have $P = P_{loss}$ and hence $R = |V|^2 / (2P_{loss}) = |V|^2 / (2P)$. Thus, R gives the magnitude of the gap voltage $|V|$ for a given input power P .

3. The Q factor gives the resonant bandwidth $\delta\omega$ through (4).

Transit Time Factor:

In an accelerator, the RF power is fed into the acceleration cavity to maintain a gap voltage. For simplicity, we assume that the electric field in the gap is uniform over a distance d and zero elsewhere (Fig. 2),

$$E_z(z) = \begin{cases} E_g, & -d \leq z \leq 0 \\ 0, & \text{otherwise} \end{cases} \quad (5)$$

Thus, the electric field is

$$E_z(z, t) = \text{Re}[E_z(z)e^{j\omega t}] = \begin{cases} E_g \cos \omega t & -d \leq z \leq 0 \\ 0, & \text{otherwise} \end{cases} \quad (6)$$

Assuming that an electron has a constant velocity $v_0 \mathbf{e}_z$ and it passes the middle plane ($z = -\frac{d}{2}$) at time t_1 , we can write its orbit as

$$z = -\frac{d}{2} + v_0(t - t_1) \quad (7)$$

or t as a function of the electron position z : $t = t_1 + \frac{z}{v_0} + \frac{d}{2v_0}$ (8)

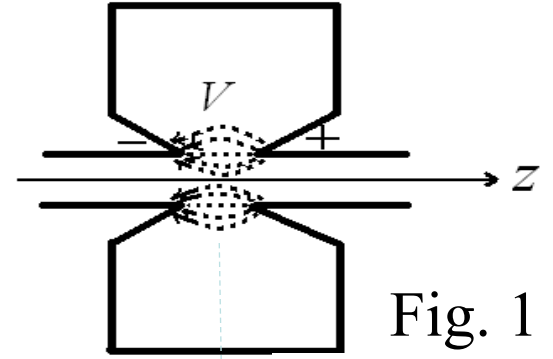


Fig. 1

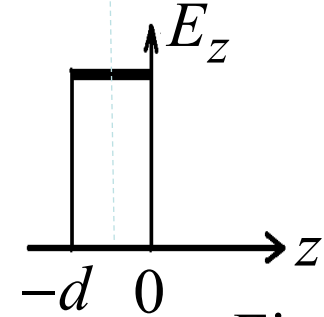


Fig. 2

Parameters of an Open-End Cavity (continued)

Rewrite
$$\begin{cases} E_z(z, t) = \begin{cases} E_g \cos \omega t & -d \leq z \leq 0 \\ 0, & \text{otherwise} \end{cases} \end{cases} \quad (6)$$

$$\begin{cases} t = \frac{z}{v_0} + \frac{d}{2v_0} + t_1 \end{cases} \quad (8)$$

Sub. (8) for t in (6), we obtain the gap electric field E_z seen by a charged particle:

$$E_z(\text{on particle}) = \begin{cases} E_g \cos\left[\frac{\omega}{v_0}\left(z + \frac{d}{2} + v_0 t_1\right)\right], & -d \leq z \leq 0 \\ 0, & \text{otherwise} \end{cases} \quad (9)$$

Thus, due to the time variation of $E_z(z, t)$ during the particle's passage time, the particle does not see a constant E_z , although E_z in the gap is spatially uniform at any instant of time.

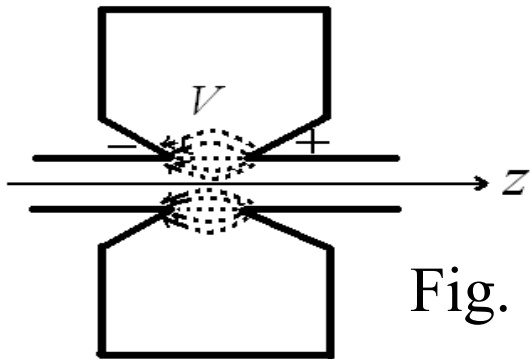


Fig. 1

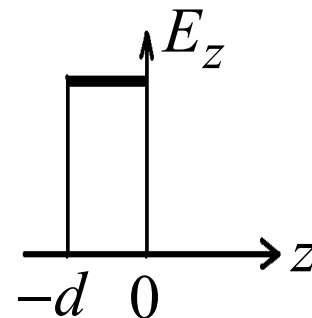


Fig. 2

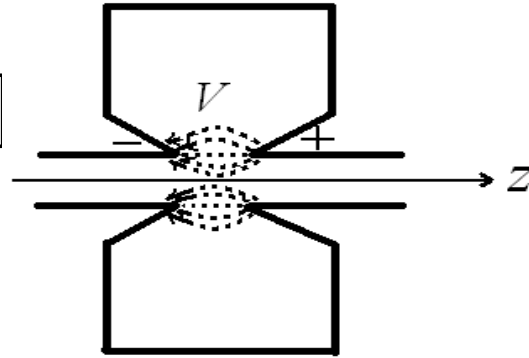
Parameters of an Open-End Cavity (continued)

The work done by $E_z(z, t)$ on the particle during its passage through the cavity gap is

$$\begin{aligned}
 W &= -e \int_{-d}^0 E_z(\text{on electron}) dz = -e E_g \int_{-d}^0 \cos \left[\frac{\omega}{v_0} \left(z + \frac{d}{2} + v_0 t_1 \right) \right] dz \\
 &= -e E_g d \left[\frac{\sin \frac{\omega d}{2 v_0}}{\frac{\omega d}{2 v_0}} \right] \cos \omega t_1 = -e E_g d M \cos \omega t_1
 \end{aligned} \tag{10}$$

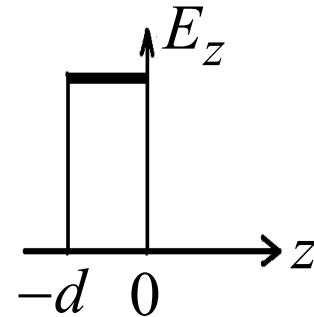
where

$$\begin{cases} M \equiv \frac{\sin \frac{\theta_g}{2}}{\frac{\theta_g}{2}} \quad [\text{Transit time factor}] \\ \theta_g \equiv \omega \frac{d}{v_0} \quad [\text{Transit angle}] \end{cases} \tag{11}$$



θ_g is the total phase variation of $E_z(z, t)$ during the particle's transit time ($\frac{d}{v_0}$). Since $\theta_g > 0$, we always have $|M| < 1$.

For present-day accelerators, $v_0 \approx c$.



Parameters of an Open-End Cavity (*continued*)

Rewrite
$$W = -eE_g dM \cos \omega t_1 \quad (10)$$

Since $|M| < 1$ (see Fig. 3), the maximum energy gained or lost by the particle, $eE_g dM$ (when $\cos \omega t_1 = \pm 1$), in passing through the cavity is always less than the *instantaneous* maximum value: $eE_g d$.

For this reason, in accelerator literature, *effective* values of gap voltage and shunt impedance are defined and often used:

$$\begin{cases} V_{eff} = MV \\ R_{eff} = M^2 R = \frac{|V_{eff}|^2}{2P_{loss}} \end{cases} \quad (13)$$

where $M = \frac{\sin \frac{\theta_g}{2}}{\frac{\theta_g}{2}}$ is the transit time factor.

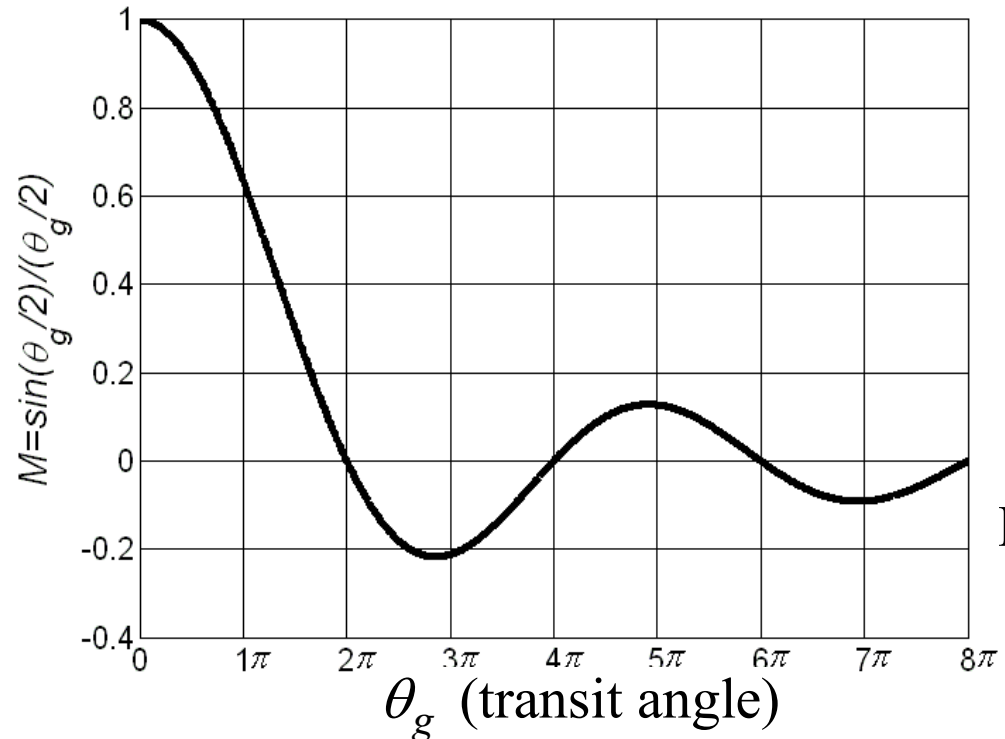
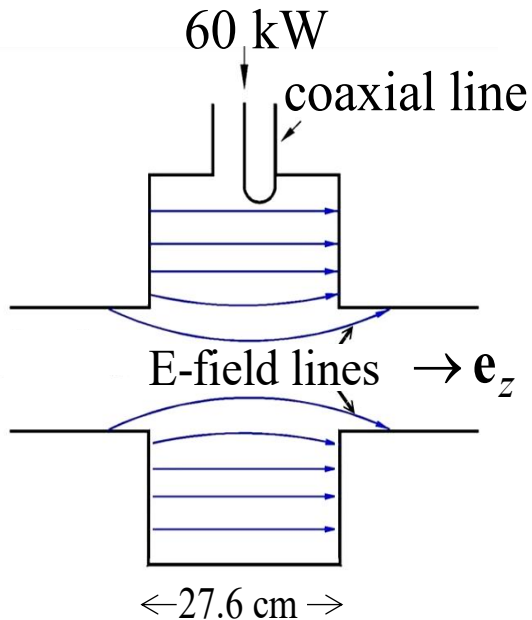


Fig. 3

An Example of Open-End Cavity : the DORIS I Cavity Used in the NSRRC Storage Ring

Dimensions:



Parameters:

$$f_0 = 500 \text{ MHz}$$

$$Q = 37000$$

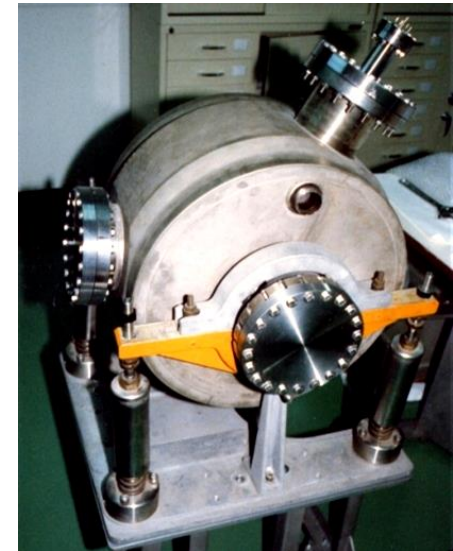
$$R_{eff} = 3 \times 10^6 \ \Omega$$

$$P = 60 \text{ kW}$$

$$V_{eff} = 600 \text{ kV}$$

$$M = 0.587$$

DORIS I cavity



If 60 kW is input into the empty cavity to excite the mode. Then, in the steady state, all 60 kW is dissipated on the walls ($P_{loss} = 60 \text{ kW}$),

$$\text{Thus, } R_{eff} = \frac{|V_{eff}|^2}{2P_{loss}} \quad [(13)] \Rightarrow V_{eff} = 600 \text{ kV} \quad \left[\Rightarrow \text{Maximum energy gained by an electron} \right]$$

Equivalent Circuit for an Open-End Cavity

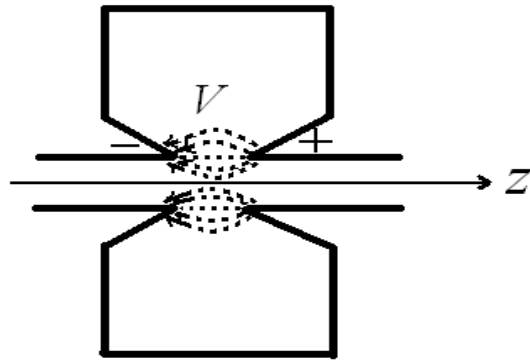


Fig. 1

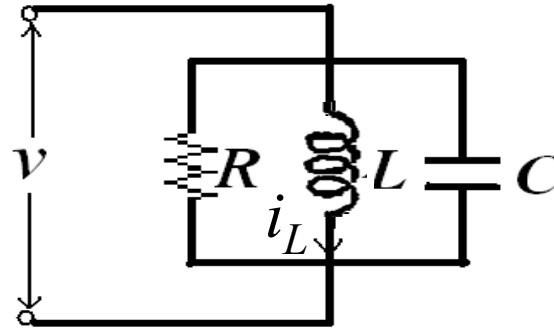
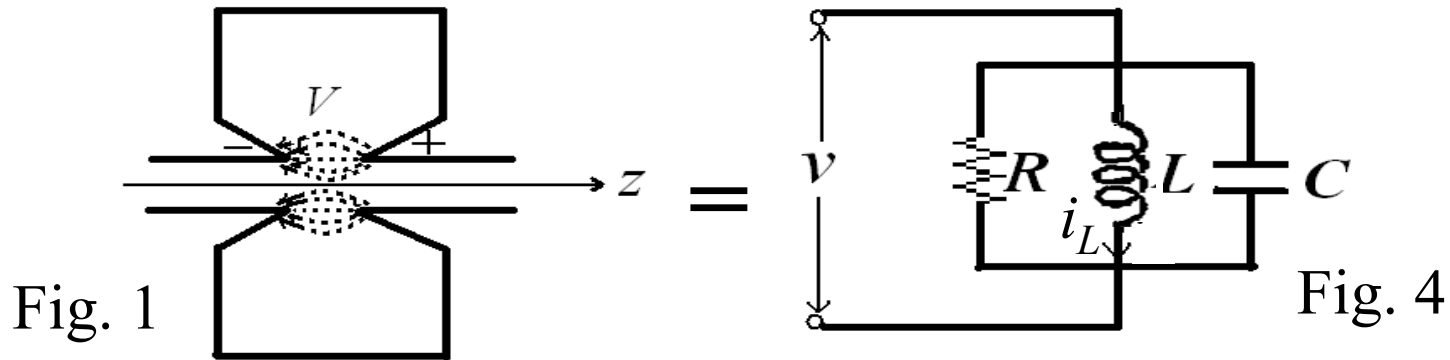


Fig. 4

Cavities like the one in Fig.1 are often too complex to be examined analytically. Instead, it can be described by an equivalent circuit, which yields the parameters of interest : ω_0 , Q , and R .

Fig.4 shows a commonly used equivalent circuit (Collin, Sec.7.1). The equivalent circuit has a resistance R , a resonant frequency ω_0 and a quality factor Q [ω_0 and Q are derived below and also in Lecture Notes, Ch.3, Appendix A, Eqs.(10) and (13)]. Thus, what we need are the proper values of R , C , and L to give the equivalent circuit the same R , ω_0 , and Q as those of the cavity. This is done below.

Equivalent Circuit for an Open Cavity (continued)



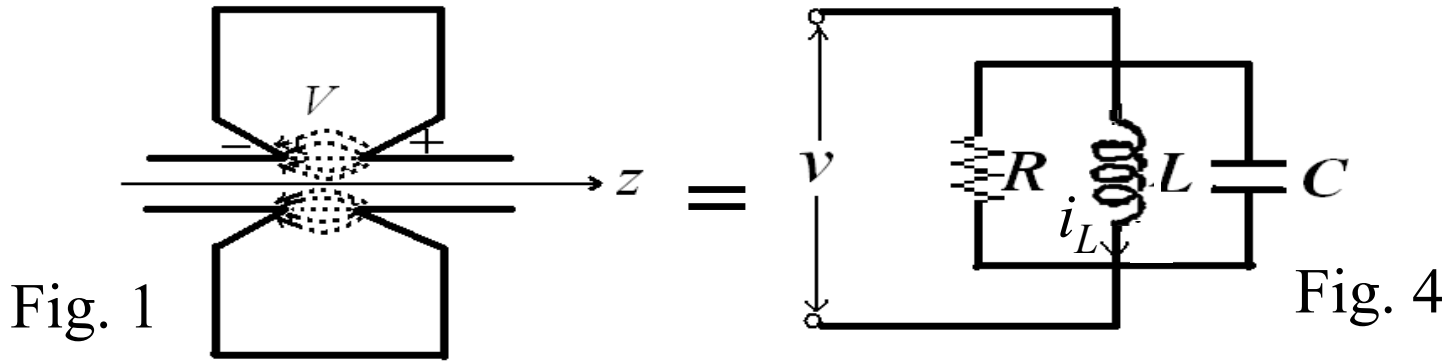
For the circuit in Fig. 4, let W_e , W_m be the average E- and B-field energies, P_{loss} be the power dissipation, and Q be the quality factor.

Then,
$$\begin{cases} W_e = \frac{1}{4} C |v|^2 & (14) \\ W_m = \frac{1}{4} L |i_L|^2 = \frac{1}{4} \frac{|v|^2}{\omega^2 L} & (15) \\ P_{loss} = \frac{1}{2} \frac{|v|^2}{R} & (16) \\ Q = \frac{\omega W_f}{P_{loss}} = \frac{\omega(W_e + W_m)}{P_{loss}} & (17) \end{cases}$$

$v = j\omega L i_L$, where $j\omega L$ is the impedance of L .
[Lecture Notes, Ch. 3, Appendix A, Eq. (14)].

For the cavity, we have $R = \frac{1}{2} |V|^2 / P_{loss}$ [(2)]. Comparing this with (16), R of the equivalent circuit is to be specified at the same value.

Equivalent Circuit for an Open Cavity (*continued*)



Rewrite
$$\begin{cases} W_e = \frac{1}{4} C |v|^2 & [(14)]; & W_m = \frac{1}{4} L |i_L|^2 = \frac{1}{4} \frac{|v|^2}{\omega^2 L} & [(15)] \\ P_{loss} = \frac{1}{2} \frac{|v|^2}{R} & [(16)]; & Q = \frac{\omega(W_e + W_m)}{P_{loss}} & [(17)] \end{cases}$$

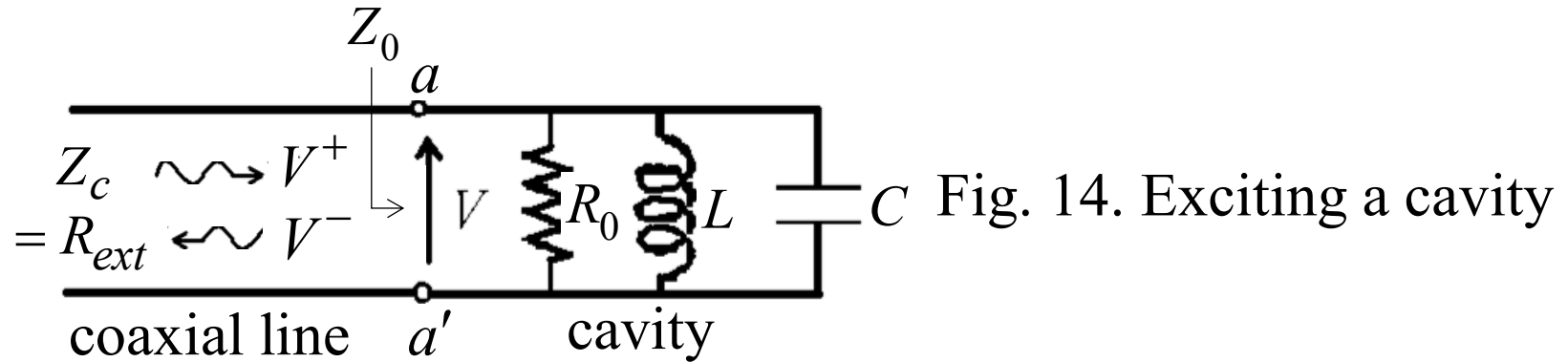
At $\omega = \omega_0$, we have $W_e = W_m$ [Lecture Notes, Ch. 3, Appendix A,

Eq. (12)]. Thus,
$$\begin{cases} (14), (15) \Rightarrow \omega_0^2 = \frac{1}{LC} & (18) \\ (14), (16), (18) \Rightarrow Q = \frac{2\omega_0 W_e}{P_{loss}} = \omega_0 RC = \frac{R}{\omega_0 L} & (19) \end{cases}$$

Thus, using ω_0 , Q of the cavity, we get L , C from (18), (19).

With R , L , and C specified in this way, Figs. 1 and 4 have the same R , ω_0 , and Q . As shown next, the equivalence goes beyond this.

Critical Coupling, Undercoupling, and Overcoupling



Rewrite
$$\begin{cases} |V|^2 = \frac{4|V^+|^2 R_0^2}{(R_0 + R_{ext})^2 [1 + (2Q_L \frac{\Delta\omega}{\omega_0})^2]} \\ \frac{\Delta P}{P} = \frac{4R_0 R_{ext}}{(R_0 + R_{ext})^2 [1 + (2Q_L \frac{\Delta\omega}{\omega_0})^2]} \end{cases} \quad (45)$$

$$\frac{\Delta P}{P} = \frac{4R_0 R_{ext}}{(R_0 + R_{ext})^2 [1 + (2Q_L \frac{\Delta\omega}{\omega_0})^2]} \quad (49)$$

Under the conditions:
$$\begin{cases} \omega = \omega_0 \text{ (i.e. } \Delta\omega = 0) \\ \text{and } R_0 = R_{ext} \end{cases} \quad (50a)$$

$$\text{and } R_0 = R_{ext} \quad (50b)$$

$(45) \Rightarrow |V|^2 = |V^+|^2$ and $(49) \Rightarrow \Delta P = P$. Either $|V|^2 = |V^+|^2$ or $\Delta P = P$ implies that the incident power has all entered into the cavity (i.e. a perfect match). This is called critical coupling.

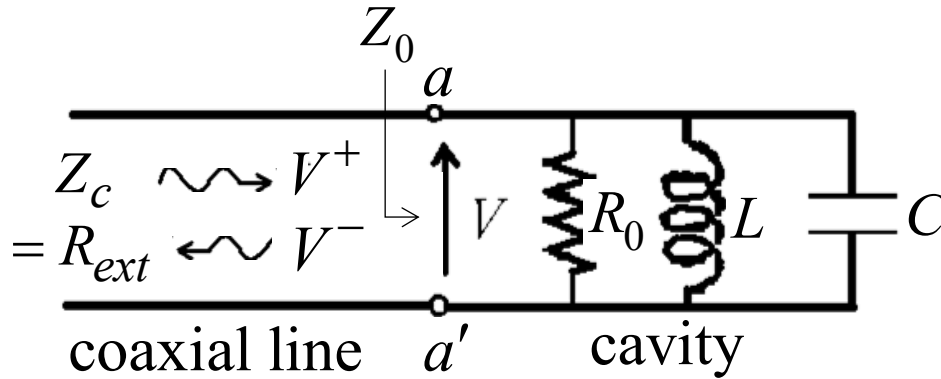


Fig. 14. Exciting a cavity

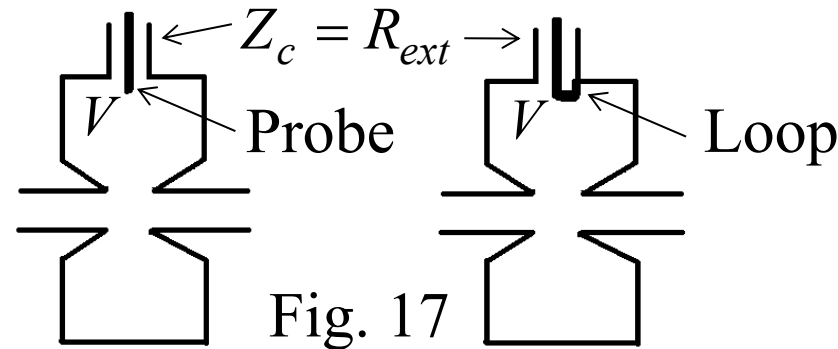
Eq. (36) gives $Q_0 = \omega_0 R_0 C$ and $Q_{ext} = \omega_0 R_{ext} C$. Thus, one of the critical coupling conditions, $R_0 = R_{ext}$ [(50b)], can also be expressed as

$$Q_{ext} = Q_0 \quad \text{i.e.} \quad [\text{External } Q] = [\text{Unloaded } Q] \quad (51)$$

A coupling coefficient (β) is often used to characterize the degree of matching with a cavity. It is defined as

$$\beta \equiv \frac{Q_0}{Q_{ext}} \quad (52)$$

$\beta < 1$, the cavity is said to be undercoupled to the feeding line
 $\beta = 1$, the cavity is said to be critically coupled to the feeding line
 $\beta > 1$, the cavity is said to be overcoupled to the feeding line

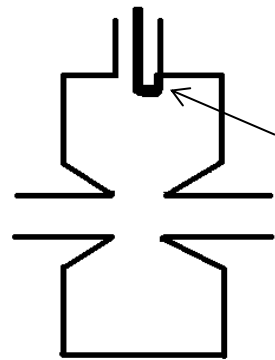


Question: Fig. 17 shows 2 coaxial feeding line with a probe or a loop at the end. What parameters are being changed when we "tune" the coupling strength by varying the probe length or loop orientation?

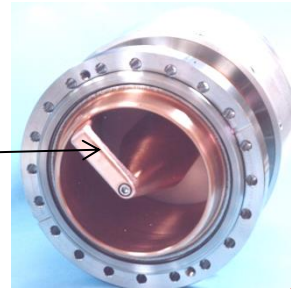
$$\text{Rewrite } P_{ext} = \frac{|V|^2}{2R_{ext}} \text{ [(34)]; } R_0 = \frac{|V|^2}{2P_0} \text{ [(35)]; } Q_{ext} = \frac{\omega_0 W_f}{P_{ext}} \text{ [(32)]}$$

Let's assume the same field energy (W_f) and ω_0 . Then, P_0 (Ohmic loss) and Q_0 ($= \omega_0 W_f / P_0$) are the same. Also, R_{ext} (R_c of the coaxial line) is fixed. When the probe or loop is tuned, the (local) gap voltage V can vary a lot. Hence, by (34) and (35), P_{ext} and R_0 can be changed a lot. As a result, by (32), Q_{ext} can also be changed a lot. This makes it possible to achieve critical coupling: $Q_{ext} = Q_0$ ($\Rightarrow R_0 = R_{ext}$).

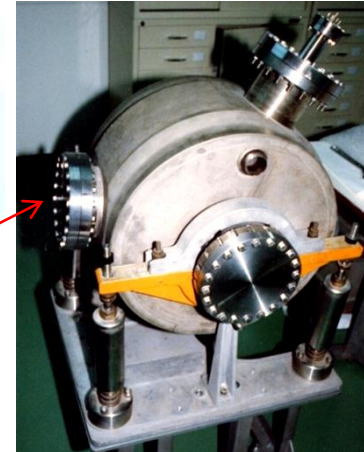
Fig. 18



Loop

Port for
loop coupling

NSRRC cavity



Significance and Example of Critical Coupling:

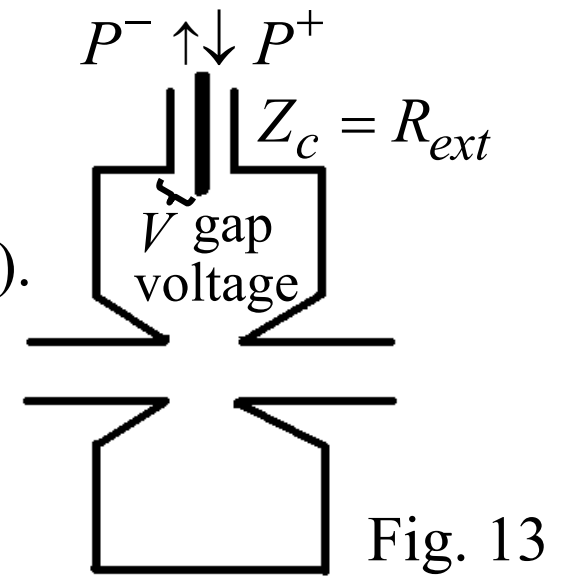
In feeding a cavity, reflections can cause interferences with other signals. In the case of high input power (e.g. 60 kW for the NSRRC cavity), reflections can also waste energy and, worse, damage the power generator. Thus, the coupling structure needs to be tuned to minimize the reflection.

For the NRSSC cavity, loop coupling is used (Fig. 18). Critical coupling (i.e. no reflection) can be achieved by rotating the coupling loop to vary Q_{ext} until $Q_{ext} = Q_0$ [(51)].

A Physical Picture of Critical Coupling:

In Fig. 13, there are two sources for P^- : (1) Reflection of P^+ at the port; and (2) Energy leakage from the cavity to the coaxial line. How can there be no P^- under critical coupling? The reason is that there are *two* sources for P^- . When the critical coupling conditions are met, the fields of the two sources are equal in amplitude, but 180° out of phase. Hence, they cancel exactly (no P^-).

From another point of view, if the gap voltage is V and there is no V^- . Then, at the gap, $V^- + V^+ = V$ reduces to $V^+ = V$, which implies a power of $|V|^2 / (2R_{ext})$ is fed into the cavity. Then, in order to maintain a steady state, this power must equal the power dissipated in the cavity: $\frac{|V|^2}{2R_{ext}} = \frac{|V|^2}{2R_0}$ or $R_{ext} = R_0$ (the critical coupling condition).



Cavity application – 3GHz chopper of TLS LINAC

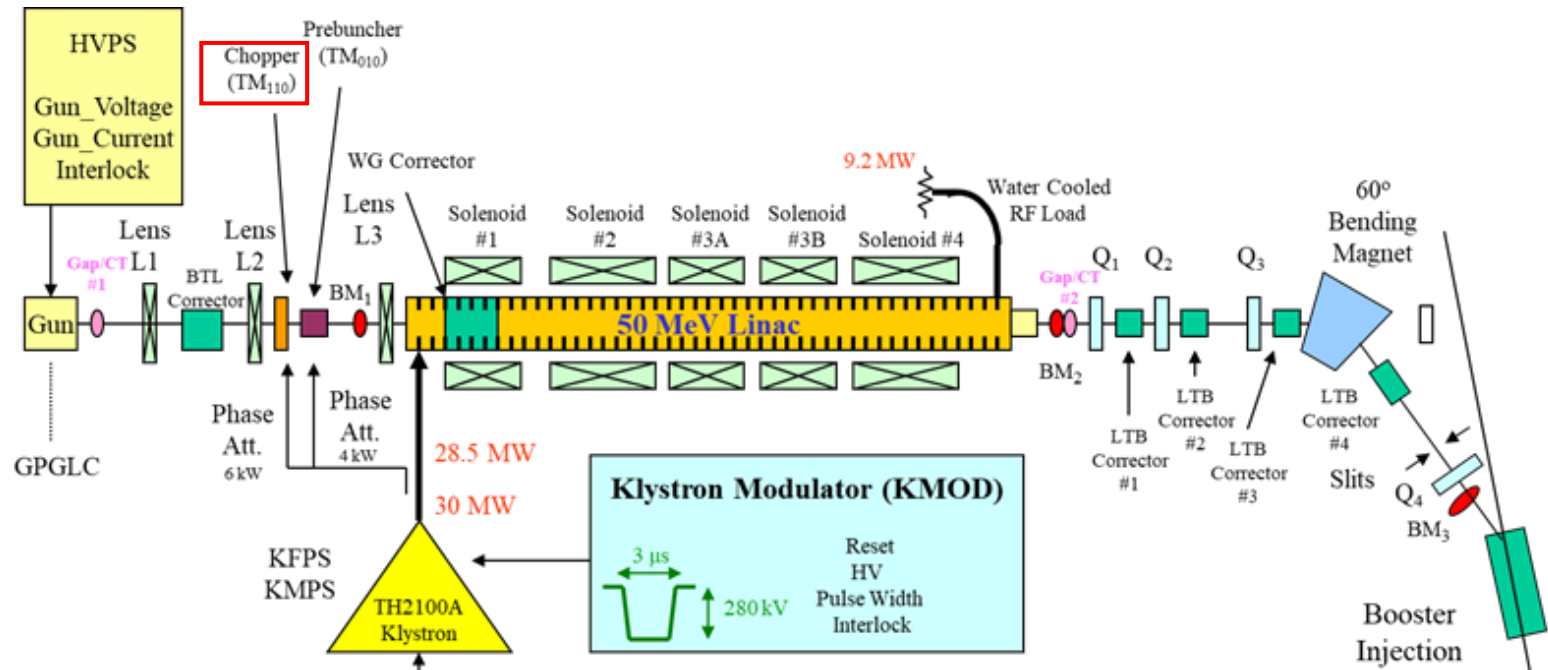
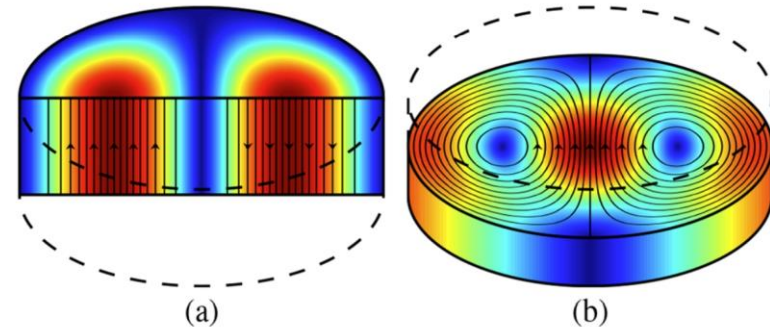


Illustration of the 3GHz chopper operating at TM₁₁₀ mode is shown in figure-4. The applied rf magnetic field, shown in the figure, compensates the DC-biased magnetic field at 3GHz and chops the DC electron pulse into 3GHz bunch train.

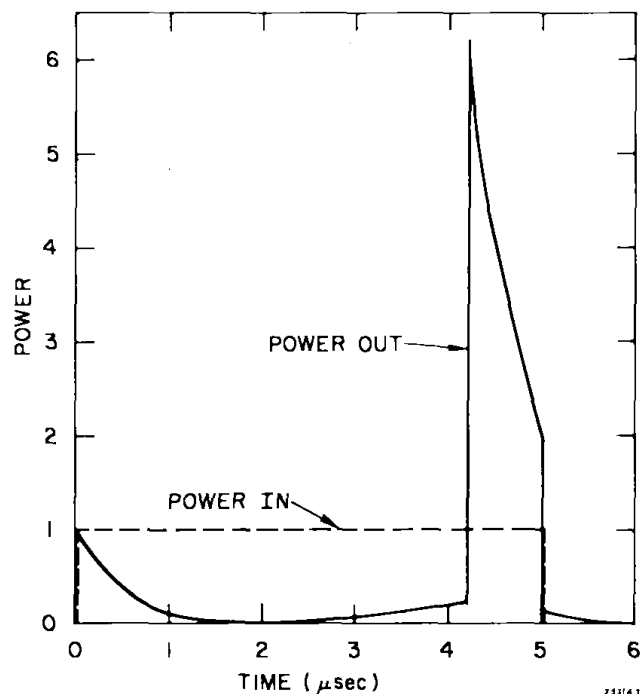


Chopper cavity (a) Longitudinal electric and (b) transverse magnetic field distribution of the TM₁₁₀ mode.

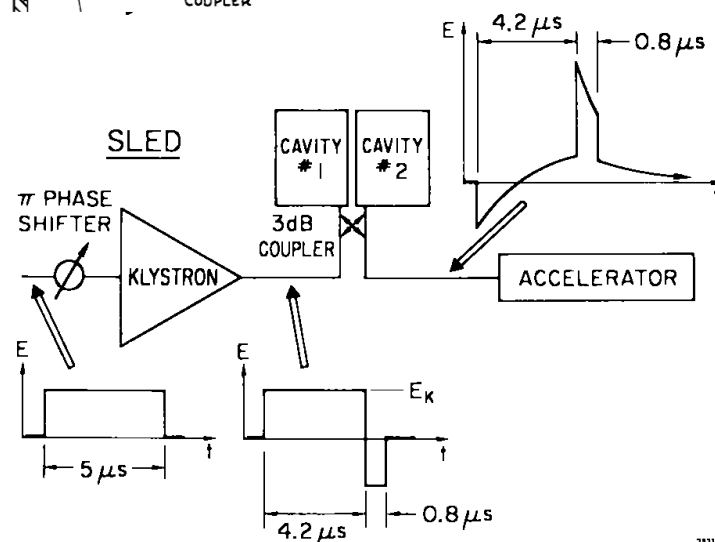
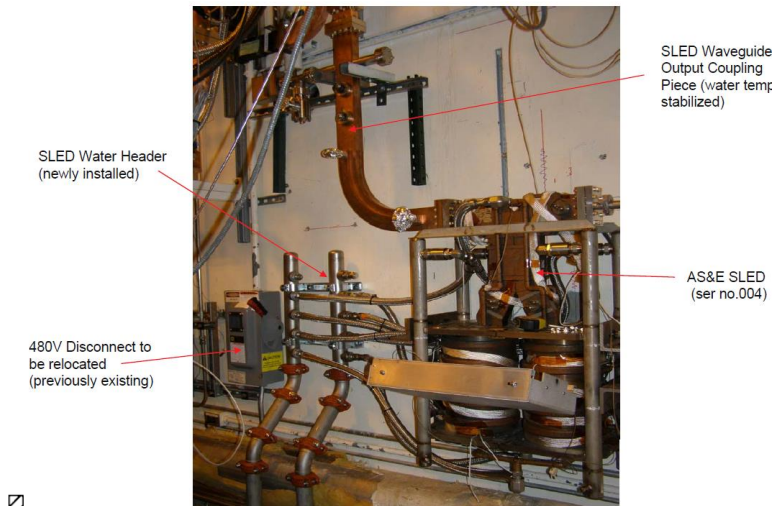
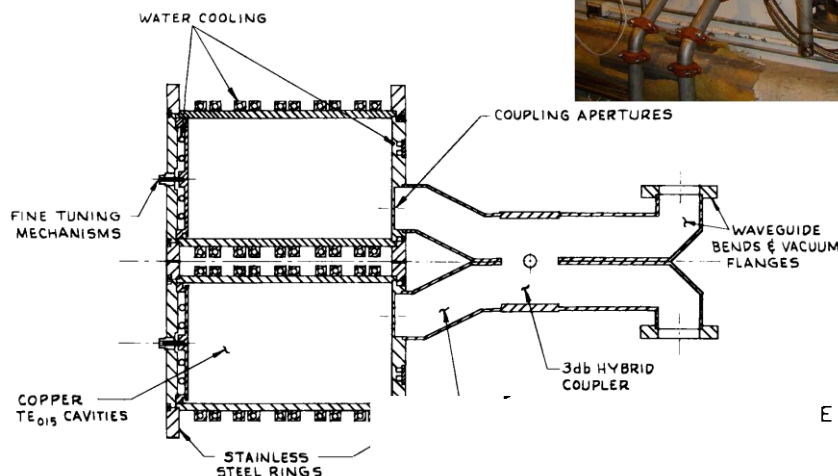
Cavity application – SLED

SLED = SLAC Energy Doubler

- A method of achieving RF pulse-compression through the use of high-Q resonant cavities.
- The cavities store klystron energy during a large fraction of each pulse and then discharge this energy rapidly into the accelerator during the remainder of the pulse.



SLED output power waveform



Cavity application – DAWON(KOREA) SLED

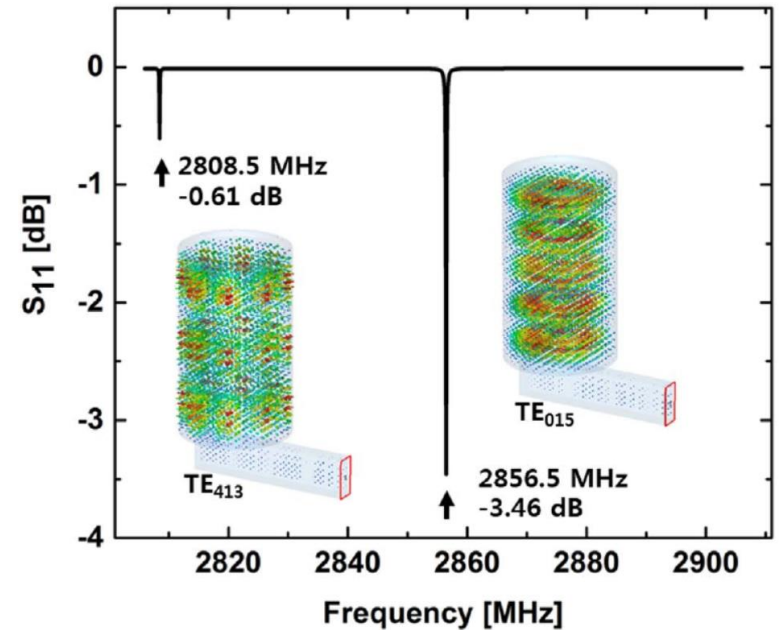
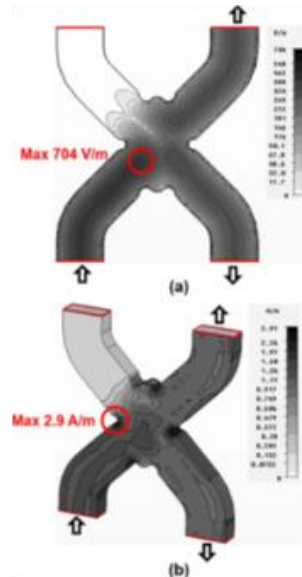
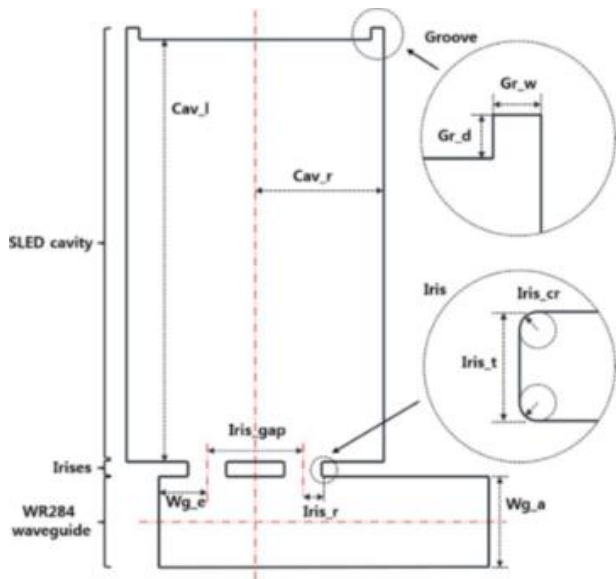
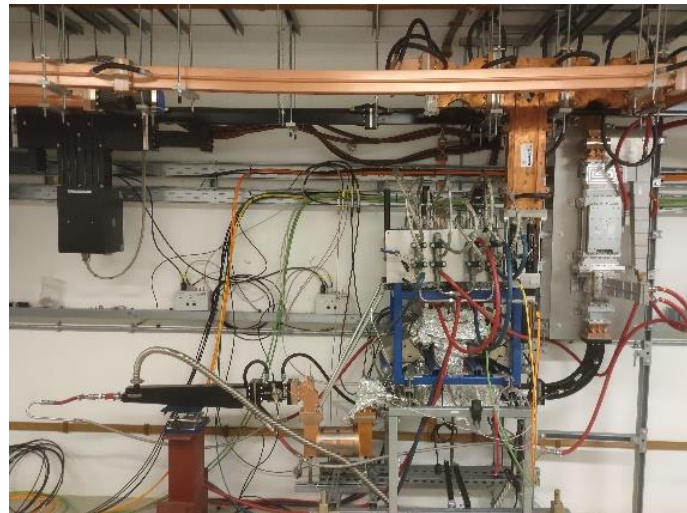
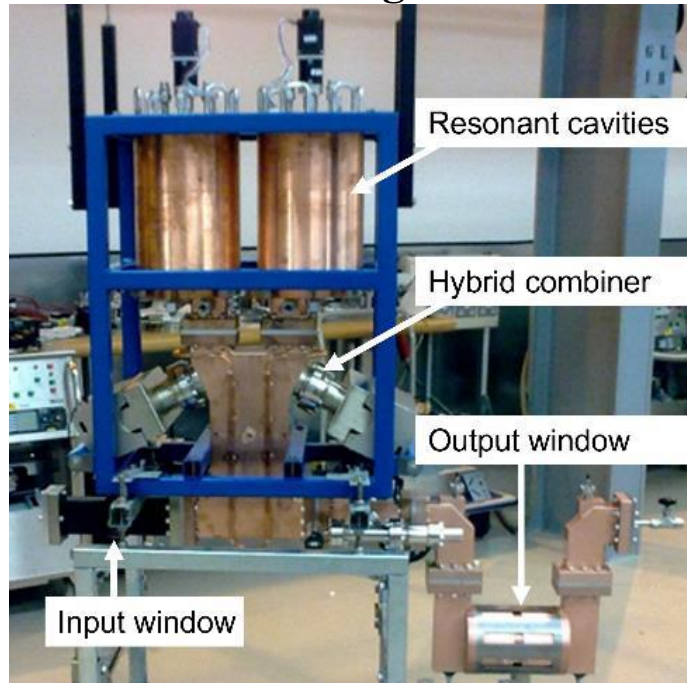


Table 2. Results of the analytical calculation and the MWS simulation of several resonant modes around 2856 MHz for the SLED cavity.

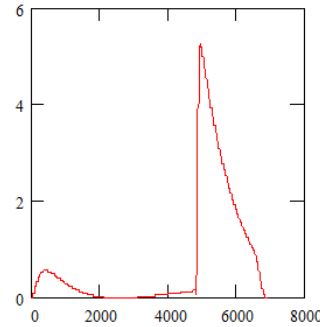
Resonant mode	Without groove			With groove	
	Calculation	MWS Simulation	Q-value	MWS Simulation	Q-value
	Frequency (MHz)	Frequency (MHz)		Frequency (MHz)	
TE116	2811.22	2811.34	46411		
TE413	2813.11	2813.21	36781		
TE123	2818.76	2818.9	84572		
TM115	2856.02	2856.15	50794	2838.7	49641
TE015	2856.02	2856.16	106550	2856.13	107290
TM023	2896.32	2896.46	50679		
TM016	2901.90	2902.04	51260		
TE315	2966.38	2966.53	46168		

Cavity application – SLED Flat Pulse Operation

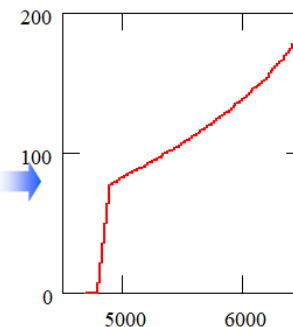
Diamond Light Source



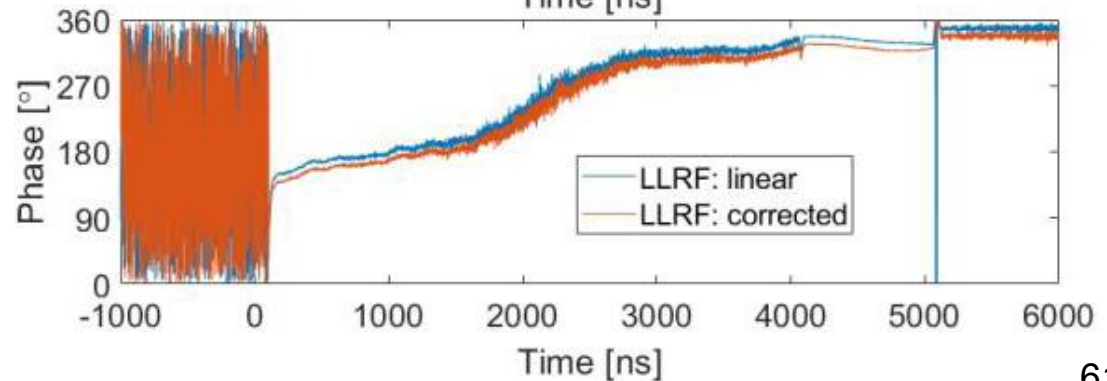
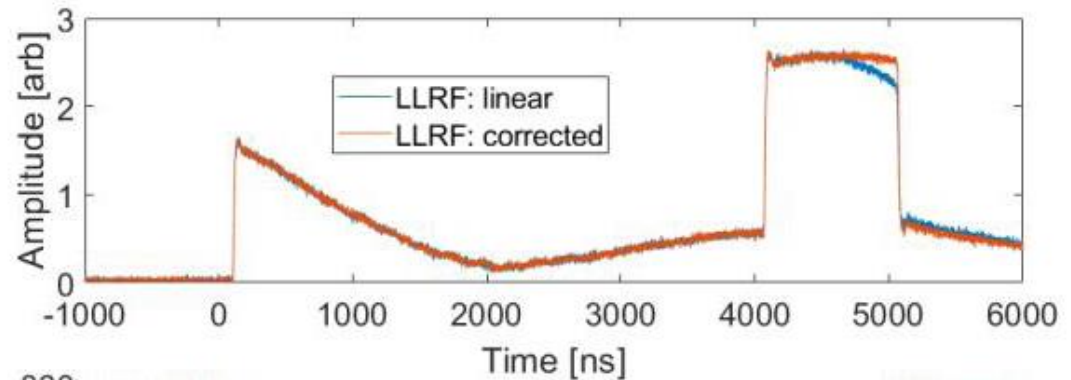
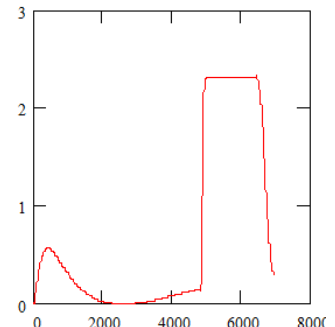
Standard "SLED" Pulse



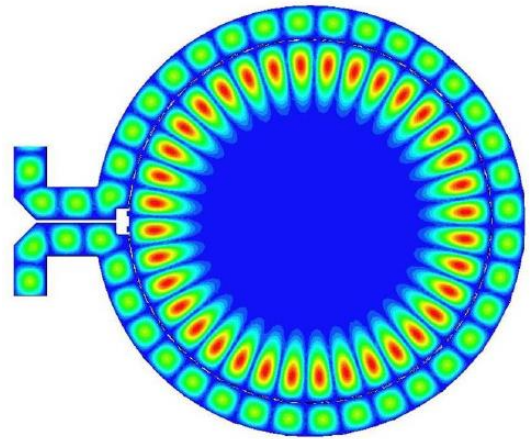
RF phase modulation



Flat pulse



Cavity application – SLED-II BOC (Barrel Open Cavity)



C-band BOC of Swiss FEL
Single cavity, no power hybrid

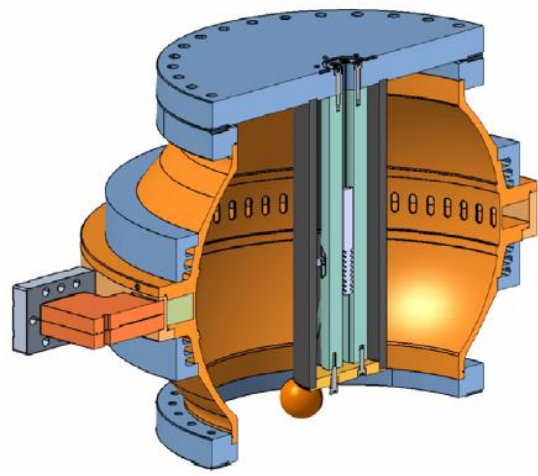


Table 1: Main Parameters of BOC

Pulse compressor	Design parameter
Type	Barrel Open cavity
Frequency	5.712 GHz
Resonant mode	TM _{18,1,1}
Diameter	492 mm
Number of coupling slots	70
Q	216000
Coupling factor (β)	10
Max. input power	50 MW
RF input pulse length	3 μ s
RF compressed pulse length	330 ns
Energy multiplication factor (M)	2.13
Repetition rate	100 Hz

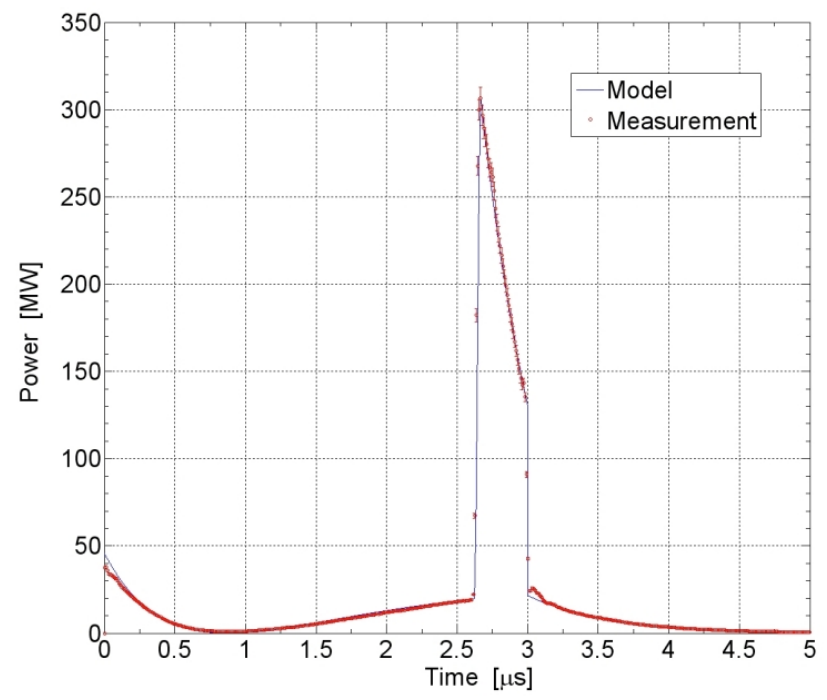
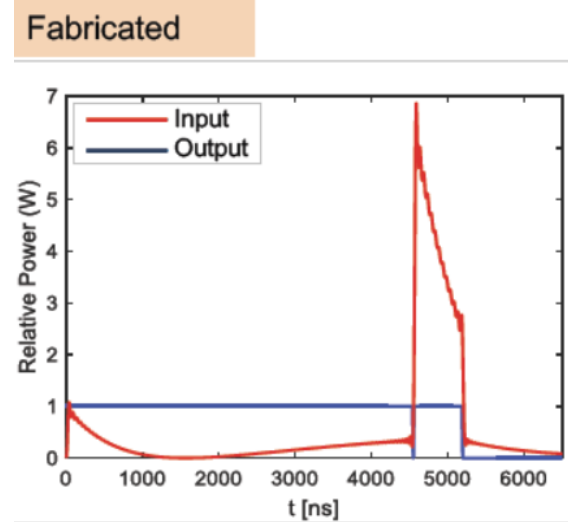
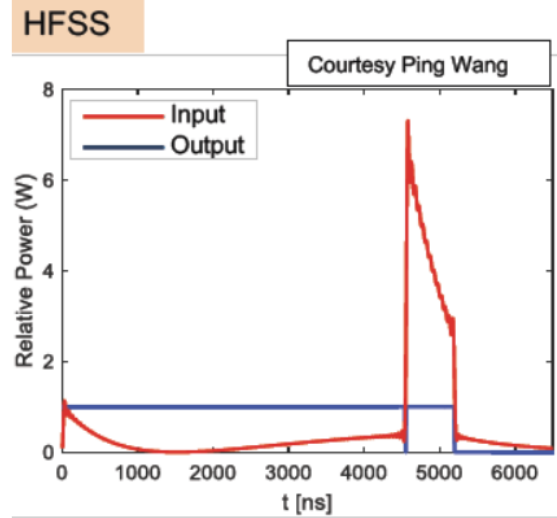
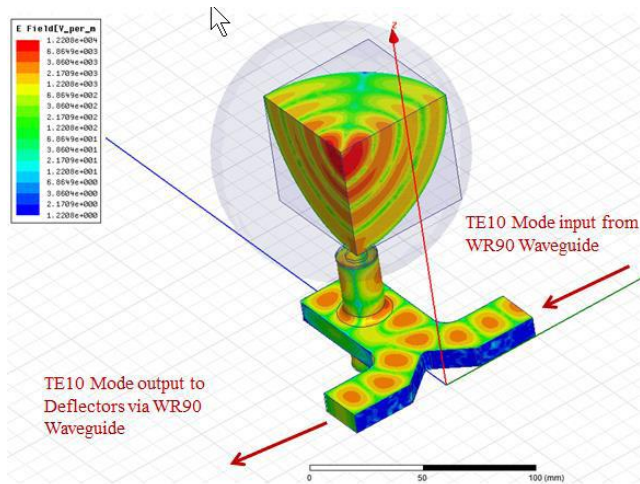


Figure 8: Compression of a 50 MW, 3 μ s rectangular pulse.

Cavity application – SLED-III SCPC (SPHERICAL PULSE COMPRESSOR)



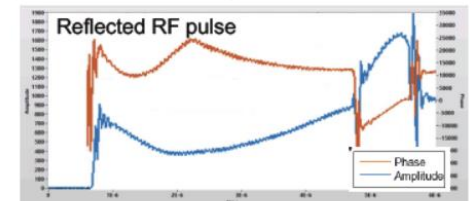
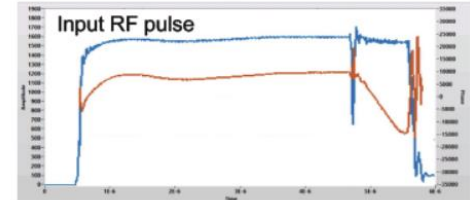
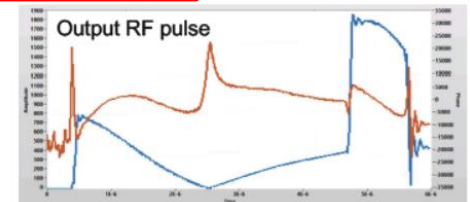
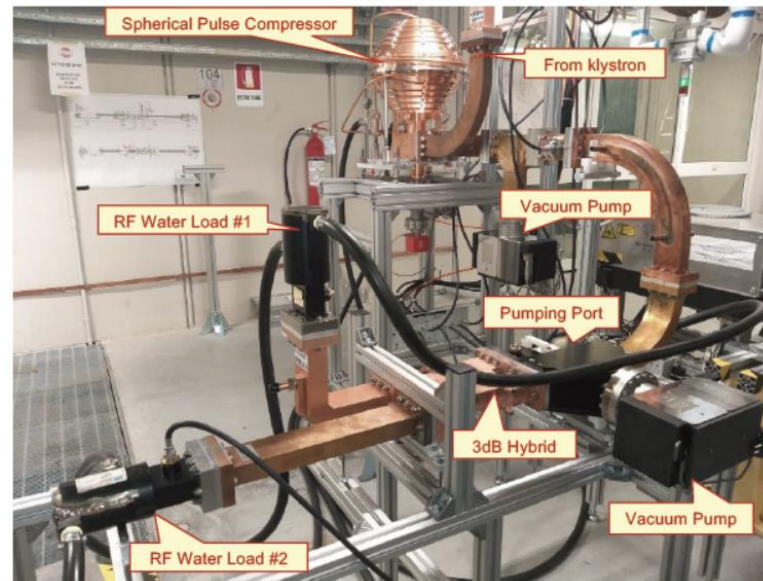
Elettra SCPS Test Results

Phase I (90 MW)

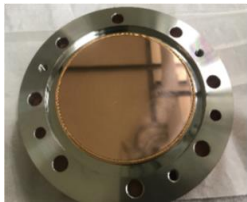
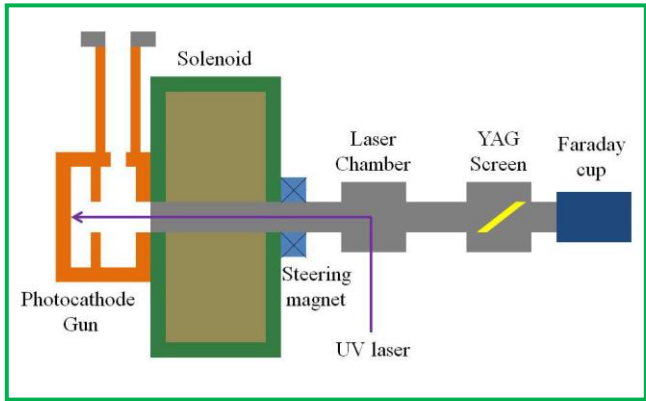
- ❑ Rep. Rate: 50 Hz
- ❑ Start Date: 06-12-2022
- ❑ End Date: 21-12-2022
- ❑ Output power: 90MW, 700 ns
- ❑ Input power: 26 MW, 4000 ns
- ❑ Operating temperature: 32.25 °C

Phase II (100 MW)

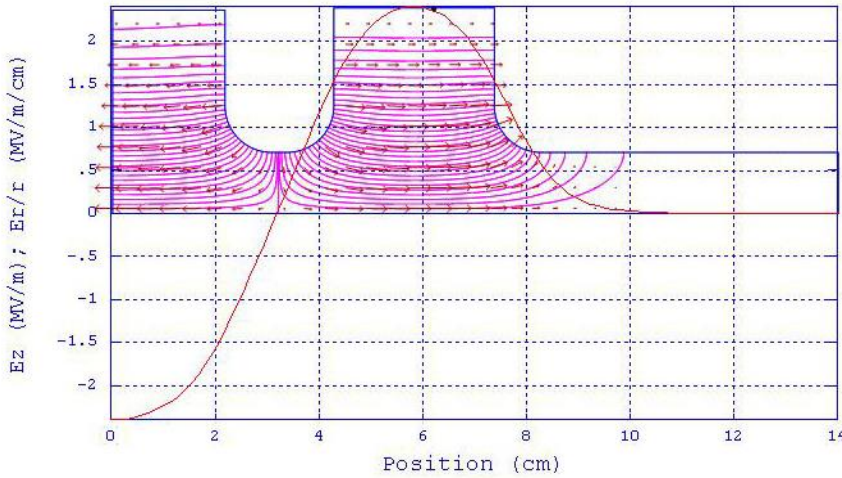
- ❑ Rep. Rate: 50 Hz
- ❑ Start Date: 23-03-2023
- ❑ End Date: 31-03-2023
- ❑ Output power: 100 MW, 700 ns
- ❑ Input power: 29 MW, 4000 ns
- ❑ Operating temperature: 31.47 °C



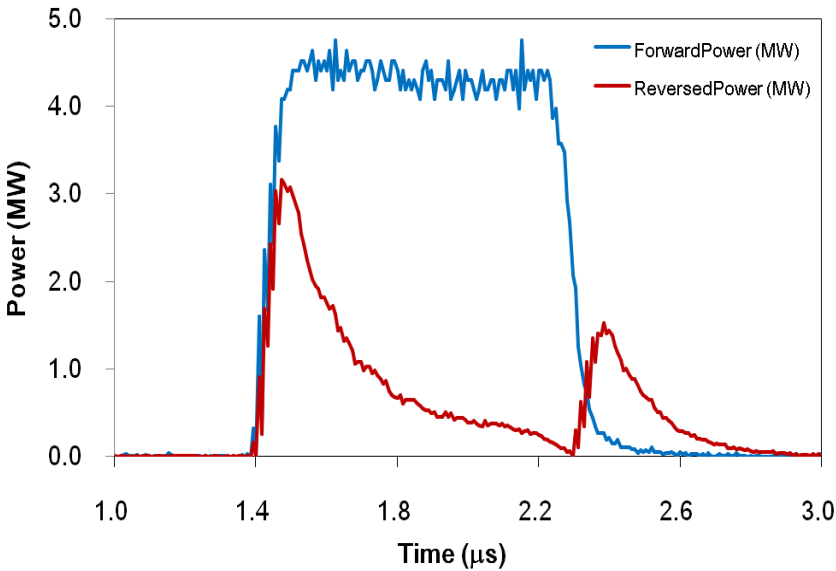
Cavity application – NSRRC Photocathode RF Gun



Cu cathode



Parameter	Value
Frequency	2.99822 GHz (@55°C)
Q_0	~8000
Coupling coefficient	0.7
Peak field at the cathode	50 MV/m
Beam energy after gun	2.5 MeV
UV laser pulse duration (FWHM)	3 ps
Cathode quantum efficiency	$\sim 1 \times 10^{-5}$



Forward and reverse power of the Gun

Vacuum Electronics

Vacuum electronics addresses electron-wave interactions in a vacuum, usually for radiation generation. It involves a much broader frequency range than the microwave band (e.g. X-ray free electron laser, FEL). This chapter covers only the microwave regime.

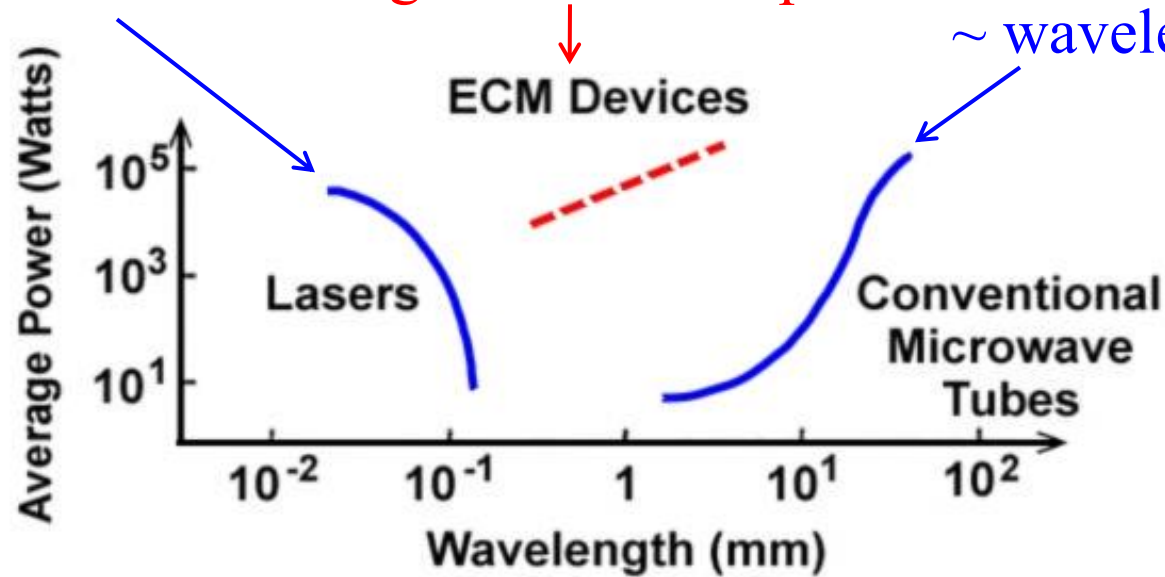
	Conventional Microwave Electronics	Relativistic Electronics
Examples ,	TWT, Klystron, Magnetron	ECM, FEL
Frequency	$< 10^{11}$ Hz	10^{10} Hz – X-ray
Power	$< 10^6$ W	10^4 W – 10^{10} W
Electron Energy	$< 10^5$ V	10^3 V – 10^{10} V
Beam Current	$< 10^2$ A	1 A – 10^6 A
Basic Equations	Circuit equations + Fluid equations	Maxwell equations + Relativistic particle eqs.

Power Capabilities of Laser and Microwave Tubes

One photon per
excitation,
Large interaction
space

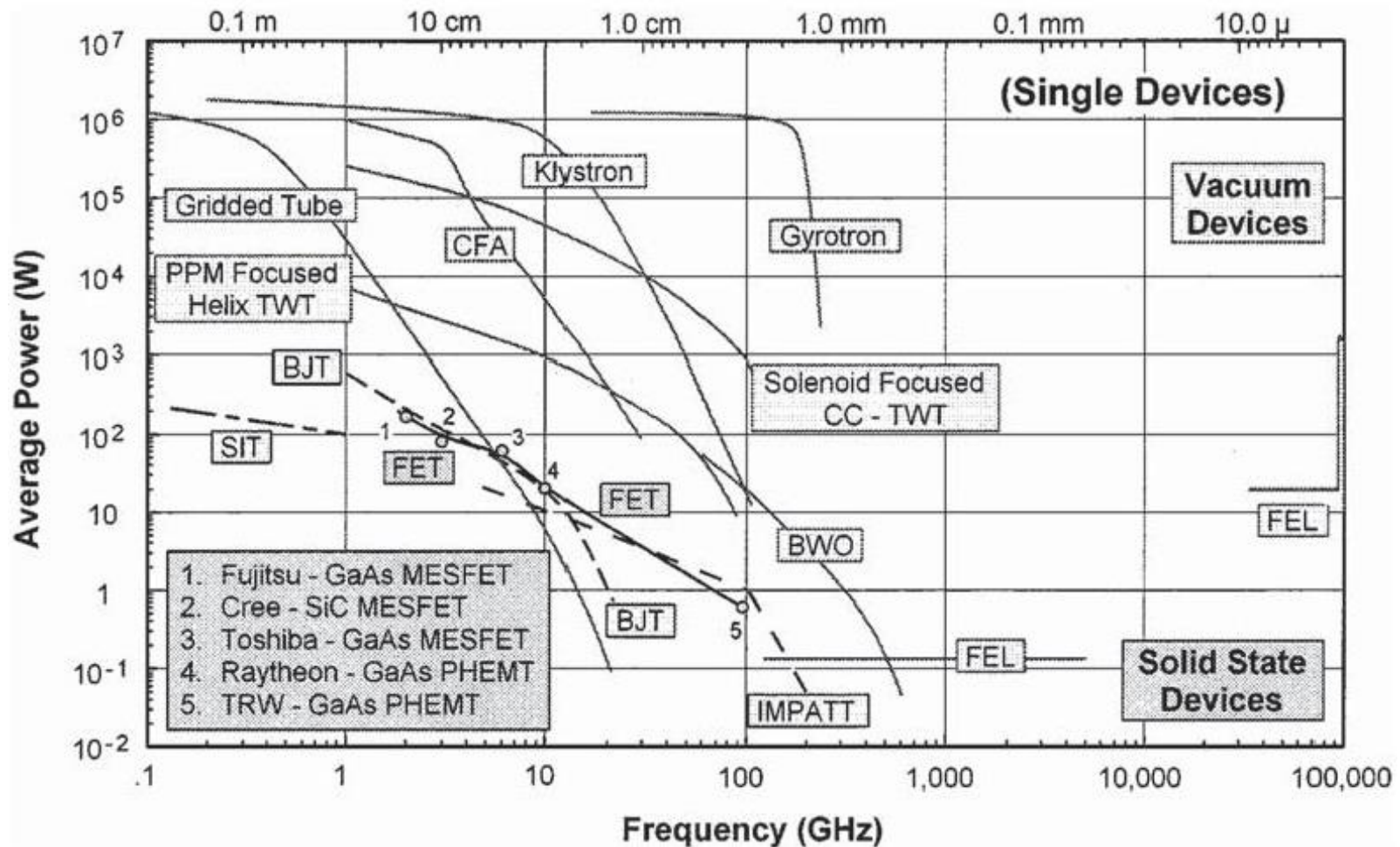
Multiple photon per
electron,
Large interaction space

Multiple photon per
excitation,
Interaction space
 \sim wavelength



The figure above compares the power capabilities of lasers and microwave tubes. Lasers are quantum mechanical devices, while the conventional microwave tubes and ECM (a new type of microwave tubes) are vacuum electronic devices. The term "microwave tube" refers to microwave generators requiring a vacuum environment for the electron-wave interaction

Introduction of Microwave Tubes



An Overview of Microwave Tubes

Microwave tubes (or simply "tubes") are the main subject of this chapter. They have a long history of research and are still being enriched by new physical insights and the discovery of novel types of tubes. Microwave tubes are widely used in our daily life.

Tubes are bulkier than solid state microwave devices, but they generate much higher power. The basic types of microwave tubes are listed below (and will be discussed later).

Conventional Microwave Tubes: matured in the 1960s

Cornerstones: {
1. Traveling Wave Tube (TWT)
2. Klystron
3. Magnetron

Relativistic Microwave Tubes: 1970s-present

Cornerstone: Gyrotron [a device based on a relativistic effect called the electron cyclotron maser (ECM)]

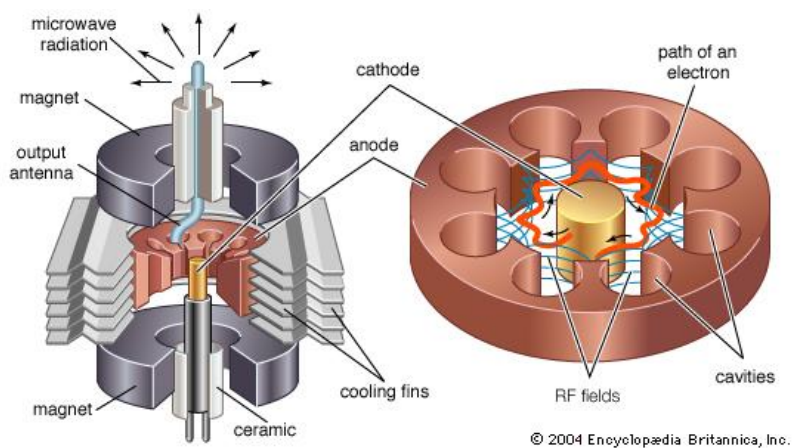
An Overview of Microwave Tubes

<u>Amplifier</u>	<u>Oscillator</u>	<u>Interaction Process</u>
Gridded Tube	Gridded Tube	Grid control of the beam current
Klystron	1.Two Cavity Oscillator 2.Extended Interaction Oscillator 3.Reflex Klystron	Velocity Modulation with resonant cavities
1.Helix TWT 2.Coupled Cavity TWT	Backward wave Oscillator	Velocity Modulation with traveling wave structure
Crossed Field Amplifier	1.Carcinotron(M-type BWO) 2.Fixed Frequency Magnetron 3.Coaxial Magnetron 4.Voltage Tuned Magnetron	Crossed Field
Gyrotron	Gyrotron	Spiraling beam

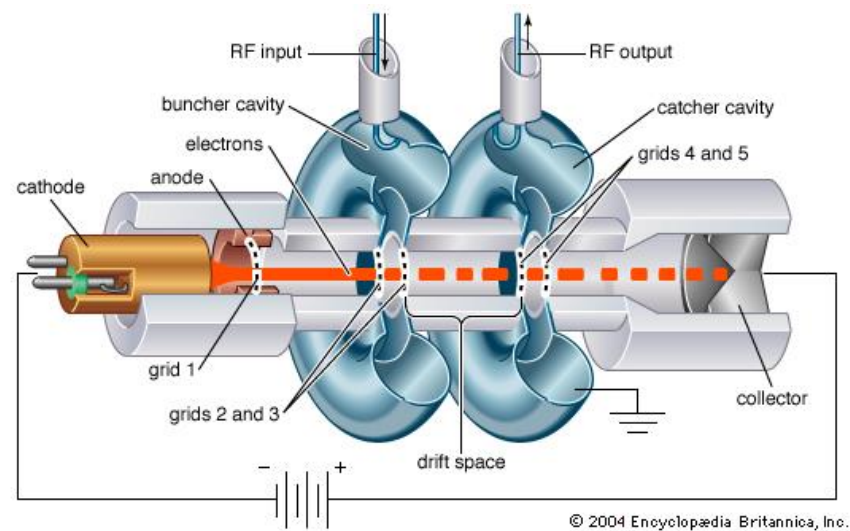
※ **Linear beam tubes are called O-type devices.**

※ **Crossed-field tubes are called M-type devices.**

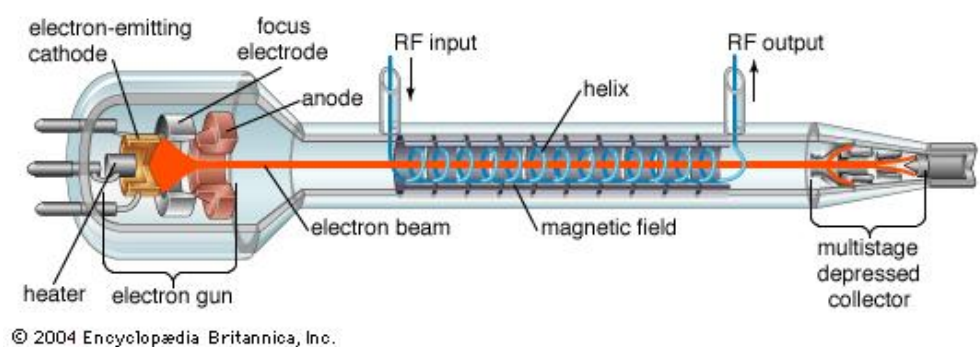
Conventional Microwave Electronics



Magnetron

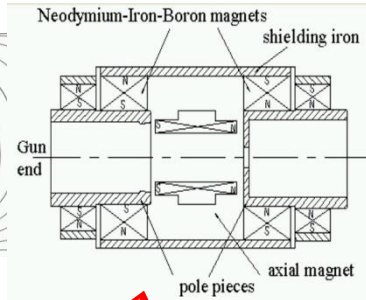
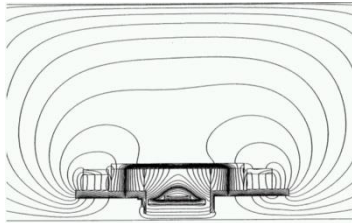


Klystron



Helix TWT

Microwave Source R&D



CAD

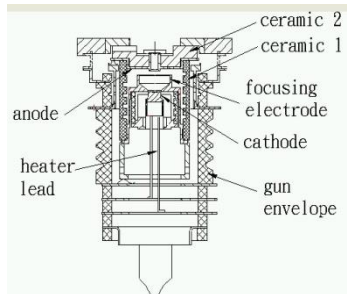
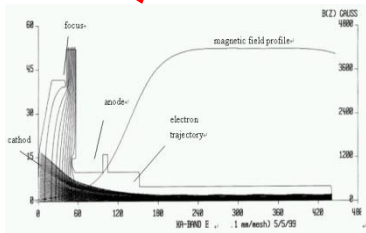
Engineering
Drawing

Precision
Machining

Brazing

EIKA
Assembly

Hot
Test



Conditions Required for the Generation of Coherent Radiation - Common to All Types of Microwave Tubes

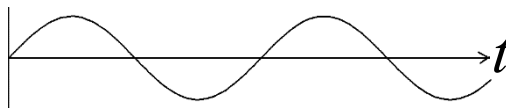
1. A mechanism for the RF fields to *bunch* a DC electron beam into an AC electron beam (Microwave tubes are distinguished by their bunching mechanisms).
2. *Synchronism* between the bunched electrons and the RF fields.

$$\text{Let } \begin{cases} J \text{ (electron current)} = \begin{cases} J_0 \text{ [DC]} \\ J_0 \sin \omega t \text{ [AC]} \end{cases} \\ E \text{ (wave electric field)} = E_0 \sin \omega t \end{cases}$$

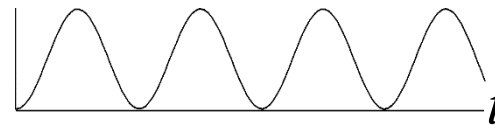
$$\text{Then, } P \text{ (power)} = JE = \begin{cases} J_0 E_0 \sin \omega t \text{ [DC]} \\ J_0 E_0 \sin^2 \omega t \text{ [AC]} \end{cases}$$

$$\Rightarrow \langle P \rangle_t \begin{cases} = 0 \text{ [DC], no energy exchange} \\ \neq 0 \text{ [AC], energy exchange} \end{cases}$$

$\sin \omega t$

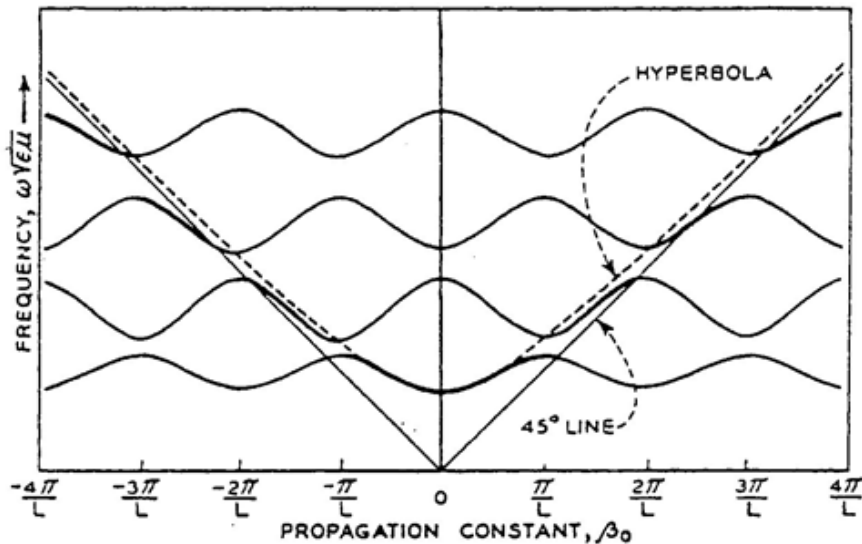
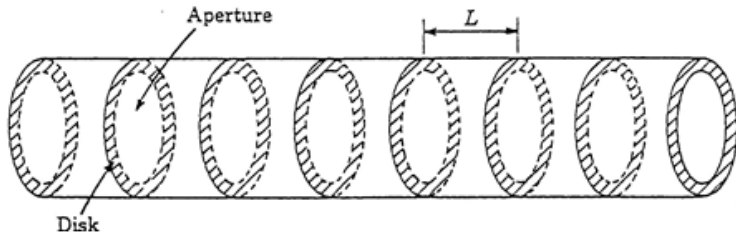


$\sin^2 \omega t$



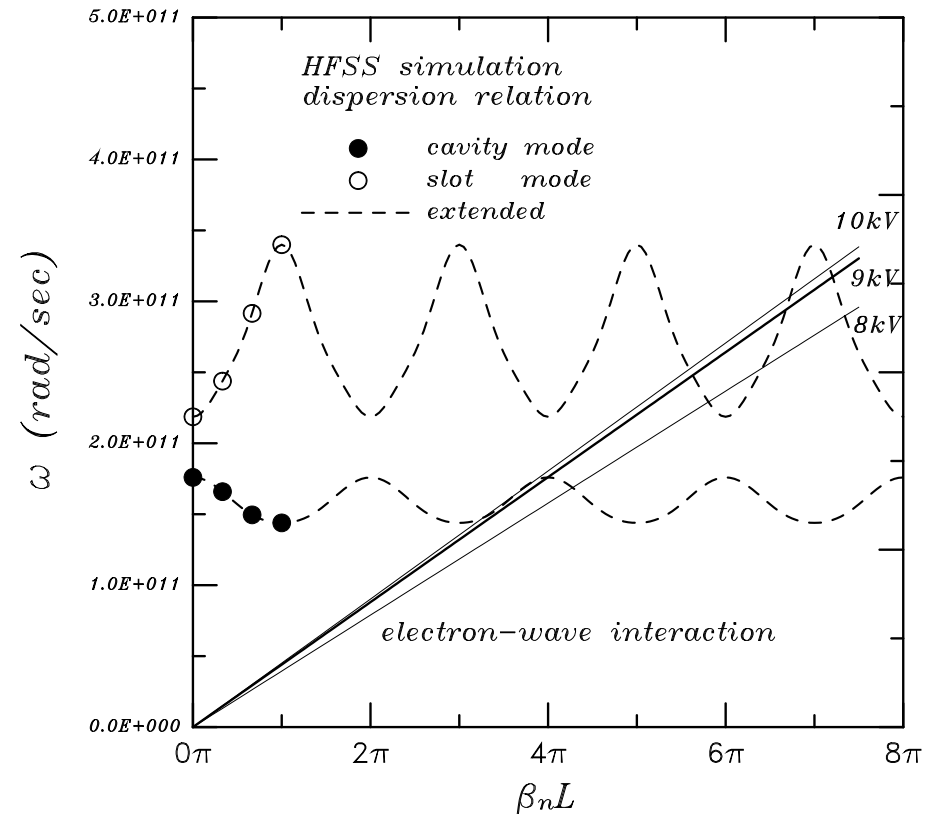
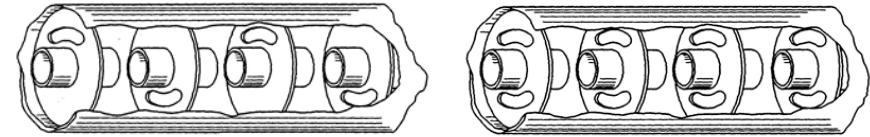
Waves in Periodic Structures

weak periodic loading



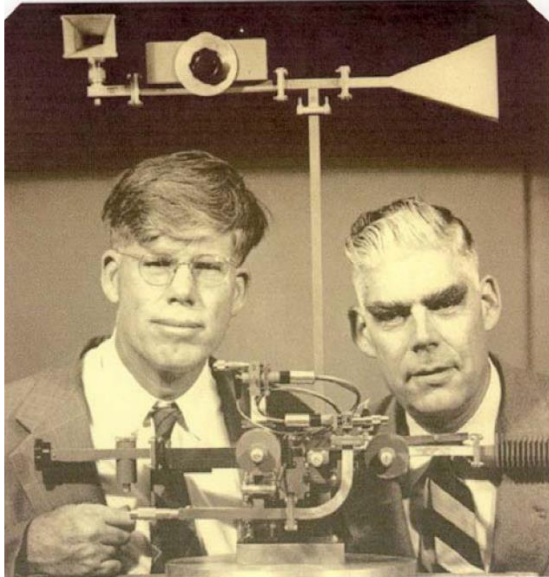
ω-β Diagram of slow wave structure

strong periodic loading

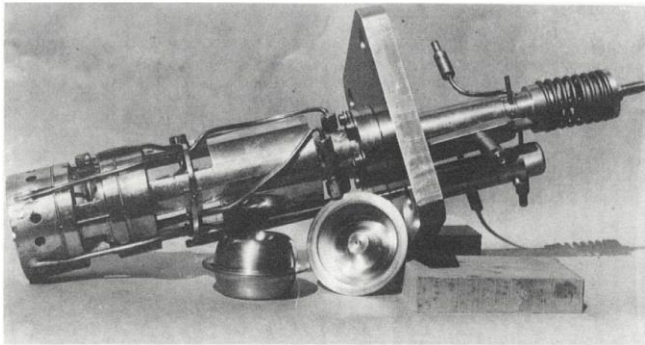


ω-β Diagram of slow wave structure

Klystrons



The first klystron invented by the Varian brothers at Stanford



The Stanford “Model A” klystron



Table 1: Typical 5045 Operating Parameters

Operating Parameter	Value
Frequency	2.856 GHz
Beam Voltage	350 kV
Pervance	$2.0 \mu\text{A}/\text{V}^{1.5}$
Peak Output Power	65 MW
Average Output Power	41 kW
RF Pulse Width	3.5 μs
Pulse Rep. Rate	180 Hz
Gain	50 dB
3 dB Bandwidth	20 MHz
Saturated Efficiency	45%
Cathode Current Density	8 A/cm ²

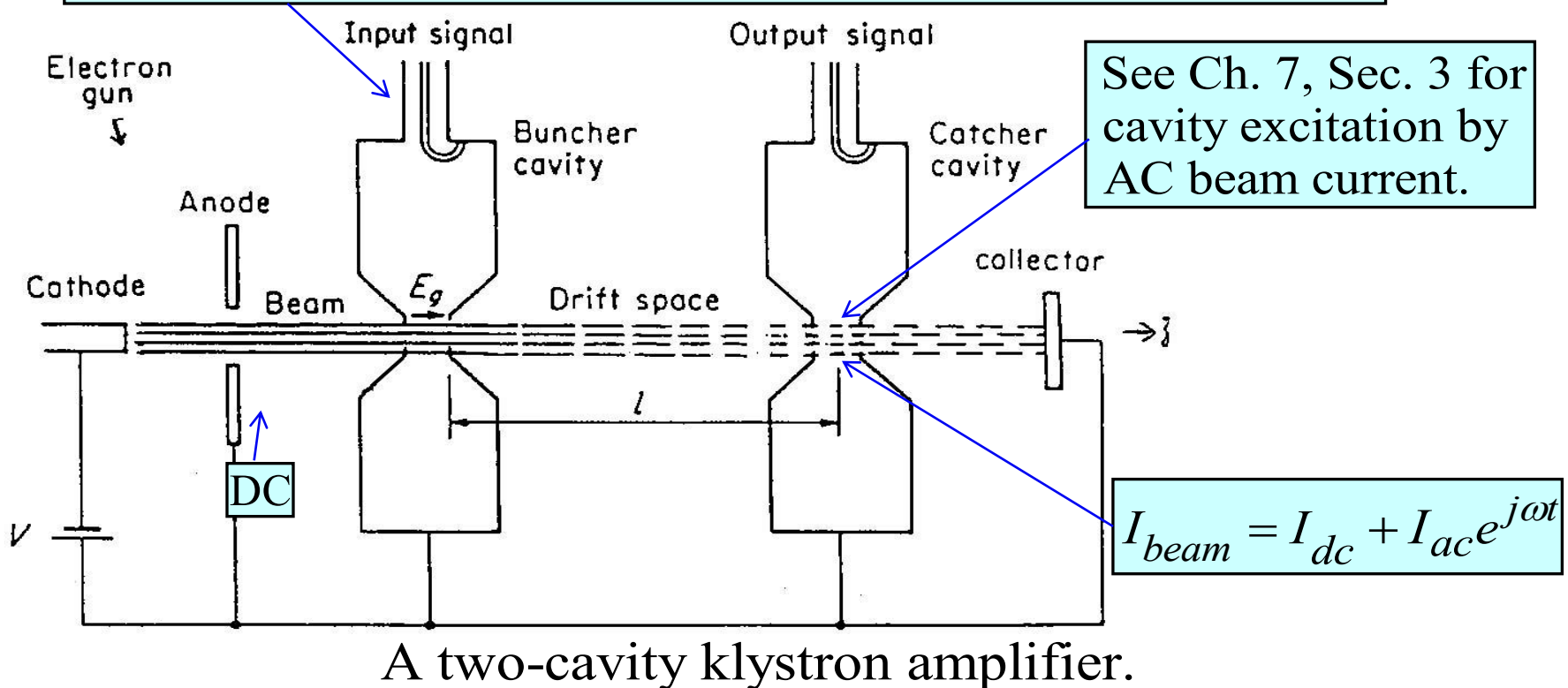
The SLAC S-band klystron

Design Principle of the Klystron

Principle of the klystron amplifier:

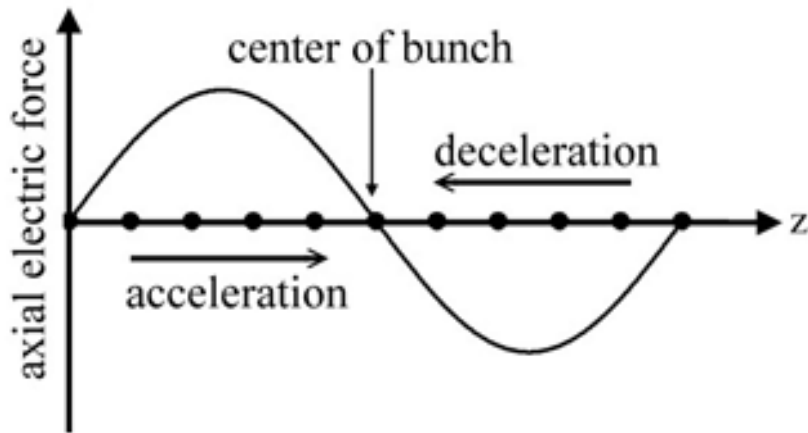
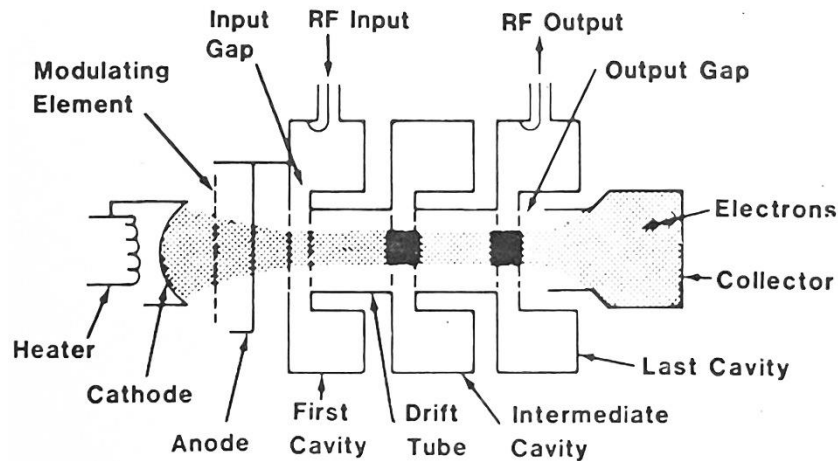
$\left\{ \begin{array}{l} \text{velocity modulation} \\ \text{in buncher cavity} \end{array} \right\} \Rightarrow \left\{ \begin{array}{l} \text{electron bunching} \\ \text{in the drift space} \end{array} \right\} \Rightarrow \left\{ \begin{array}{l} \text{density} \\ \text{modulation} \end{array} \right\}$

See Ch. 7, Sec. 5 for cavity excitation by external coupling.



Design Principle of the Klystron

Elements of a Three-Cavity Klystron Amplifier



DC beam under a HF electric field

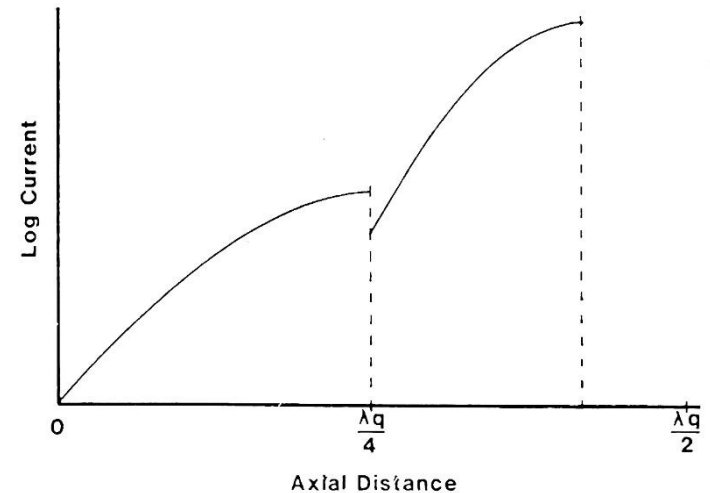
Plasma Frequency

$$\begin{cases} \omega_{pe} \equiv \sqrt{\frac{4\pi n_0 e^2}{m_e}} [= 5.64 \times 10^4 \sqrt{n_0 (\text{cm}^{-3})} \frac{\text{rad}}{\text{sec}}] \\ \omega_{pi} \equiv \sqrt{\frac{4\pi n_0 e^2}{m_i}} [= \sqrt{\frac{m_e}{m_i}} \omega_{pe} \ll \omega_{pe}] \end{cases}$$

For (18) to have a non-trivial solution ($E_{1k} \neq 0$), ω can only have a single frequency given by $\omega^2 = \omega_{pe}^2 + \omega_{pi}^2 = \omega_p^2$ (19)

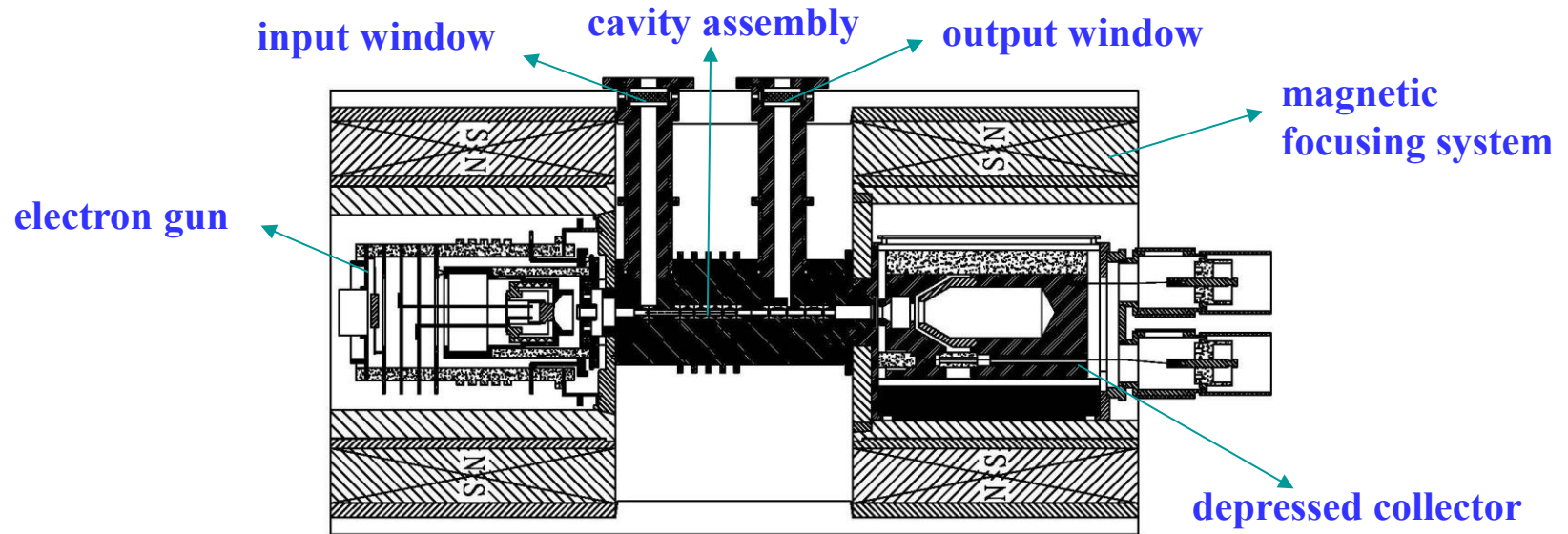
where $\omega_p^2 \equiv \omega_{pe}^2 + \omega_{pi}^2$ (20)

ω_p is called the plasma frequency. It is a characteristic frequency of the plasma most frequently encountered in plasma studies.

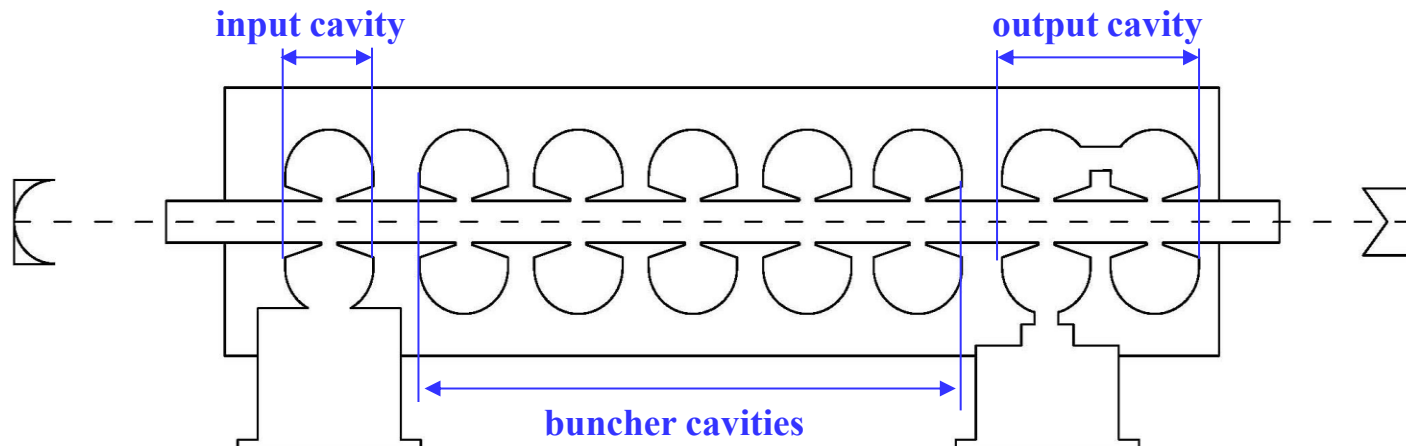


RF Current Growth in Beam in a Three-Cavity Klystron Amplifier

Klystron Assembly



Interaction Circuit



Tuning of the Multi-cavity klystron

(1) Synchronously tuning (for maximum gain)

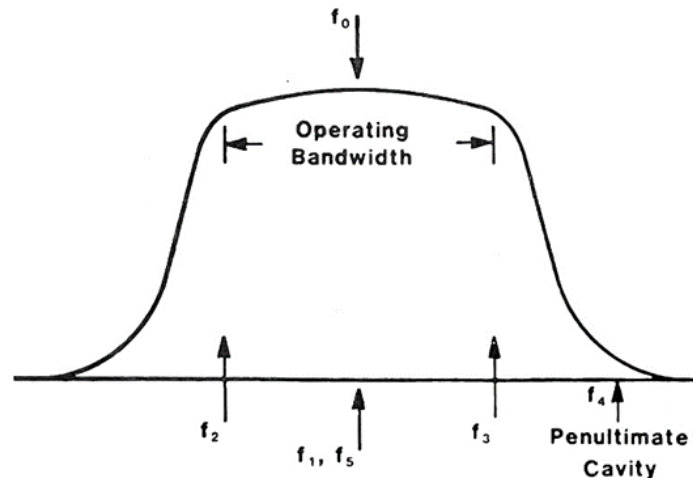
All cavities are tuned to the same frequency, which is also referred to as gain tuning. Generally, each cavity provides a gain of about 15-20 dB, so a klystron amplifier with four resonant cavities is expected to offer a total gain of over 50 dB.

(2) Efficiency tuning (for maximum efficiency)

The penultimate cavity (i.e. next-to-the last cavity) is tuned upward in frequency (making it inductive at the operating frequency) . If the resonant frequency of the penultimate cavity is increased, the bandwidth will be widened. Although the gain will decrease by about 10 dB, efficiency tuning will enhance the bunching efficiency of the electron beam, resulting in a 15-20% increase in power output.

(3) Broadband tuning (for wide bandwidth)

A klystron is typically a narrow-bandwidth microwave source. Usually, stagger tuning is employed, sacrificing high gain to achieve a wider bunching bandwidth. Stagger tuning involves adjusting the resonant frequencies of different cavities above or below the center frequency to increase the overall bandwidth.



Thales TH2100 Klystron

RF performance

Frequency	2 998.5	2 998.5	MHz	
RF output power				
• peak	37	45.1	MW	
• average	17	20	kW	
Peak RF drive power	200	200	W	max.
- 1 dB bandwidth	10	10	MHz	min.
RF pulse duration	4.5	4.5	μs	max.
Saturated gain	53.5	55	dB	typ.
Efficiency	45	43	%	typ.

Electrical characteristics

Anode voltage	279	307	kV	typ.
Beam current	295	340	A	typ.
Heater voltage	30	30	V	max.
Heater current	28	28	A	max.



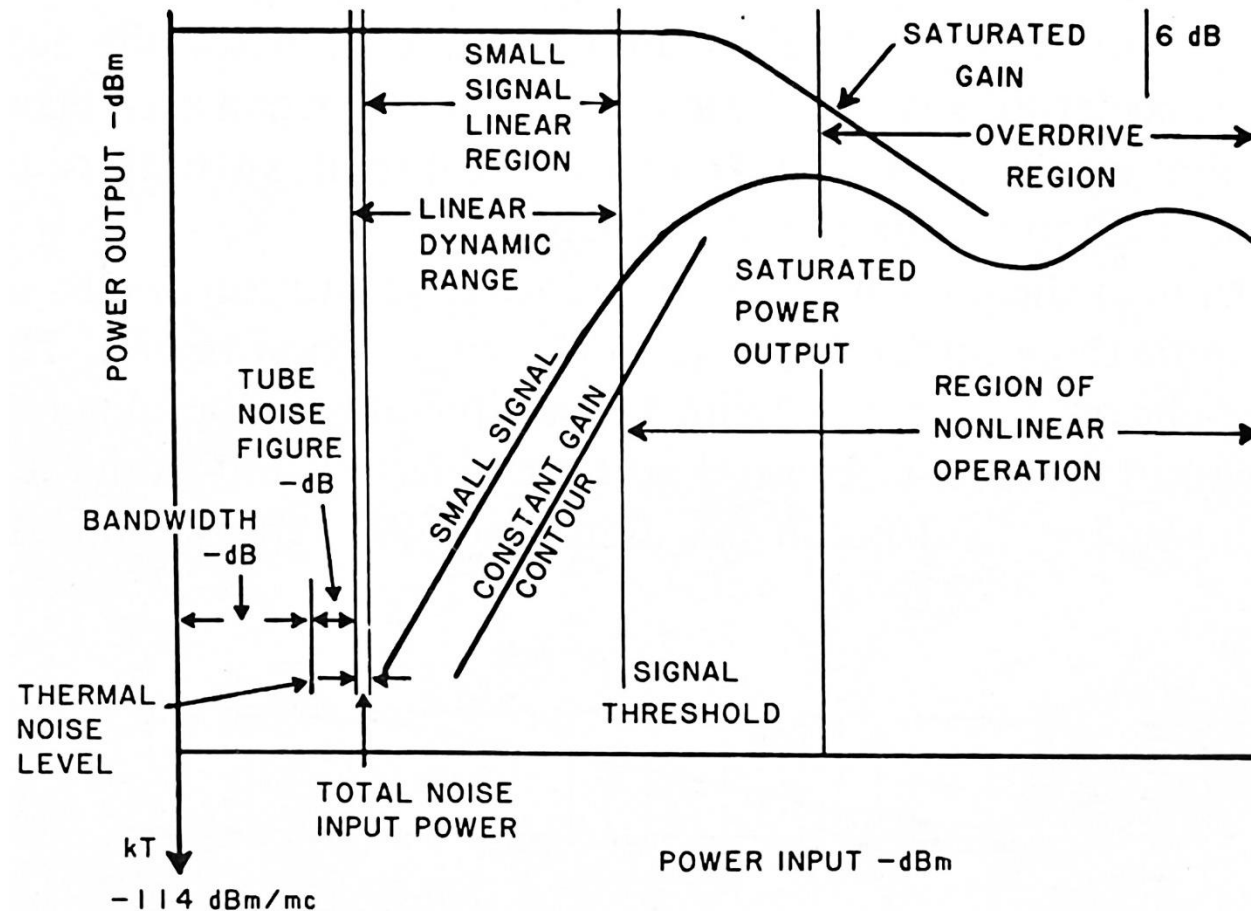
Canon E37310A Pulsed Klystron

Typical Operation

Frequency	2998 MHz
Peak beam voltage	293 kV
Peak beam current	320 A
Beam pulse width	6.2 μ s
RF pulse duration	4.0 μ s
Drive power	374W
Peak output power	35.5MW
Efficiency	38.8%
Gain	49.7dB
Filament voltage	18.3Vac
Filament current	18.4Aac



Design Principle of the Klystron



Transfer Curve of rf amplifier

Small-Signal Analysis

Ka-Band Klystron

$V_0 \equiv 14000$ Beam Voltage (V)
 $I_0 \equiv 0.5$ Beam Current (A)
 $f_0 \equiv 35$ Center Frequency (GHz)
 $a \equiv 0.000375$ Tunnel Radius (m)
 $b \equiv 0.000225$ Beam Radius (m)

Remember to update the shape factor d2 if the fill-factor changes.

$$\beta_e = 3.212 \times 10^7 \beta_q = 169.200 \gamma_a = 1.173$$

Empirical expression for Q_e of the output cavity - not used in the gain calculation: $I_{rf} \equiv 1.5$

$$Q_{eN} := \frac{V_0}{I_0} \frac{1}{RQ_N \left[\frac{2}{\sigma(\sigma+1)} (M_N)^2 I_{rf} \right]}$$

(11)

$$Q_{eN} = 176.205$$

Number of Klystron Cavities: $N \equiv 6$

Gun Microperveance (uA/V^{1.5}) $K \equiv 0.302$

Brillouin Field (gauss) $B_{br} = 2.397 \times 10^3$

Beam current density (A/cm²) $J_{beam} = 314.380$ Cathode current density (A/cm²) $J_{cathode} := 5$

Gun convergence $\frac{J_{beam}}{J_{cathode}} = 63$

Cavity Rs/Q (Ohms)	External Q and Qo	Cavity Frequency (GHz)	Gap-Gap L (m)	Gap Length (m)	Coupling coefficient at r=a	Total coupling coefficient
$RQ_1 \equiv 128$	$Q_{e1} \equiv 350$ $Q_{o1} \equiv 2000$	$f_1 \equiv 34.98$	$L_1 \equiv 0$	$d_1 \equiv 0.0004$	$Ma_1 \equiv 0.919$	$M = \begin{pmatrix} 0.711 \\ 0.711 \\ 0.711 \\ 0.711 \\ 0.711 \\ 0.711 \end{pmatrix}$
$RQ_2 \equiv 128$	$Q_{e2} \equiv \infty$ $Q_{o2} \equiv 2000$	$f_2 \equiv 34.9$	$L_2 \equiv 0.005$	$d_2 \equiv 0.0004$	$Ma_2 \equiv 0.919$	
$RQ_3 \equiv 128$	$Q_{e3} \equiv \infty$ $Q_{o3} \equiv 2000$	$f_3 \equiv 35.09$	$L_3 \equiv 0.005$	$d_3 \equiv 0.0004$	$Ma_3 \equiv 0.919$	
$RQ_4 \equiv 128$	$Q_{e4} \equiv \infty$ $Q_{o4} \equiv 2000$	$f_4 \equiv 35.09$	$L_4 \equiv 0.005$	$d_4 \equiv 0.0004$	$Ma_4 \equiv 0.919$	
$RQ_5 \equiv 128$	$Q_{e5} \equiv \infty$ $Q_{o5} \equiv 2000$	$f_5 \equiv 35.17$	$L_5 \equiv 0.005$	$d_5 \equiv 0.0004$	$Ma_5 \equiv 0.919$	
$RQ_6 \equiv 218$	$Q_{e6} \equiv 350$ $Q_{o6} \equiv 2000$	$f_6 \equiv 35.00$	$L_6 \equiv 0.0047$	$d_6 \equiv 0.0004$	$Ma_6 \equiv 0.919$	

$P3 := PPmax - 3$ $P1 := PPmax - 1$

Number of Data Points npoints $\equiv 256$

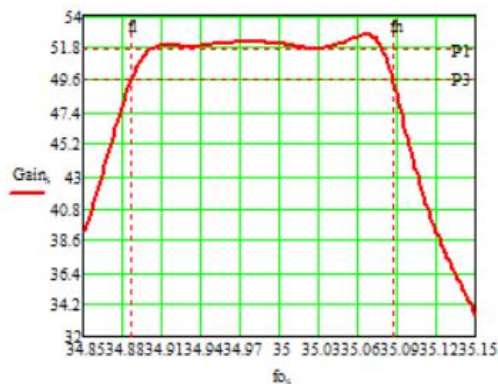
Calculation Bandwidth (GHz) $BW \equiv 0.30$

Plot Markers $f_1 = 34.886$ $f_2 = 35.088$ $PPmax = 52.633$ dB

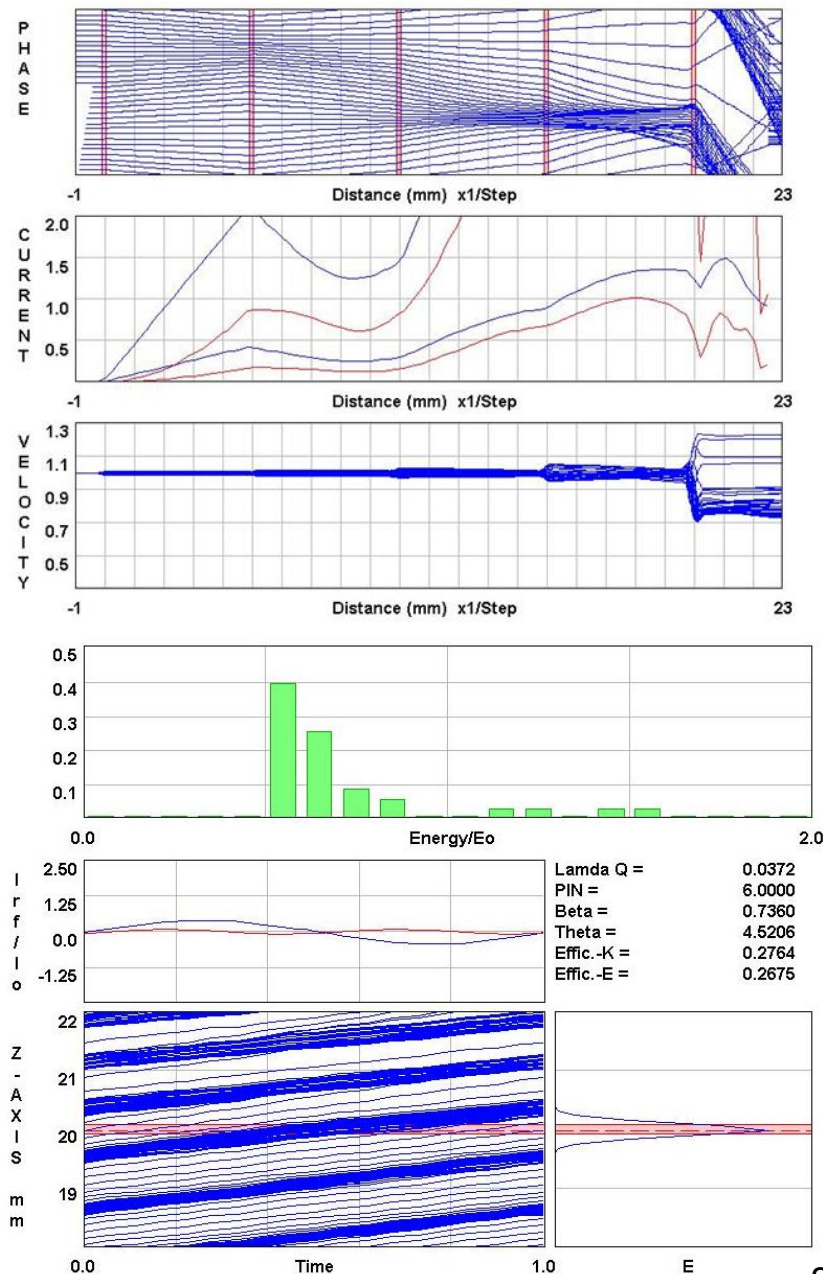
Gain at center frequency $PP0 = 52.002$ dB

1dB Bandwidth (GHz) $Bndwtdb = 0.179$ % $BW(1dB)$ $bw1 = 0.512$

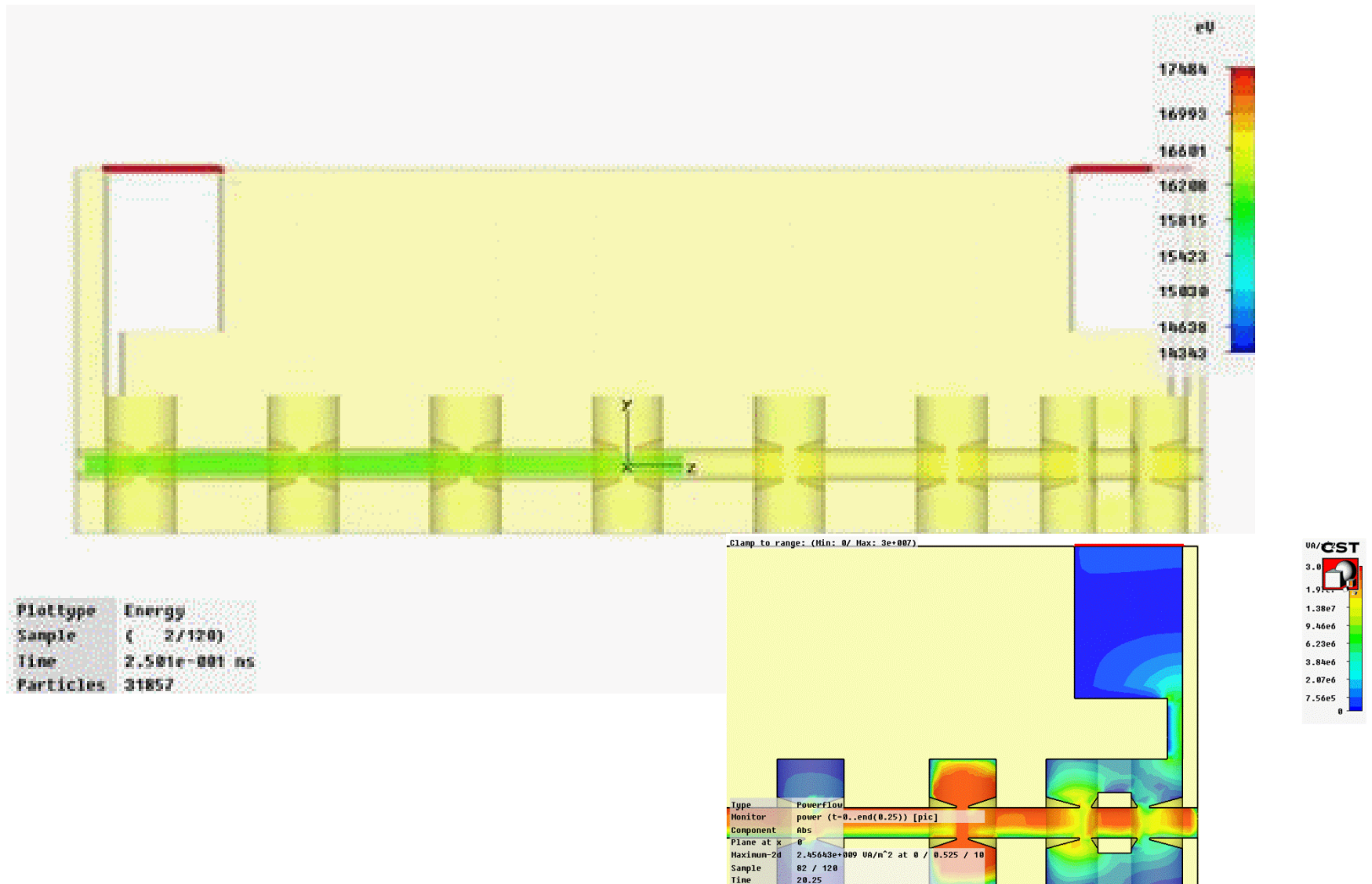
3dB Bandwidth (GHz) $Bndwth = 0.202$ % $BW(3dB)$ $bw3 = 0.576$



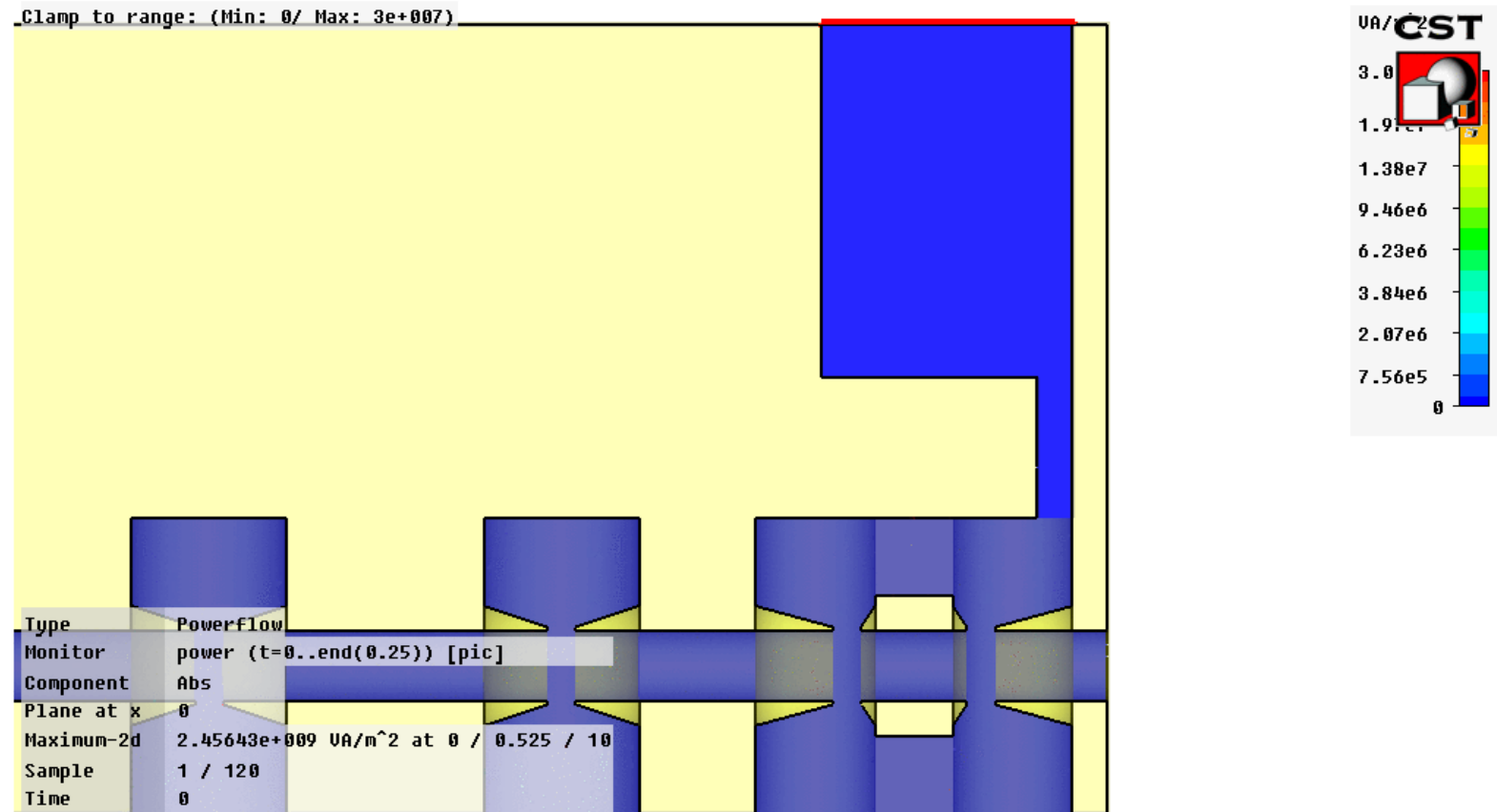
Big-Signal Analysis



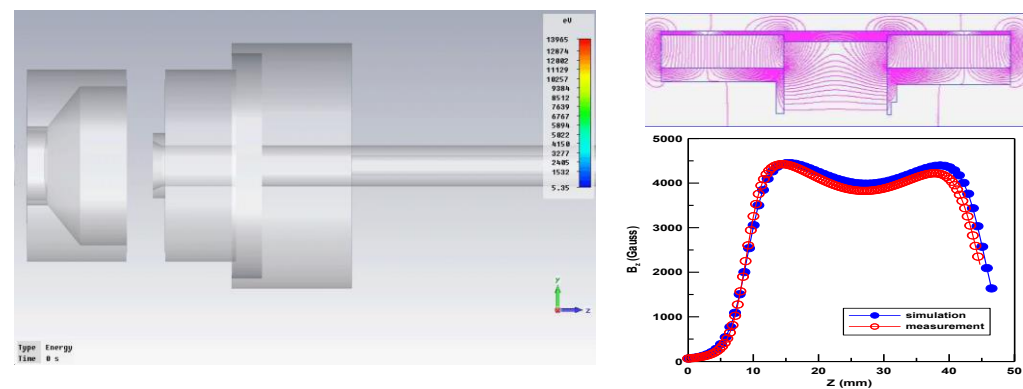
Principle of Beam-Wave Interaction



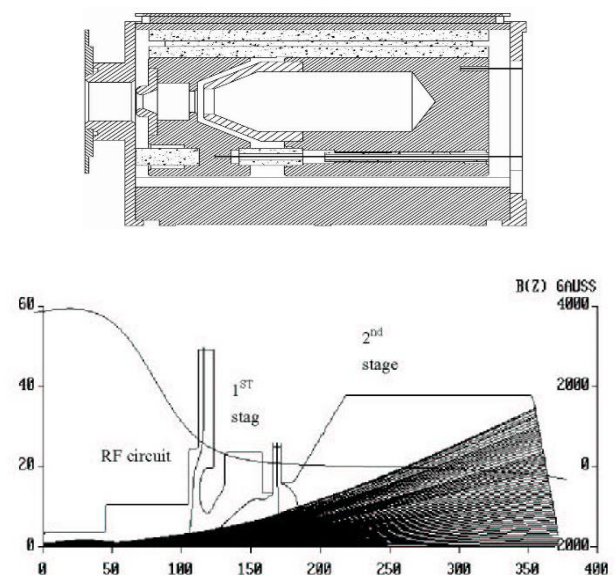
Principle of beam-wave interaction



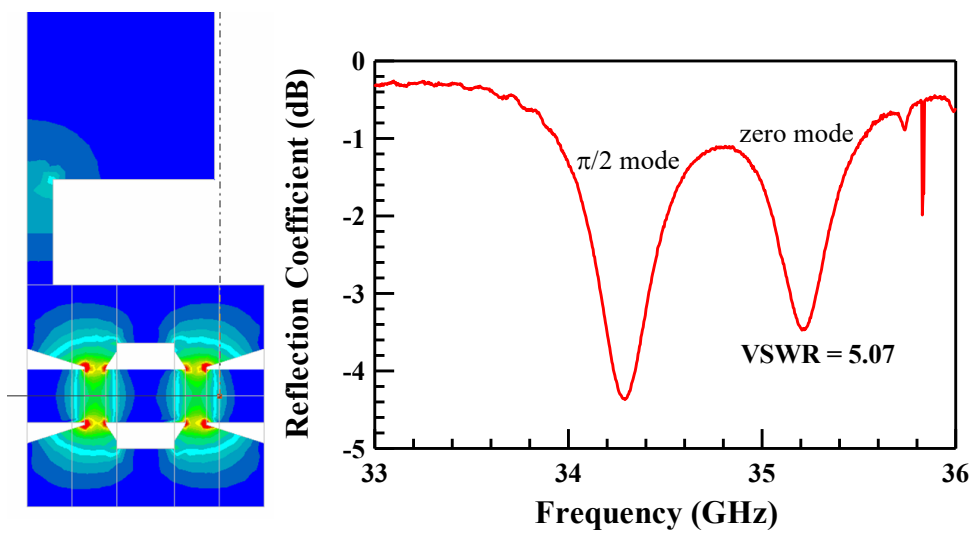
Simulation of the Klystron



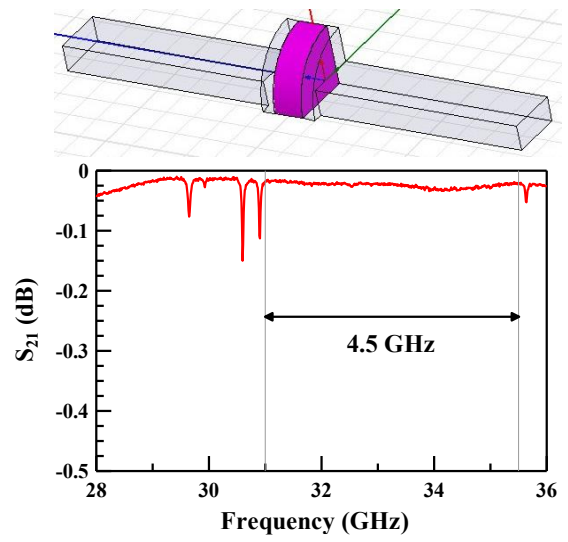
E-Gun and Magnetic Focusing System



Collector Simulation

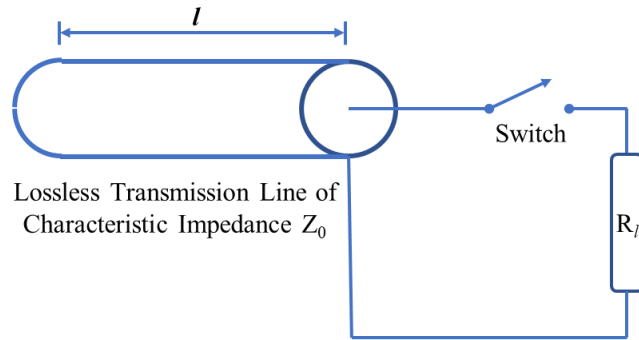


Interaction Structure

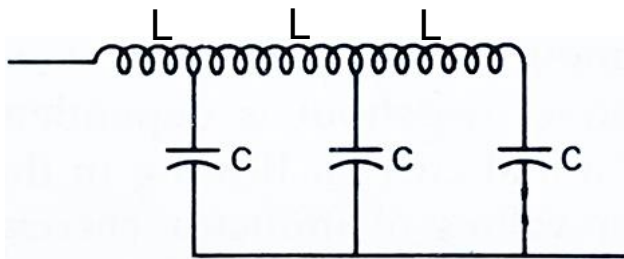


Pillbox Window

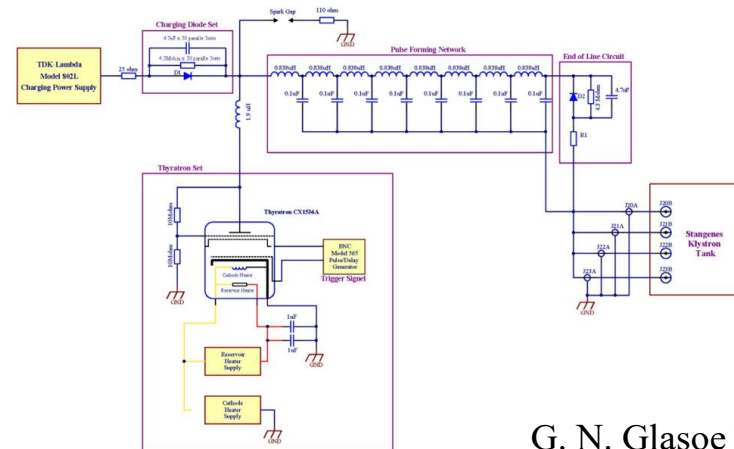
Line-type Modulator of Klystron



$$\text{impedance } R = \sqrt{\frac{L}{C}}$$



Guillemin E type pulse forming networks

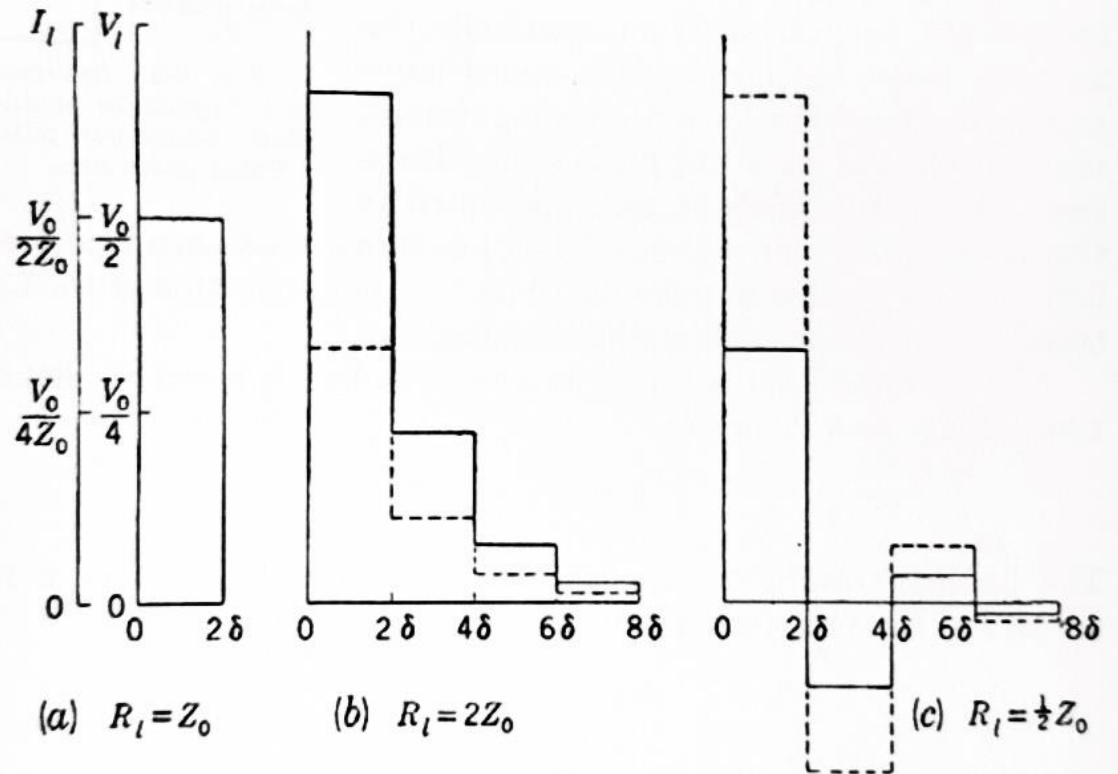


$$i(l) = \frac{V_0}{Z_0 + R_l} \left\{ 1 - U(t - 2\delta) - \frac{Z_0 - R_l}{Z_0 + R_l} [U(t - 2\delta) - U(t - 4\delta)] + \left(\frac{Z_0 - R_l}{Z_0 + R_l} \right)^2 [U(t - 4\delta) - U(t - 6\delta)] - \dots \right\}$$

$$U(\Delta t) = 1 \text{ for } \Delta t > 0$$

$$U(\Delta t) = 0 \text{ for } \Delta t < 0$$

$$\Delta t = (t - n\delta), \quad n = 2, 4, 6, \dots$$



Thales and Canon Klystron comparison

Thales TH2100 klystron



Canon E37310A klystron



	Thales TH2100	Canon E37310A
Frequency (MHz)	2998.5 ± 1	2.997.5~2.999.5
Peak Cathode Voltage (kV)	300 (276)	295 (291)
Peak Inverse Beam Voltage (kV)	70	80
Peak Cathode Current (A)	310 (281)	345 (315)
Peak Drive Power (W)	400	1000
Peak RF Output Power (MW)	37.5 (35.1)	36 (35.6)
Pulse Width (duration) (μs)	7 (75%, 6.5 μs)	7.5 (75%)
Pulse Width (duration, RF) (μs)	4.5 ± 0.5	4.5 (-3 dB)
Pulse Repetition Rate (Hz)	100	120
Gain (dB)	(55.1)	(48)
Efficiency η (%)	(45.2)	(39)
Oil Tank Turn Ratio	TLS : 20, TPS : 13	New Oil Tank : 14
Klystron Impedance (Ω)	TLS : 2.419 (2.46), TPS : 5.7	3.8 (4.11)
Focusing magnet (solenoid/set)	3	6
Charging Voltage (kV)	46.2 (42.5)	39.3 (38.8)

※ The black value is the official specification.

※ (.....) The FAT data are in red brackets. THALES : No. 2100-018, CANON : S/N 21E002A

HBI Modulator PFN Impedance : 1.14 ~ 4.123 Ω

(each capacitor set : 0.1 μF, each inductor (tuning range): 130 nH ~ 1700 nH)

TPS PPT Modulator PFN Impedance : 5.5 ~ 6 Ω

(each capacitor set : 0.025 μF, each inductor : 800 nH)

TPS LINAC Klystron Modulator analysis

Thales TH2100 Klystron :

#210-113, $V_{\text{catode}} = 272 \text{ kV}$, $I_{\text{cathode}} = 286.2 \text{ A}$, Impedance = 950Ω (secondary side)

- Pulse transformer turns ratio 1:13 \rightarrow Primary side impedance $R_{T13} = 5.62 \Omega$

Canon Klystron E37310A Impedance :

SN21E002A, $V_{\text{catode}} = 291 \text{ kV}$, $I_{\text{cathode}} = 315 \text{ A}$, Impedance = 923.8Ω (secondary side)

- Pulse transformer turns ratio 1:14 \rightarrow Primary side impedance $R_{C14} = 4.7 \Omega$
- Pulse transformer turns ratio 1:15 \rightarrow Primary side impedance $R_{C15} = 4.1 \Omega$
- Pulse transformer turns ratio 1:18 \rightarrow Primary side impedance $R_{C18} = 2.85 \Omega$

Charging 43 kV

1. $\frac{R_{P0}}{R_{P0}+R_{T13}} = \frac{5.66}{5.66+5.62} = 0.5 \Rightarrow V_m : V_k = 1 : 1 \Rightarrow (1st) 21.5 \text{ kV} \Rightarrow (2nd) 279.5 \text{ kV}$
2. $\frac{R_{P0}}{R_{P0}+R_{C14}} = \frac{5.66}{5.66+4.7} = 0.55 \Rightarrow V_m : V_k = 1 : 0.83 \Rightarrow (1st) 19.5 \text{ kV} \Rightarrow (2nd) 273 \text{ kV}$
3. $\frac{R_{P0}}{R_{P0}+R_{C15}} = \frac{5.66}{5.66+4.1} = 0.58 \Rightarrow V_m : V_k = 1 : 0.72 \Rightarrow (1st) 18.0 \text{ kV} \Rightarrow (2nd) 270 \text{ kV}$
4. $\frac{R_{P0}}{R_{P0}+R_{C18}} = \frac{5.66}{5.66+2.85} = 0.67 \Rightarrow V_m : V_k = 1 : 0.5 \Rightarrow (1st) 14.3 \text{ kV} \Rightarrow (2nd) 257 \text{ kV}$
5. $\frac{R_{P1}}{R_{P1}+R_{C18}} = \frac{4.7}{4.7+2.85} = 0.62 \Rightarrow V_m : V_k = 1 : 0.61 \Rightarrow (1st) 16.3 \text{ kV} \Rightarrow (2nd) 293 \text{ kV}$

PPT (RI) Modulator (18 sections):

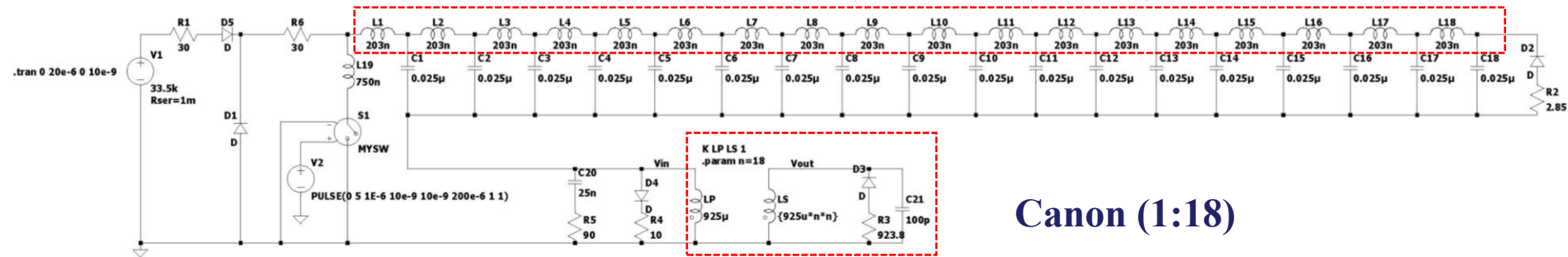
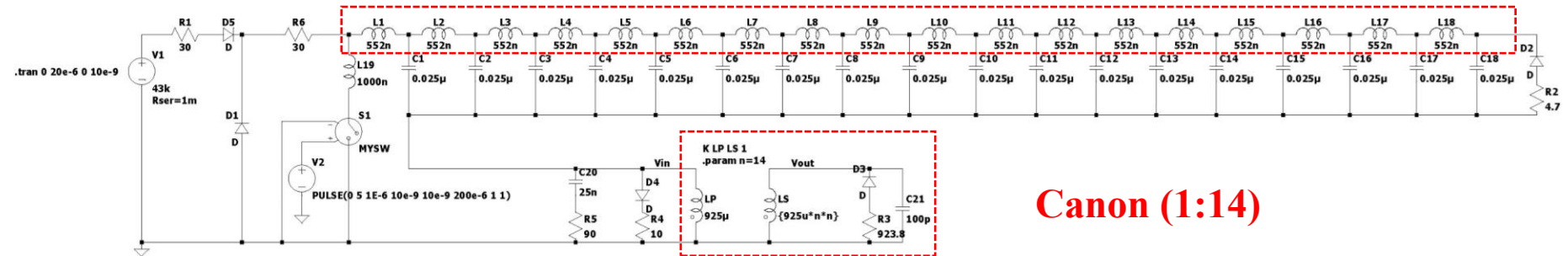
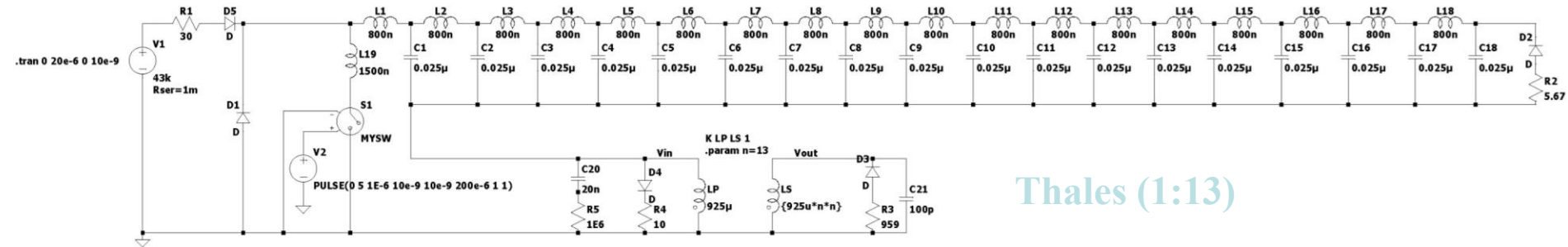
$$\begin{cases} L_0 = 800 \text{ nH} \\ C = 25 \text{ nF} \end{cases} \rightarrow \text{Primary side impedance: } R_{P0} = 5.66 \Omega$$

$$\begin{cases} L_0 = 552 \text{ nH} \\ C = 25 \text{ nF} \end{cases} \rightarrow \text{Primary side impedance: } R_{P1} = 4.7 \Omega$$

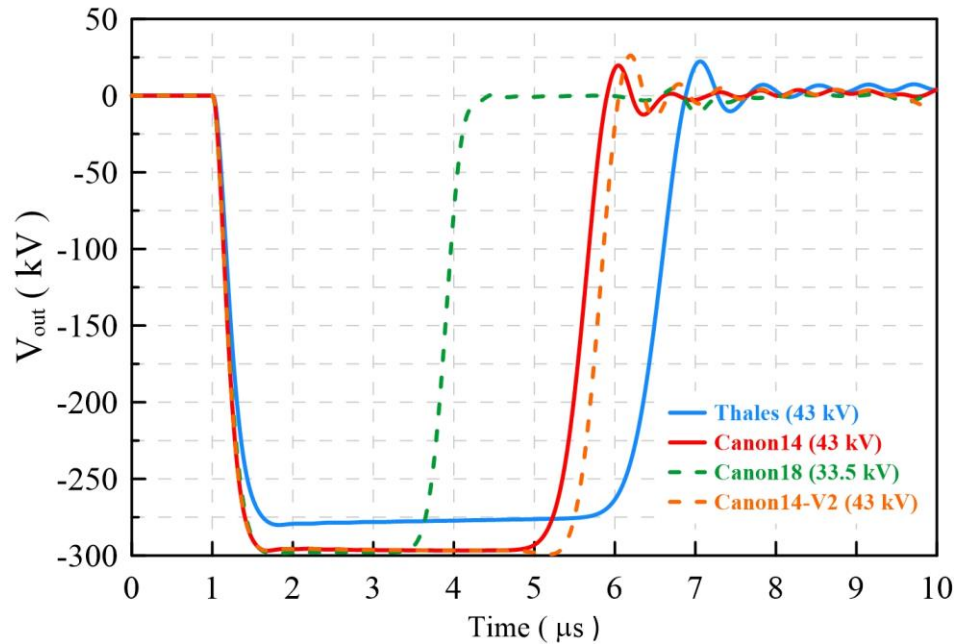
$$\begin{cases} L_1 = 420 \text{ nH} \\ C = 25 \text{ nF} \end{cases} \rightarrow \text{Primary side impedance: } R_{P2} = 4.1 \Omega$$

$$\begin{cases} L_2 = 203 \text{ nH} \\ C = 25 \text{ nF} \end{cases} \rightarrow \text{Primary side impedance: } R_{P3} = 2.85 \Omega$$

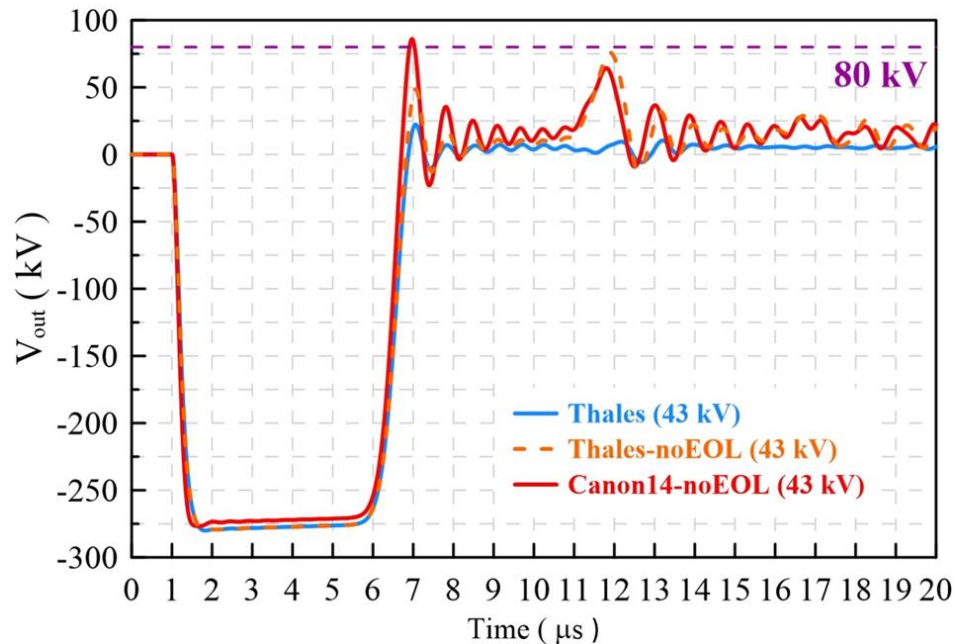
TPS Modulator PFN Analysis (matching design)



TPS LINAC Klystron Modulator analysis

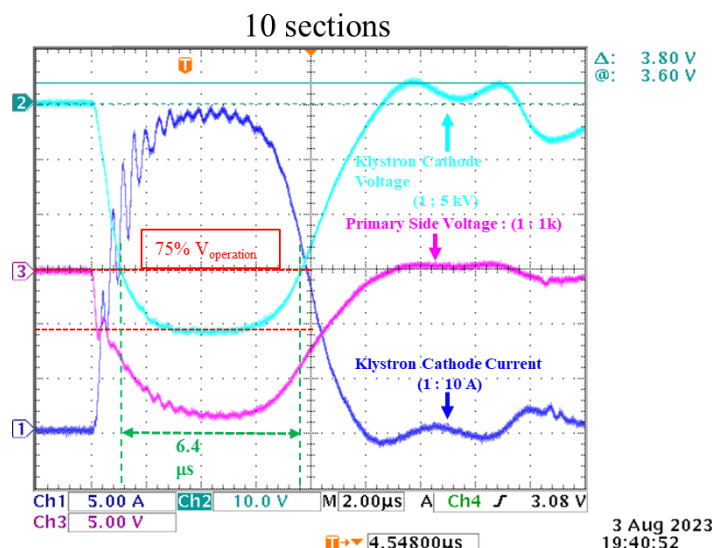
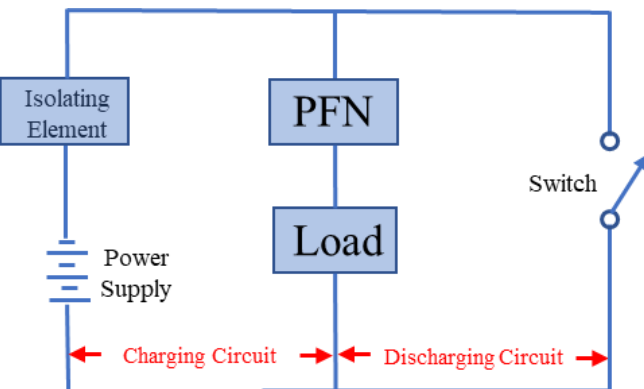


Matching Analysis

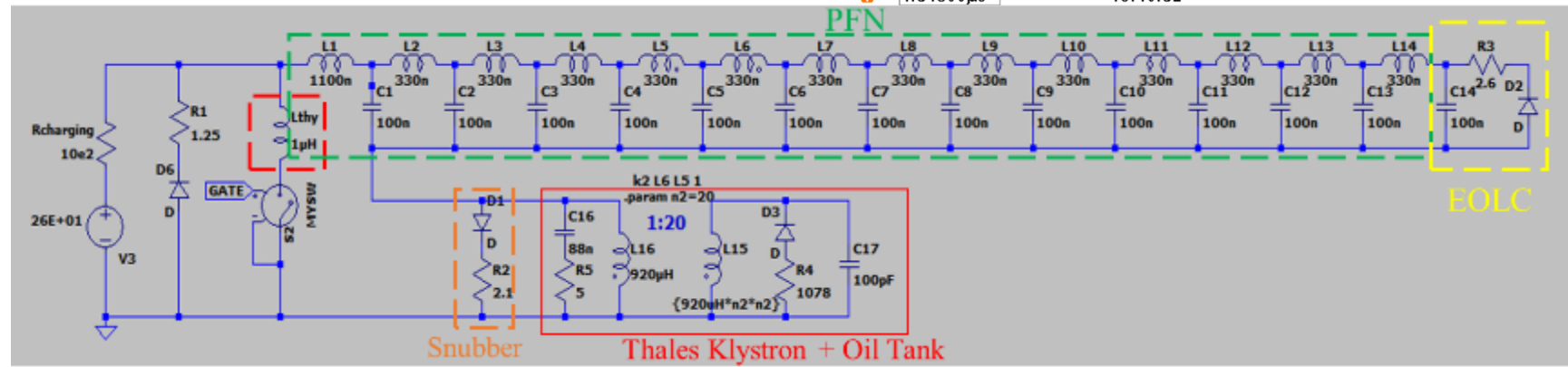


Mismatching Analysis

Modification of the TLS Pulse RF System



3 Aug 2023
19:40:52



Thank You !

And God Said

$$\nabla \cdot E = \frac{\rho}{\epsilon_0}$$

$$\nabla \cdot B = 0$$

$$\nabla \times E = - \frac{\partial B}{\partial t}$$

$$\nabla \times B = \mu_0 J + \mu_0 \epsilon_0 \frac{\partial E}{\partial t}$$

and then there was
"Light"